CATALYTIC CONVERSION OF BIO-DERIVED 5-HMF INTO VALUE ADDED DERIVATIVES

A Thesis submitted to Gujarat Technological University

for the Award of

Doctor of Philosophy

in

Chemical Engineering

by

Rana Srujal Pravinchandra

(Enrollment Number - 189999911009)

under supervision of

Dr. Paresh H. Rana

(Professor, Chemical Engineering Department,

L. D. College of Engineering, Ahmedabad, Gujarat, India)

GUJARAT TECHNOLOGICAL UNIVERSITY, AHMEDABAD

December – 2024

CATALYTIC CONVERSION OF BIO-DERIVED 5-HMF INTO VALUE ADDED DERIVATIVES

A Thesis submitted to Gujarat Technological University

for the Award of

Doctor of Philosophy

in

Chemical Engineering

by

Rana Srujal Pravinchandra

(Enrollment Number - 189999911009)

under supervision of

Dr. Paresh H. Rana

(Professor, Chemical Engineering Department,

L. D. College of Engineering, Ahmedabad, Gujarat, India)

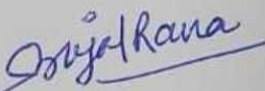# GUJARAT TECHNOLOGICAL UNIVERSITY,

AHMEDABAD

December – 2024

DECLARATION

I declare that the thesis entitled **"CATALYTIC CONVERSION OF BIO-DERIVED 5-HMF INTO VALUE ADDED DERIVATIVES"** submitted by me for the degree of Doctor of Philosophy is the record of research work carried out by me during the period from **July-2018** to **July-2024** under the supervision of **"Dr. Paresh H. Rana"** and this has not formed the basis for the award of any degree, diploma, associateship, fellowship, titles in this orany other University or other institution of higher learning.

I further declare that the material obtained from other sources has been duly acknowledged in the thesis. I shall be solely responsible for any plagiarism or other irregularities, if noticed in the thesis.

Signature of the Research Scholar: ....*Srujal Rana*........... Date: 02|12|2024

Name of Research Scholar: **Rana Srujal Pravinchandra (Enrollment Number - 189999911009)**

Place: **GTU, Ahmedabad**

CERTIFICATE

I certify that the work incorporated in the thesis "**CATALYTIC CONVERSION OF BIO-DERIVED 5-HMF INTO VALUE ADDED DERIVATIVES**" submitted by **Mr. Rana Srujal Pravinchandra (Enrollment Number - 189999911009)** was carried out by the candidate under my supervision/guidance. To the best of my knowledge: (i) the candidate has not submitted the same research work to any other institution for any degree/diploma, Associateship, Fellowship or other similar titles (ii) the thesis submitted is a recordof original research work done by the Research Scholar during the period of study under my supervision, and (iii) the thesis represents independent research work on the part of the Research Scholar.

Signature of Supervisor: ....

Date: 02|12|2024

Name of Supervisor: **Dr. Paresh H. Rana**

Place: **L.D. College of Engineering, Ahmedabad, Gujarat, India**

COURSE-WORK COMPLETION CERTIFICATE

This is to certify that **Mr. Rana Srujal Pravinchnadra** enrolment number – **189999911009** is enrolled for PhD program in the branch **Chemical Engineering** of Gujarat Technological University, Ahmedabad.

(Please tick the relevant option(s))

☐ He has been exempted from the course-work (successfully completed during M.Phil Course)

☐ He has been exempted from Research Methodology Course only (successfully completedduring M.Phil Course)

☑ He has successfully completed the PhD course work for the partial requirement for the award of PhD Degree. His performance in the course work is as follows-

Grade Obtained in Research Methodology [PH001]	Grade Obtained in Self-Study Course/ Contact Program [PH002]
BB	AB

Supervisor's Sign: ....

Name of Supervisor: **Dr. Paresh H. Rana**

ORIGINALITY REPORT CERTIFICATE

It is certified that PhD Thesis titled "CATALYTIC CONVERSION OF BIO-DERIVED 5-HMF INTO VALUE ADDED DERIVATIVES" by Mr. Rana Srujal Pravinchandra (Enrollment Number - 189999911009) has been examined by us. We undertake the following:

a.   Thesis has significant new work / knowledge as compared already published or are under consideration to be published elsewhere. No sentence, equation, diagram, table, paragraph or section has been copied verbatim from previous work unless it is placed under quotation marks and duly referenced.

b.   The work presented is original and own work of the author (i.e. there is no plagiarism). No ideas, processes, results or words of others have been presented as Author own work.

c.   There is no fabrication of data or results which have been compiled / analyzed.

d.   There is no falsification by manipulating research materials, equipment or processes, or changing or omitting data or results such that the research is not accurately represented in the research record.

e.   The thesis has been checked using **DrillBit Plagiarism Check** (copy of originality report attached) and found within limits as per GTU Plagiarism Policy and instructions issued from time to time (i.e. permitted similarity index <= 10%).

Signature of the Research Scholar: ...Srujal Rana...   Date: 02/12/2024

Name of Research Scholar: **Mr. Rana Srujal Pravinchandra**

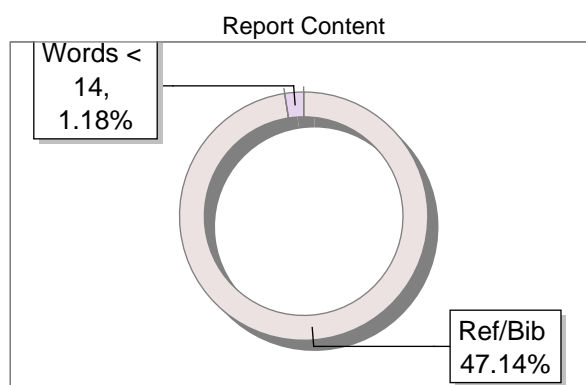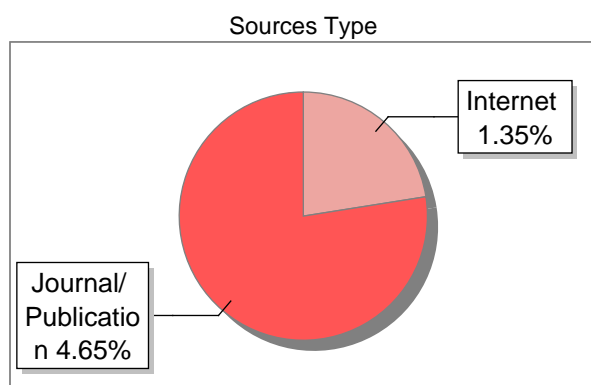Signature of Supervisor: ....   Date: 02/12/2024

Name of Supervisor: **Dr. Paresh H. Rana**

Place: **GTU, Ahmedabad**

DrillBit

The Report is Generated by DrillBit Plagiarism Detection Software

---

Submission Information

Author Name	srujal
Title	Srujal Rana
Paper/Submission ID	2181598
Submitted by	srujal.rana@scet.ac.in
Submission Date	2024-07-29 19:05:21
Total Pages, Total Words	133, 29884
Document type	Thesis

Result Information

Similarity **6 %**

| 1 | 10 | 20 | 30 | 40 | 50 | 60 | 70 | 80 | 90 |

Sources Type

Internet 1.35%
Journal/Publication 4.65%

Report Content

Words < 14, 1.18%
Ref/Bib 47.14%

Exclude Information

Quotes	Excluded
References/Bibliography	Excluded
Source: Excluded < 14 Words	Excluded
Excluded Source	**0 %**
Excluded Phrases	Not Excluded

Database Selection

Language	English
Student Papers	Yes
Journals & publishers	Yes
Internet or Web	Yes
Institution Repository	Yes

A Unique QR Code use to View/Download/Share Pdf File

18	worldwidescience.org	<1	Internet Data
20	www.intechopen.com	<1	Publication
22	www.researchgate.net	<1	Internet Data
23	www.intechopen.com	<1	Publication
24	Pharmacological application of barium containing bioactive glass in ga by Paliwal-2018	<1	Publication
25	springeropen.com	<1	Internet Data
26	Significance of the Mn-Oxidation State in Catalytic and Noncatalytic Promotional by Karakurt-2020	<1	Publication
27	dovepress.com	<1	Internet Data
31	One-step synthesis of hierarchical Zn-ZSM-11 via a facile ZnO route by Yu-2014	<1	Publication
33	An alternative method for the synthesis of functional AuWO3 materials by Durn-lvarez-2018	<1	Publication

Ph.D. THESIS NON-EXCLUSIVE LICENSE TO GUJARAT TECHNOLOGICAL UNIVERSITY

In consideration of being a Research Scholar at Gujarat Technological University, and in the interests of the facilitation of research at the University and elsewhere, I, **Mr. Rana Srujal Pravinchandra** having (Enrollment Number) **189999911009** hereby grant a non-exclusive, royalty free and perpetual license to the University on the following terms:

a.   The University is permitted to archive, reproduce and distribute my thesis, in whole or in part, and/or my abstract, in whole or in part (referred to collectively as the "Work") anywhere in the world, for non-commercial purposes, in all forms of media;

b.   The University is permitted to authorize, sub-lease, sub-contract or procure any of the acts mentioned in paragraph (a);

c.   The University is authorized to submit the Work at any National / International Library, under the authority of their "Thesis Non-Exclusive License";

d.   The Universal Copyright Notice (©) shall appear on all copies made under the authorityof this license;

e.   I undertake to submit my thesis, through my university, to any Library and Archives. Any abstract submitted with the thesis will be considered to form part of the thesis.

f.   I represent that my thesis is my original work, does not infringe any rights of others, including privacy rights, and that I have the right to make the grant conferred by this non-exclusive license.

g.   If third party copyrighted material was included in my thesis for which, under the terms of the Copyright Act, written permission from the copyright owners is required, I have obtained such permission from the copyright owners to do the acts mentioned in paragraph (a) above for the full term of copyright protection.

h.   I understand that the responsibility for the matter as mentioned in the paragraph (g) rests with the authors / me solely. In no case shall GTU have any liability for any acts

/ omissions / errors / copyright infringement from the publication of the said thesis or otherwise.

i.   I retain copyright ownership and moral rights in my thesis, and may deal with the copyright in my thesis, in any way consistent with rights granted by me to my university in this non-exclusive license.

j.   GTU logo shall not be used /printed in the book (in any manner whatsoever) being published or any promotional or marketing materials or any such similar documents.

k.   The following statement shall be included appropriately and displayed prominently in the book or any material being published anywhere: "The content of the published work is part of the thesis submitted in partial fulfilment for the award of the degree of Ph.D. in **Chemical Engineering** of the "Gujarat Technological University".

l.   I further promise to inform any person to whom I may hereafter assign or license my copyright in my thesis of the rights granted by me to my University in this nonexclusive license. I shall keep GTU indemnified from any and all claims from the Publisher(s) or any third parties at all times resulting or arising from the publishing or use or intendeduse of the book / such similar document or its contents.

m.   I am aware of and agree to accept the conditions and regulations of Ph.D. including allpolicy matters related to authorship and plagiarism.
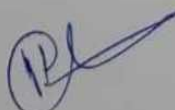
Date: 02|12|2024

Srijel Rana

Signature of the Research Scholar

Place: **GTU, Ahmedabad**

Recommendation of the Supervisor: **Recommended**

Recommendation of the Co-Supervisor (if any): **N.A.**

Signature of Supervisor

THESIS APPROVAL FORM

The viva-voce of the PhD Thesis submitted by **Mr. Rana Srujal Pravinchandra** (Enrollment Number - **189999911009**) entitled **"CATALYTIC CONVERSION OF BIO-DERIVED 5-HMF INTO VALUE ADDED DERIVATIVES"** was conducted on 02 /12/ 2024 at Gujarat Technological University(12.00 pm)
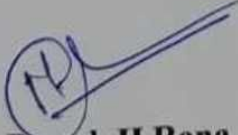
(Please tick any one of the following options)

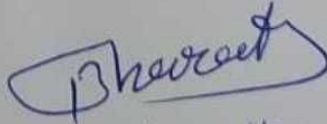☑ The performance of the candidate was satisfactory. We recommend that he/she be awarded the PhD degree.

☐ Any further modifications in research work recommended by the panel after 3 months from the date of first viva-voce upon request of the Supervisor or request of Independent Research Scholar after which viva-voce can be re-conducted by the same panel again.
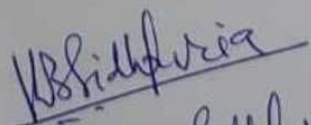
(Briefly specify the modifications suggested by the panel)

☐ The performance of the candidate was unsatisfactory. We recommend that he/she should not be awarded the PhD degree.

Dr. Bharatkumar Modhera

1) (External Examiner 1) Name and Signature

Dr. Paresh H.Rana

Prof. (Dr.) Paresh H Rana
Name and Signature of Supervisor with
Chemical Engg. Dept.
L. D. College of Engineering.
Ahmedabad-380015

Dr. Kalpesh Sidhpuria

2) (External Examiner 2) Name and Signature

X

ABSTRACT

This study examines the significant impact of fossil fuel-derived energy on human life, emphasizing the associated problems such as resource depletion, price uncertainties, and environmental issues. Acknowledging the urgency to explore renewable alternatives, the focus shifts to biomass as a carbon-based, low-cost, and environmentally friendly resource. The conversion of biomass-derived platform molecules into valuable chemicals is explored, with a particular emphasis on the potential of biomass-derived chemicals as platform chemicals for industrial-scale production.

The research delves into the transformation of lignocellulosic biomass, specifically 5-hydroxymethylfurfural (HMF), into biofuel candidates, exemplified by 5-ethoxymethylfurfural (EMF). Challenges related to EMF's molecular stability when blended with regular diesel are discussed, prompting the exploration of alternatives such as di-ethers and 2,5-bis(alkoxymethyl)furans (BAMFs) with superior blending properties.

The catalytic processes, including conventional hydrogenation and catalytic transfer hydrogenation (CTH), are examined, highlighting CTH's advantages in terms of safety, storage, and reduced unit operations. The synthesis of BAMFs from HMF through CTH, employing various catalysts, is presented as a promising one-pot approach. The study underscores the economic viability, catalytic activity, stability, and selectivity of the chosen catalysts, focusing on their role in the reductive etherification of HMF.

The abstract concludes by emphasizing the importance of a one-pot process for the catalytic conversion of 5-HMF to BAMF, highlighting economic benefits, high selectivity, and the potential of BAMF as a biofuel candidate. Overall, the research contributes valuable insights into sustainable energy development and the efficient utilization of biomass resources for biofuel production.

ACKNOWLEDGEMENT

I am immensely grateful to my parents (**Mr. Pravinchandara C. Rana** and **Mrs. Jyoti P. Rana**), my brother, my daughter **Preesha**, and my relatives for their love, unwavering support, tremendous patience, trust, and encouragement.

Finally, I cannot adequately describe the endless love and constant support of my dearest wife, **Jayana S. Rana**. Her constant encouragement criticism and admiration have set new horizons for me to reach in every aspect of my life. I acknowledge her endless patience during my study and thank the Almighty for the inspirational strength she has provided.

<div align="right">

SRUJAL P.RANA

</div>

DEDICATED

TO

ALMIGHTY

TABLE OF CONTENTS

into valuable chemicals

LIST OF ABBREVIATION

5-HMF: 5-Hydroxymethylfurfural

5-EMF: 5-Ethoxymethylfurfural

BAMFs: 2,5-bis(alkoxymethyl)furans

BMMF: 2,5-bis(Methoxymethyl)furans

BHMF: 2,5-bis(Hydroxymethyl)furan

BPMF: 2,5-bis(Propoxymethyl)furans

MPV: Meerwein–Ponndorf–Verley

CTH: Catalytic Transfer Hydrogenation

GHG: Green House Gases

TEM: Transmission Electron Microscopy

PXRD: Powder X-ray diffraction

FTIR: Fourier Transform Infrared Spectroscopy

TPD: Temperature Programmed Desorption

Py-IR: Pyridine Infrared Spectroscopy

LAS-Lewis Acidic Sites

BAS-Bronsted Acidic Sites

EDS- Energy Dispersive Spectroscopy

MMF-Methoxymethylfurfural

AMF-Alkoxymethylfurfural

BBMF-Bis(2-Butoxymethylfuran)

BIPMF-2,5-Bis(isopropoxymethyl)furan

BEMF-2,5-Bisethoxymethylfuran

BSBMF-2,5-bis-(secbutoxymethyl)furan

LIST OF FIGURES

LIST OF TABLES

LIST OF APPENDICES

CHAPTER – 1

INTRODUCTION

1.1 Introduction

Human life undergoes significant impacts due to the energy derived from fossil fuels. The extensive utilization of fossil fuel resources has resulted in numerous issues such as depletion of reserves, price uncertainties, and environmental problems(1–3). Consequently, there is an urgent need to explore renewable resources as an alternative to fossil fuels (4–6). Biomass, being a carbon-based renewable resource, possesses several advantages, including low cost, environmental friendliness, and widespread availability, making it a crucial source for the sustainable development of valuable chemicals (7–9). Therefore, the conversion of biomass-derived platform molecules into valuable chemicals and derivatives represents an attractive approach(10,11). Bio-refinery has emerged as a viable route to maximize biomass utilization, with biomass-derived chemicals such as 5-hydroxymethylfurfural (5-HMF), levulinic acid, furfurals, sugar alcohols, lactic acid, succinic acid, and phenols considered as platform chemicals (12–14). These platform chemicals can further be used for the industrial-scale production of various important chemicals.

Various methods for transforming lignocellulosic biomass into platform chemicals, such as 5-hydroxymethylfurfural (HMF), have been reported recently. HMF can be converted into polymer building blocks and potential biofuel candidates, such as 5-ethoxymethylfurfural (EMF). EMF, produced by etherifying HMF with ethanol, is considered as a promising bio-diesel or additive due to its high energy density compare to commercial gasoline or diesel (15).

Gruter et al. (16) observed that the aldehyde group in EMF affects molecular stability when blended with regular diesel, causing phase separation. Alternatively, products like di-ethers and 2,5-bis(alkoxymethyl)furans (BAMFs) exhibit higher energy densities and better blending properties with diesel(17) . Cao et al.(18) reported complete miscibility of 2,5-bismethoxymethylfuran (BMMF) with diesel. The synthesis of BAMFs from HMF involves two catalytic systems: conventional hydrogenation using H_2 gas and catalytic transfer hydrogenation (CTH). CTH is preferred due to its ability to completely reduce carbonyl compounds through the Meerwein–Ponndorf–Verley (MPV) reaction using formic acid and alcohols as hydrogen donors(19–22).

Researchers have combined hydrogenation and etherification to produce BAMFs from HMF, making the process economically viable by reducing production costs and simplifying operations. The CTH method allows selective conversion of HMF to 2,5-bis(hydroxymethyl)furan (BHMF) through MPV reaction, followed by the conversion of BHMF to various BAMFs. The choice of catalyst and solvent significantly influences the yield and selectivity of the process (13,23–34).

In conclusion, the exploration of renewable resources, particularly the conversion of biomass into valuable chemicals and biofuels, is crucial for sustainable development. The one-pot process for synthesizing BAMF from 5-HMF using a mixed catalyst represents a promising approach with economic advantages and high selectivity. The choice of catalysts and solvents plays a vital role in determining the efficiency and yield of the process.

1.2 Motivation of study

Currently, the global demand for energy and chemicals relies heavily on fossil resources such as petroleum, coal, and natural gas. However, their use is rapidly increasing in transportation and industrial sectors, leading to the swift depletion of these sources. Additionally, the GHG emissions from these fossil resources are contributing significantly

to global warming, posing a serious threat to society. The use of non-degradable materials and hazardous, toxic, and polluting chemicals is also increasing with the advancement of civilization. This has led to severe health hazards for humans and environmental threats. Therefore, a primary challenge for researchers is to find alternative options for fuels, chemicals, and materials. Lignocellulosic biomass is a promising sustainable and eco-friendly alternative, as it is abundant on earth and, most importantly, a renewable source of organic carbon.

India is having highest population in world and about 30-40 % Indian population presently living in urban area and this leads to increase in generation of bio-waste every year (35). So, there is huge potential in India for harnessing bioenergy from the bio-waste. India is agriculture based country so there is various agro based sources are available in plenty. This can able to generate biomass which has the potential to produce biofuels. Biomass, being a carbon-based renewable resource, possesses several advantages, including low cost, environmental friendliness, and widespread availability, making it a crucial source for the sustainable development of valuable chemicals(7–9). Therefore, the conversion of biomass-derived platform molecules into valuable chemicals and derivatives represents an attractive approach(10,11). Bio-refinery has emerged as a viable route to maximize biomass utilization, with biomass-derived chemicals such as 5-hydroxymethylfurfural (5-HMF), levulinic acid, furfurals, sugar alcohols, lactic acid, succinic acid, and phenols considered as platform chemical (13,36,37). These platform chemicals can further be used for the industrial-scale production of various important chemicals.

1.3 Aims and objectives for the present study

The present work principally aims at one-pot reductive etherification of 5-HMF to value added products. Wet impregnation and post synthesis method is used for deposition of

metals on the supports in the search of novel catalyst. The prepared catalyst is characterized by TEM, EDS, PXRD, FTIR, NH_3-TPD and Py-IR.

The objectives are:

Synthesis of BAMF via one pot reductive etherification.

To evaluate the performance of Zr over various support employed to achieve higher conversion for HMF and higher selectivity for the desirable products 2,5 Bis propoxy methyl furan (BPMF).

To explore the effect of Lewis and Bronsted acidity of catalyst on catalytic activity and study the effect of process parameters like temperature, metal loading and time on conversion and selectivity.

To study the performance of metals over HZSM-5 support employed and explores metal support interaction to achieve higher conversion for HMF and higher selectivity for the desirable products 2,5 Bis propoxy methyl furan (BPMF).

1.4 Outlines of thesis

Chapter 1 describes Introduction, motivation of study and aims and objectives of the current study.

Chapter 2 discuss about the literature review on catalytic conversion of 5-HMF to value added derivatives and brief on catalyst characterization methods.

Chapter 3 describes catalytic conversion of 5-HMF to valuable chemicals.

Chapter 4 presents One pot reductive etherification of 5-HydroxyMethylFurfural into biofuel (2, 5-Bis (Propoxymethyl) Furan (BPMF)) using various catalyst such as $ZrO(OH)_2$, Hβ, HY, HZSM-5, Zr-Mont , Zr supported on various zeolites, mixed catalyst $ZrO(OH)_2$ and Zr-Hβ.

Chapter 5 explains Effect of tunable acidic properties on the selectivity of biofuel candidate 2, 5-Bis (PropoxyMethyl) Furan (BPMF) using Sn- Hβ and Sn-dAlHβ catalysts.

Chapter 6 Study of the performance of metals over HZSM-5 support employed and explores metal support interaction to achieve higher conversion for HMF and higher selectivity for the desirable products 2,5 Bis propoxy methyl furan (BPMF).

Chapter 7 summarizes the research work and assesses the contribution of present study.

REFERENCES

1. Zhou CH, Xia X, Lin CX, Tong DS, Beltramini J. Catalytic conversion of lignocellulosic biomass to fine chemicals and fuels. Chem Soc Rev. 2011;40(11):5588.

2. Zhang Z, Song J, Han B. Catalytic Transformation of Lignocellulose into Chemicals and Fuel Products in Ionic Liquids. Chem Rev. 2017 May 24;117(10):6834–80.

3. Hu L, Lin L, Wu Z, Zhou S, Liu S. Recent advances in catalytic transformation of biomass-derived 5-hydroxymethylfurfural into the innovative fuels and chemicals. Renewable and Sustainable Energy Reviews. 2017 Jul;74:230–57.

4. Tollefson J. Can the world kick its fossil-fuel addiction fast enough? Nature. 2018 Apr;556(7702):422–5.

5. Hu L, Zhao G, Hao W, Tang X, Sun Y, Lin L, et al. Catalytic conversion of biomass-derived carbohydrates into fuels and chemicals via furanic aldehydes. RSC Adv. 2012;2(30):11184.

6. Xu C, Arancon RAD, Labidi J, Luque R. Lignin depolymerisation strategies: towards valuable chemicals and fuels. Chem Soc Rev. 2014;43(22):7485–500.

7. Wang J, Xi J, Wang Y. Recent advances in the catalytic production of glucose from lignocellulosic biomass. Green Chem. 2015;17(2):737–51.

8. Zhang Z, Deng K. Recent Advances in the Catalytic Synthesis of 2,5-

Furandicarboxylic Acid and Its Derivatives. ACS Catal. 2015 Nov 6;5(11):6529–44.

9. Liu B, Zhang Z. Catalytic Conversion of Biomass into Chemicals and Fuels over Magnetic Catalysts. ACS Catal. 2016 Jan 4;6(1):326–38.

10. Binder JB, Raines RT. Simple Chemical Transformation of Lignocellulosic Biomass into Furans for Fuels and Chemicals. J Am Chem Soc. 2009 Feb 11;131(5):1979–85.

11. Sheldon RA, Arends IWCE, Hanefeld U. Green Chemistry and Catalysis [Internet]. 1st ed. Wiley; 2007 [cited 2024 Feb 8]. Available from: https://onlinelibrary.wiley.com/doi/book/10.1002/9783527611003

12. Bozell JJ, Petersen GR. Technology development for the production of biobased products from biorefinery carbohydrates—the US Department of Energy's "Top 10" revisited. Green Chem. 2010;12(4):539.

13. Mika LT, Cséfalvay E, Németh Á. Catalytic Conversion of Carbohydrates to Initial Platform Chemicals: Chemistry and Sustainability. Chem Rev. 2018 Jan 24;118(2):505–613.

14. Nicholas KM, editor. Selective Catalysis for Renewable Feedstocks and Chemicals [Internet]. Cham: Springer International Publishing; 2014 [cited 2024 Feb 8]. (Topics in Current Chemistry; vol. 353). Available from: https://link.springer.com/10.1007/978-3-319-08654-5

15. Ras E, Maisuls S, Haesakkers P, Gruter G, Rothenberg G. Selective Hydrogenation of 5-Ethoxymethylfurfural over Alumina-Supported Heterogeneous Catalysts. Adv Synth Catal. 2009 Dec;351(18):3175–85.

16. Gerardus Johannes Maria Gruter. 5-SUBSTITUTED 2-

(ALKOXYMETHYL)FURANS. US 8,231,693 B2, 2012.

17. De Jong E, Vijlbrief T, Hijkoop R, Gruter GJM, Van Der Waal JC. Promising results with YXY Diesel components in an ESC test cycle using a PACCAR Diesel engine. Biomass and Bioenergy. 2012 Jan;36:151–9.

18. Cao Q, Liang W, Guan J, Wang L, Qu Q, Zhang X, et al. Catalytic synthesis of 2,5-bis-methoxymethylfuran: A promising cetane number improver for diesel. Applied Catalysis A: General. 2014 Jul;481:49–53.

19. Ikariya T, Blacker AJ. Asymmetric Transfer Hydrogenation of Ketones with Bifunctional Transition Metal-Based Molecular Catalysts. Acc Chem Res. 2007 Dec 1;40(12):1300–8.

20. Wang D, Astruc D. The golden age of transfer hydrogenation. Chem Rev. 2015 Jul 8;115(13):6621–86.

21. Osatiashtiani A, Lee AF, Wilson K. Recent advances in the production of γ-valerolactone from biomass-derived feedstocks via heterogeneous catalytic transfer hydrogenation. J of Chemical Tech & Biotech. 2017 Jun;92(6):1125–35.

22. Xue Z, Jiang J, Li G, Zhao W, Wang J, Mu T. Zirconium–cyanuric acid coordination polymer: highly efficient catalyst for conversion of levulinic acid to γ-valerolactone. Catal Sci Technol. 2016;6(14):5374–9.

23. Leng Y, Shi L, Du S, Jiang J, Jiang P. A tannin-derived zirconium-containing porous hybrid for efficient Meerwein–Ponndorf–Verley reduction under mild conditions. Green Chem. 2020;22(1):180–6.

24. Zhou S, Dai F, Xiang Z, Song T, Liu D, Lu F, et al. Zirconium–lignosulfonate

polyphenolic polymer for highly efficient hydrogen transfer of biomass-derived oxygenates under mild conditions. Applied Catalysis B: Environmental. 2019 Jul;248:31–43.

25. Rojas-Buzo S, García-García P, Corma A. Hf-based metal–organic frameworks as acid–base catalysts for the transformation of biomass-derived furanic compounds into chemicals. Green Chem. 2018;20(13):3081–91.

26. Li H, He J, Riisager A, Saravanamurugan S, Song B, Yang S. Acid–Base Bifunctional Zirconium N-Alkyltriphosphate Nanohybrid for Hydrogen Transfer of Biomass-Derived Carboxides. ACS Catal. 2016 Nov 4;6(11):7722–7.

27. Hu L, Li N, Dai X, Guo Y, Jiang Y, He A, et al. Highly efficient production of 2,5-dihydroxymethylfuran from biomass-derived 5-hydroxymethylfurfural over an amorphous and mesoporous zirconium phosphonate catalyst. Journal of Energy Chemistry. 2019 Oct;37:82–92.

28. Wei J, Cao X, Wang T, Liu H, Tang X, Zeng X, et al. Catalytic transfer hydrogenation of biomass-derived 5-hydroxymethylfurfural into 2,5-bis(hydroxymethyl)furan over tunable Zr-based bimetallic catalysts. Catal Sci Technol. 2018;8(17):4474–84.

29. Hu D, Hu H, Jin H, Zhang P, Hu Y, Ying S, et al. Building hierarchical zeolite structure by post-synthesis treatment to promote the conversion of furanic molecules into biofuels. Applied Catalysis A: General. 2020 Jan;590:117338.

30. Jae J, Mahmoud E, Lobo RF, Vlachos DG. Cascade of Liquid-Phase Catalytic Transfer Hydrogenation and Etherification of 5-Hydroxymethylfurfural to Potential Biodiesel Components over Lewis Acid Zeolites. ChemCatChem. 2014 Feb;6(2):508–13.

31. Luo J, Yu J, Gorte RJ, Mahmoud E, Vlachos DG, Smith MA. The effect of oxide acidity on HMF etherification. Catal Sci Technol. 2014;4(9):3074–81.

32. Lewis JD, Van de Vyver S, Crisci AJ, Gunther WR, Michaelis VK, Griffin RG, et al. A Continuous Flow Strategy for the Coupled Transfer Hydrogenation and Etherification of 5-(Hydroxymethyl)furfural using Lewis Acid Zeolites. ChemSusChem. 2014 Aug;7(8):2255–65.

33. Shinde S, Rode C. Cascade Reductive Etherification of Bioderived Aldehydes over Zr-Based Catalysts. ChemSusChem. 2017 Oct 23;10(20):4090–101.

34. Wei J, Wang T, Liu H, Li M, Tang X, Sun Y, et al. Highly Efficient Reductive Etherification of 5-Hydroxymethylfurfural to 2,5-Bis(Alkoxymethyl)Furans as Biodiesel Components over Zr-SBA Catalyst. Energy Tech. 2019 May;7(5):1801071.

35. Pandey B, Reba M, Joshi PK, Seto KC. Urbanization and food consumption in India. Sci Rep. 2020 Oct 14;10(1):17241.

36. Mascal M, Dutta S. Chemical-Catalytic Approaches to the Production of Furfurals and Levulinates from Biomass. In: Nicholas KM, editor. Selective Catalysis for Renewable Feedstocks and Chemicals [Internet]. Cham: Springer International Publishing; 2014 [cited 2024 May 27]. p. 41–83. (Topics in Current Chemistry; vol. 353). Available from: https://link.springer.com/10.1007/128_2014_536

37. Rajoka MI, Malik KA. Cellulase production by Cellulomonas biazotea cultured in media containing different cellulosic substrates. Bioresource Technology. 1997 Jan;59(1):21–7.

CHAPTER – 2

LITERATURE REVIEW AND

CHARACTERIZATION TECHNIQUES

2.1 Introduction

The main aim of current review is to compare the conversion and yield of HMF, BHMF and fructose to EMF, MMF and 2, 5 BAMF and its reaction conditions. Besides this the different catalyst and their activities are also discussed. It also discussed the reaction mechanism, which will helpful to design reactor.

Human life is significantly affected by energy derived from fossil fuel. The enormous use of fossil fuel resources led to creates many problems like depletion in reserves, uncertainty in price and environmental issues(1–3). In this regards, exploration of renewable resources as an alternative of fossil fuel has been become urgent needs(4–6). Biomass is a carbon based renewable resource having many advantages like, low cost, environmental friendly and availability, which makes them important source for sustainable development of valuable chemicals (7–9). Hence, conversion of biomass derived platform molecules into valuable chemical and derivatives is most attractive approach(10,11) Bio refinery is emerged as viable route to maximize the use of biomass. Biomass-derived chemicals, such as 5-hydroxymethylfurfural (5-HMF), levulinic acid, furfurals, sugar alcohols, lactic acid, succinic acid, and phenols, are considered platform chemicals. These platform chemicals can be further used for the production of a variety of important chemicals on an industrial scale. [11-14]. Various transformation method of lignocellulosic biomass to platform chemicals such as 5- hydroxymethylfurfural (HMF), which can be converted further to polymer building blocks and potential biofuel candidates, have been reported recently (12). Beside the various biomass derived liquid fuel such as 2, 5-dimethylfuran (DMF) (13–22)

and AMFs (MMF and 5-ethoxymethylfurfural (EMF)) (23–32) 2, 5 Bis-alkoxymethyl furans (BAMFs) are specifically draw more attention because -of its superior properties as biofuel. In comparison with 5- alkoxymethyl furfurals (AMFs) and bioethanol, BAMFs hold properties such as higher energy density (more than 31 MJ/L), higher boiling point, stronger chemical stability, lower water solubility, higher flashing point , lower cold filter plugging point and higher cetane number to the ordinary commercial diesel (33,34). As cetane number (80) of 2, 5 Bis-alkoxymethyl furans are higher than commercial diesel (45), it can be mix with diesels in different propositions which enhance the combustion and reduce the emissions. So, BAMFs are widely considered as potential biodiesel candidates or fuel additives with great application prospects.

BAMFs like 2,5-bis-(methoxymethyl)furan (BMMF) (35), 2,5-bis-(ethoxymethyl)furan (BEMF) (36), 2,5-bis-(propoxymethyl)furan (BPMF) (37), 2,5-bis-(isopropoxymethyl)furan (BIPMF) (38), 2,5-bis-(butoxymethyl)furan (BBMF) (39), and 2,5-bis-(secbutoxymethyl)furan (BSBMF) (40), all derived from various biomass-based substrates such as 2,5-bis-(hydroxymethyl)furan (BHMF), 5-hydroxymethylfurfural (HMF), and fructose (Fig. 2.1), hold significance in their potential use as fuels or additives for diesel fuel. Consequently, a comprehensive examination of their distinct production aspects becomes imperative. As such, this review aims to provide a detailed overview of recent advancements in the synthesis of EMF and BAMFs.
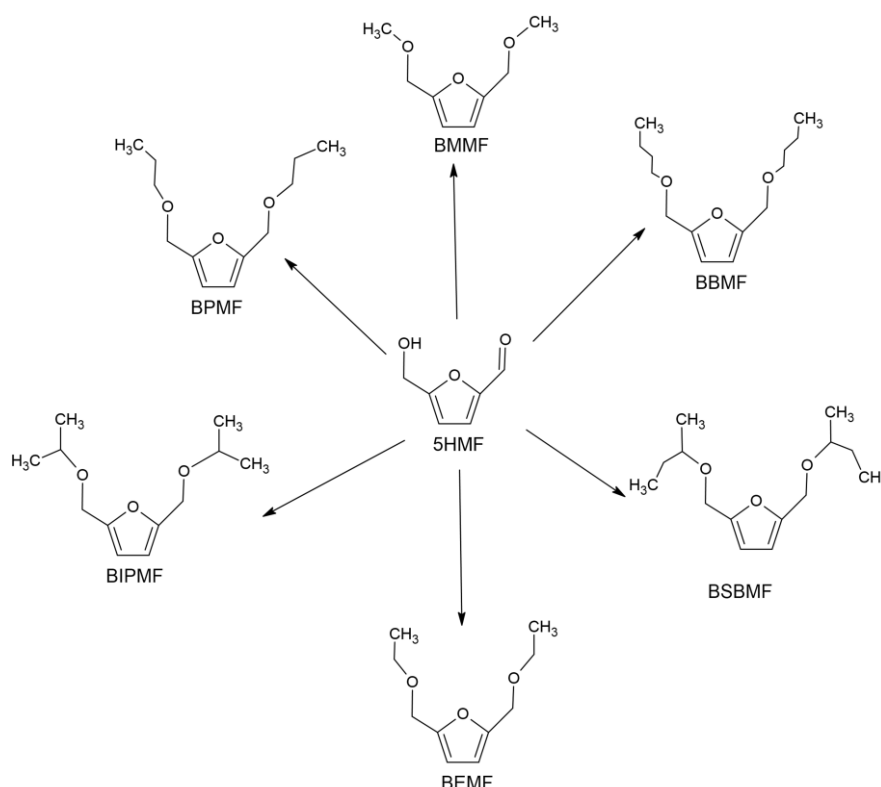
Figure 2.1 Synthesis of various BAMFs from various 5-HMF

2.2 Synthesis of AMFs

AMF, characterized by its high energy density, serves as an exceptional fuel additive. Similar to EMF production, 5-methoxymethylfurfural (MMF) can be synthesized via the etherification of HMF with methanol (41). Alternatively, fructose can directly serve as a substrate for MMF production through a tandem reaction involving fructose dehydration and HMF etherification, using methanol. This approach not only eliminates the need for separating HMF but also reduces MMF production costs. Regrettably, there have been limited studies on this process to date. In 2005, Bicker et al. (42) explored one-pot MMF production from fructose in supercritical methanol, achieving a 77.2% MMF yield using H_2SO_4 as a catalyst at 240°C in 2 sec. To address issues such as corrosiveness and high temperatures in this catalytic system, Zhu et al. (43) introduced a more moderate system in 2011, utilizing Amberlyst-15 as the catalyst in a mixture of methanol and tetrahydrofuran, resulting in a 47.0% MMF yield at 120 °C in 3 h. While the combination of supercritical

methanol and H_2SO_4 yielded higher MMF yields as compared to the methanol/tetrahydrofuran and Amberlyst-15 combination, the former had a much lower fructose concentration of 10 g L^{-1} compared to 200 g L^{-1} in the latter catalytic system (43). From an economic perspective, the latter catalytic system is preferable for one-pot MMF production from fructose. Remarkably, in 2012, Kraus and Guney (31) introduced a greener catalytic system using the acidic ionic liquid 1-methyl-3-(3-sulfopropyl)-imidazolium chloride ([MSPIM]Cl) as a bifunctional catalyst and reaction medium, resulting in a 57.0% MMF yield under the same fructose concentration of 200 g L^{-1} at 100 °C for 20 min. This innovative approach, leveraging [MSPIM]Cl's versatility, enables efficient MMF production from fructose in significantly shorter reaction time and at lower temperatures, potentially revolutionizing its application in the future fuel industry. Beyond MMF and EMF, branched or high-molecular-weight AMF is more desirable due to its superior low-temperature flow properties(44–46). In recent years, compounds like 5-isopoxymethylfurfural (IPMF) (47), 5-tert-butoxymethylfurfural (TBMF) (48), 5-octyloxymethylfurfural (OMF) (49), 5-dodecyloxymethylfurfural (DDMF) (48), and 5-hexadecyloxymethylfurfural (HDMF)(49) have been synthesized from HMF using the corresponding alcohols. Notably, all these synthesis processes employed acidic zeolites as catalysts (47–49). Interestingly, acidic zeolites with Brønsted acidity were found to be more conducive to AMF formation than those with Lewis acidity. For example, when Luo et al.(47) used H-BEA with strong Brønsted acidity as a catalyst, they achieved 97.9% selectivity for IPMF at 140°C with a fixed feed rate of 0.2 mL min^{-1}. In contrast, when Sn-BEA with strong Lewis acidity was used under the same conditions, IPMF selectivity plummeted to 9.8%. Additionally, the type and Si/Al ratio of acidic zeolites significantly affected AMF formation. For instance, in the etherification of HMF with tert-butanol, Yang et al. (44) found that using HZSM 5 with a Si/Al ratio of 80 as a catalyst resulted in

13

almost zero TBMF yield at 60°C in 3 h. However, with the same Si/Al ratio of 80, switching to HY as the catalyst substantially increased TBMF yield to 42.8%. Furthermore, when HY with a Si/Al ratio of 12 was used as a catalyst, an even higher TBMF yield of 55.5% was achieved under the same conditions. These trends were also observed in the synthesis of OMF, DDMF, and HDMF by Arias et al.(49). Thus, optimizing the acidity, type, and Si/Al ratio of acidic zeolites is crucial for achieving the desired AMF yield in HMF etherification.

2.3. Synthesis of BAMFs

To produce Biomass-Based Alkoxymethylfurans (BAMFs), commonly used starting materials include Biomass, Fructose, 5-hydroxymethylfurfural (HMF), and 2,5-bis-(hydroxymethyl)furan (BHMF). Among these, HMF plays a pivotal role, as it is obtained through the dehydration of biomass-derived carbohydrates like fructose(50–52), glucose (53–55) sucrose (56–58) starch(59,60) and cellulose(33,61) making it a crucial compound in the process.

BAMFs can be synthesized in two distinct ways using HMF: HMF is first converted into BHMF via a hydrogenation reaction, and then BHMF is transformed into BAMFs through etherification reactions. HMF is converted into Alkoxymethyl furfuryl alcohol (AMFAs) through a reduction reaction, followed by the conversion of AMFAs into BAMFs through etherification reactions. It's worth noting that when BAMFs are produced using reductive etherification , the presence of the aldehyde group (C=O) in AMFs, which exhibits strong reactivity, can lead to the formation of undesired products like 5-alkoxymethyl-2-dialkoxymethyl furans (AMDAMFs) and alkyl levulinates (ALs)(62). Additionally, in the presence of alcohols, HMF can undergo acetylation reactions, resulting in the formation of 5-(hydroxymethyl)-2-(dialkoxymethyl) furans (HMDAMFs), which can reduce the selectivity and yield of BAMFs to some extent.

14

The various reactions involved in BAMFs production are highly dependent on the types of active sites present in catalysts(38,62–65). Typically, hydrogenation reactions can be catalyzed by metal sites, Lewis acid sites, and Lewis base sites, while etherification reactions can be catalyzed by Lewis acid sites and Brønsted acid sites. Acetylation reactions, on the other hand, can be catalyzed by Lewis acid sites, Lewis base sites, and Brønsted acid sites (see Fig. 2.2).

Therefore, the extent of reactions, reaction rates, selectivity, and product distributions vary across different catalytic systems and reaction conditions. Furthermore, the distribution of products in these reactions is also influenced significantly by the content, ratio, and strength of active sites in catalysts(62–65). In summary, BAMFs production is highly influenced by the active sites of catalysts, and it can be selectively produced by fine-tuning catalyst activity.
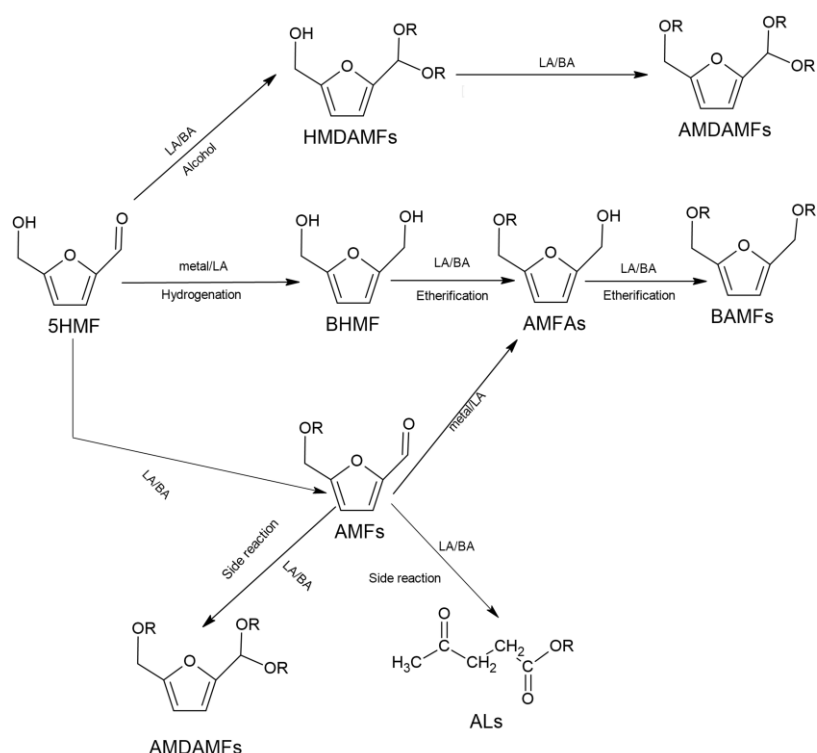
Figure 2.2 various pathways for conversion of HMF in alcohols

2.4. BHMF etherification to BAMFs

The most straightforward method for producing BAMFs is through the etherification of BHMF, which is simpler compared to using HMF and fructose(35–39,66–69). In 2012, Balakrishnan et al.(36) conducted the first study on the etherification of BHMF using ethanol as a solvent and various acid catalysts, including sulfuric acid, Amberlyst-15, p-toluenesulfonic acid (PTSA), Dowex DR2030, sulfonated silica (SiO2-SO3H), Dowex 50WX8, and Amberlite IR120. The results showed that Amberlyst-15, owing to its strong Bronsted acidity, exhibited excellent catalytic activity, yielding 80% BEMF at a mild temperature of 40°C in 16 h (36). Similarly, Han et al. (37) investigated the etherification of BHMF using 1-propanol and 1-butanol as solvents with Amberlyst-15 as the catalyst. Their findings indicated that BPMF and BBMF could be effectively produced using Amberlyst-15 as the catalyst.

Sacia et al. (66) examined the use of 5-methylfurfuryl alcohol as a solvent with Amberlyst-15 catalyst to further elucidate the reaction mechanism for the conversion of BHMF into BAMFs. The results revealed that the oxonium ion formed in the rate-limiting step rapidly reacted with a nearby nucleophile to produce BAMFs (Fig 2.3). The preference for BAMF production is due to the hydrogen-bond interaction between the two hydroxyl groups and the furan ring in BHMF. The yield of BAMFs is highly influenced by the polarity of alcohols, with highly polar alcohols leading to the formation of more by-products and a decrease in the yield of BAMFs. Consequently, the production of BMMF is more challenging with methanol due to its higher polarity, as compared to BEMF and BPMF(37,39,66).

Musolino et al. (39) reported that when using resin catalysts such as Purolite PD206, Purolite CT275DR, and Purolite CT269DR with methanol, BMMF yields of 76%, 75%,

and 99%, respectively, could be achieved at 40 °C in 24 h, attributed to the strong Bronsted acidity of the catalyst. Among the three resin catalysts, Purolite CT269DR exhibited the highest activity for BMMF production. Additionally, Musolino et al. (39) investigated the catalytic activity of Purolite CT269DR for the etherification of BHMF using various alcohols, including EtOH, 1-PrOH, 1-BuOH, 2-propanol (2-PrOH), 2-methoxyethanol (MEtOH), 2-methyl-1-propanol (MPrOH), 1-methyl-2-methoxyethanol (MMEtOH), and allyl alcohol (AlOH), resulting in BAMF yields ranging from 78% to 99% (Table 1). This highlights the excellent catalytic activity of Purolite CT269DR with different alcohols for BAMF synthesis(39).

In addition to resin catalysts, various acid catalysts were also tested for BAMF synthesis. Cao et al.(35) utilized HZSM-5 catalyst for the etherification of BHMF into BMMF. They used HZSM-5 with different Si/Al ratios (25, 38, and 300) and reported that the highest yield of 70% for BMMF was achieved with Si/Al=25, as lower Si/Al ratios provide more acidic sites and higher hydrophilicities, enhancing BMMF yield by promoting etherification reactions and removing water molecules to inhibit side reactions (35). Fang et al.(67) employed HP-HZSM-5 (hierarchical porous) for the etherification of BHMF into BAMFs at 65 °C in 12 h instead of HZSM-5. They found that with HP-HZSM-5 catalyst, a remarkable 94.5% yield of BMMF was achieved even at Si/Al ratio 43, thanks to the mesoporous structure of HP-HZSM-5, which improves mass transfer efficiency. Catalysts like HZSM-5, HP-HZSM-5, and Amberlyst-15 contain both Lewis acid and Bronsted acid sites, resulting in their excellent catalytic activity due to the synergistic effect of both site types(67).

Hu et al. (68) also examined the effect of the ratio of Bronsted acid sites to Lewis acid sites (B/L) on BAMF production. Feng et al.(70) found that reducing the B/L ratio increased BAMF production, suggesting that introducing additional Lewis acid sites can enhance

BAMF production. This hypothesis was confirmed by Fang et al.(70) and Gupta and Saha (69), who used Sn-ZSM-5 and a novel titania carbo-catalyst (a mixture of glucose (Glu), p-toluenesulfonic acid (TsOH), and titanium isopropoxide), respectively. They reported significantly higher BMMF yields of 95% and 89%, respectively, compared to catalysts without added Lewis acid sites at 65°C in 8 h. Gupta and Saha (69) also found that the titania carbo-catalyst was equally effective for producing other products, such as BEMF, BPMF, BBMF, and 2,5-bis(iso-amyloxymethyl)furan (BIAMF), with reasonable yields ranging from 88% to 95% in 8 h at temperatures ranging from 80°C to 120°C (Table 2.1).

Table 2.1 Etherification of BHMF to BAMFs

Catalyst	Solvent	Catalyst quantity (g)	Temperature (^{o}C)	Time (h)	Conversion (%)	Yield (%)	Reference
HZSM-5 (Si/Al=25)	Methanol	4	120	4	-	68	(35)
HZSM-5 (Si/Al=38)	Methanol	4	100	3	-	68	
HZSM-5 (Si/Al=300)	Methanol	4	100	3	-	69	
HZSM-5 (Si/Al=25)	Methanol	1	140	3	-	70	
HZSM-5 (Si/Al=25)	Methanol	4	100	3	-	68	
Amberlyst-15	Methanol	3.2	40	5	-	35	
Amberlyst-15	Methanol	1.6	60	5	-	35	
HP-HZSM-5	Methanol	15	65	8	100	89	(70)

(Si/Al=50)							
Sn-HZSM-5 (Si/Al=50)	Methanol	15	65	8	100	95	
Amberlyst-15	Ethanol	5	40	16	-	80	(36)
Amberlyst-15	Ethanol	5	60	5	-	74	
Amberlyst-15	Ethanol	20	40	5	-	71	
Dowex DR2030	Ethanol	5	40	16	-	66	
Dowex DR2030	Butanol	5	60	5	-	56	
Amberlyst-15	Methanol	20	60	10	-	57	(37)
Amberlyst-15	Ethanol	20	60	10	-	70	
Amberlyst-15	Propanol	20	60	10	99	72	
Amberlyst-15	Butanol	10	60	10	99	60	
Amberlyst-15	Butanol	20	50	10	99	70	
Amberlyst-15	Butanol	20	60	10	99	74	
Amberlyst-15	Butanol	20	80		99	73	
Purolite PD206	Methanol	10	40	24	-	76	(39)
Purolite CT275DR	Methanol	10	40	24	-	75	
Purolite CT269 DR	Methanol	10	40	24	-	99	
Purolite CT269 DR	Ethanol	10	40	24	-	99	
Purolite CT269 DR	AlOH	10	40	24	-	95	

Purolite CT269 DR	Propanol	10	40	24	-	97	
Purolite CT269 DR	2-Propanol	10	40	24	-	93	
Purolite CT269 DR	Butanol	10	40	24	-	78	
Purolite CT269 DR	MEtOH	10	40	24	-	99	
Purolite CT269 DR	MPrOH	10	40	24	-	91	
Purolite CT269 DR	MMEtOH	10	40	24	-	83	
HP-HZSM-5 (Si/Al=43)	Methanol	10	65	12	-	94.5	(67)
HZSM-5 (Si/Al=35)	Ethanol	2	140	*	90.1	59.7	(68)
HP-HZSM-5 (Si/Al=50)	Ethanol	2	140	*	100	76.9	
HP-HZSM-5 (Si/Al=100)	Ethanol	2	140	*	100	81.2	
HP-HZSM-5 (Si/Al=150)	Ethanol	2	140	*	100	83.7	
Glu-Ts-OH-Ti	Methanol	0.04	70	8	-	89	(69)
Glu-Ts-OH-Ti	Ethanol	0.04	80	8	-	92	
Glu-Ts-OH-Ti	Propanol	0.04	100	8	-	90	

Glu-Ts-OH-Ti	Butanol	0.04	120	8	-	93	
Glu-Ts-OH-Ti	MBuOH	0.04	120	8	-	88	

^ Catalyst amount is based on the mass of BHMF ,* Space velocity 0.3h-1

Figure 2.3 Reaction mechanisms for conversion of BHMF to BAMFs

2.5. Synthesis of BAMFs from 5-HMF

As previously discussed in the earlier section regarding the generation of BAMFs directly from BHMF, which is synthesized beforehand from HMF through a hydrogenation reaction employing different acid catalysts, multiple researchers have reported a strategy involving hydrogenation followed by etherification to create BAMFs from HMF. This approach leads to a reduction in the production costs of BAMFs and simplifies the overall process by minimizing the number of unit operations. The synthesis of BAMFs from HMF utilizes two types of catalytic systems: Conventional Hydrogenation: In this method, H_2 gas is employed directly as the hydrogen source. Catalytic Transfer Hydrogenation (CTH): This approach involves a catalytic system for transferring hydrogen and facilitating the hydrogenation reaction. By utilizing these two catalytic systems, researchers aim to optimize the production of BAMFs from HMF.

2.5.1. Conventional Hydrogenation system

In conventional Hydrogenation system molecular hydrogen is used along with solvent and catalyst in production of BAMFs. Balakrishnan et al. (36) were the pioneers in reporting the etherification of DHMF with ethanol in 2012. Their findings revealed that, among various acid catalysts, such as H_2SO_4, Amberlyst-15, Amberlite IR120, Dowex 50WX8, and Dowex DR2030, Amberlyst-15 exhibited remarkable catalytic performance. It achieved an impressive 80% yield of 2,5-bis(ethoxymethyl)furan (BEMF) at a relatively low reaction temperature of 40°C over a 16-h period. These results aligned with the findings of Sacia et al. (66). Moreover, Amberlyst-15 also proved effective in the efficient production of 2,5-bis(propoxymethyl)furan (BPMF)(37) and 2,5-bis(butoxymethyl)-furan (BBMF) (37) through the etherification of DHMF with propanol and 1-butanol, respectively.

However, when methanol was used for the etherification of DHMF, the catalytic performance of Amberlyst-15 was less satisfactory. The yield of 2,5-bis(methoxymethyl)furan (BMMF) was only 57% under the conditions of 60°C in 10 h. This lower yield may be attributed to the high polarity of methanol, which led to the formation of numerous by-products (37). In response to this, Cao et al.(35) turned to acidic zeolites to achieve a better yield of BMMF. They found that among various acidic zeolites, HZSM-5 with a Si/Al ratio of 25 was the most effective for the etherification of DHMF with methanol. After 3 h at 100°C, they obtained a BMMF yield of 70%, surpassing that of HZSM-5 with Si/Al ratios of 38 or 300. The lower Si/Al ratio of the zeolite provided more acidic sites and stronger hydrophilic properties, facilitating the etherification reaction between DHMF and methanol on the catalyst's surface (35). Wu et al. (71) explored various combinations of catalysts, such as Cu/SiO_2 and HZSM-5, $Ru(OH)_x/ZrO_2$ and Amberlyst-15, and Pd/Al_2O_3, to produce BMMF, BPMF, BIPMF, and BBMF, achieving

yields ranging from 68% to 80% under different conditions (Table 2.2). In their quest to enhance BAMF yields, Wei et al.(64) synthesized nano-sized copper (Cu) and copper oxide-modified ultra-stable Y zeolite (CuO-USY).

This reaction is carried out at $130^{o}C$ and 20 bar H_2 in 3 h. Cu and CuO-USY catalyst are used for hydrogenation and etherification reaction respectively. The results show that catalyst system used results in 95.3 % yield of the BMMF. Higher yield of BMMF is because of the more no. of Lewis acid sites associated with CuO-USY and its combine action with Cu (64). He also studied the reaction kinetics of hydrogenation and etherification reaction over the Cu and Cu-USY and found that etherification reaction is fast step. So, its rate of reaction is higher as compared to hydrogenation reaction which favours the more production of BMMF. Li et al. (72) prepared cobalt (Co) based catalyst (Co-400) from Co_3O_4. Results show that the Co-400 catalyst exhibits dual activity like higher reduction capacity and strong etherification capacity. Which leads to higher yield of BMMF 98.5% at $140^{o}C$ and 20 bar H_2 in 1 h. Although with use of Cu, CuO-USY and Co-400 catalysts conventional hydrogenation shows good performance there are many disadvantage associated with it. Conventionally, H_2 has been the primary choice as the hydrogen donor in selective hydrogenation processes due to its widespread availability and its ease of activation on many metal surfaces. However, there are several drawbacks associated with using H_2 in these processes.

Firstly, the low solubility of H_2 in most solvents necessitates high hydrogen pressures to achieve the desired conversion and yield. Handling high-pressure systems introduces safety concerns and increases infrastructure costs, which can be a significant economic barrier to the production of DHMF.

Additionally, H_2 is primarily derived from non-renewable fossil resources, making its production cost notably high. Moreover, H_2 is highly flammable in air, and its

transportation can be inconvenient and risky. Furthermore, H_2 is challenging to disperse in various solvents, leading to low utilization efficiency. Considering these practical and economic factors, using H_2 as a hydrogen donor in selective hydrogenation processes may not be the most cost-effective or secure approach.

To address these challenges and improve the security and economics of selective hydrogenation, researchers have been developing novel catalytic pathways that do not require the addition of external molecular H_2. These alternative approaches aim to provide safer, more cost-effective, and environmentally friendly methods for hydrogenation reactions.

Table 2.2 Synthesis of different BAMFs using molecular H_2

Catalyst	Solvent	Catalyst qunatity (g)	H_2 Pressure (bar)	Temp. (^{o}C)	Time (h)	Conv. (%)	Yield (%)	Reference
HZSM-5 (Si/Al=25)	Methanol	4	25	120	4	100	70	(35)
HZSM-5 (Si/Al=38)	Methanol	4	25	100	3	100	68	
HZSM-5 (Si/Al=300)	Methanol	4	25	100	3	100	69	
HZSM-5 (Si/Al=25)	Methanol	4	25	140	3	100	68	
HZSM-5 (Si/Al=25)	Methanol	4	25	100	3	100	59	
CuSiO$_2$, HZSM-5	Methanol	10,10	25	120	12	100	68	

(Si/Al=25)								
Pt/Al$_2$O$_3$, Amberlyst-15	Ethanol	0.5, 5	14	60	18	-	55	(36)
Pt/Al$_2$O$_3$, Amberlyst-15	Ethanol	1,5	14	60	18	-	59	
Amberlyst-15	Methanol	20	15-30	60	10	-	57	(37)
Amberlyst-15	Ethanol	20	15-30	60	10	-	70	
Ru (OH)$_x$/ZrO$_2$. Amberlyst-15	Propanol	20	15-30	60	10	99	74	
Ru (OH)$_x$/ZrO$_2$. Amberlyst-15	Butanol	10	15-30	60	10	99	71	
Amberlyst-15	Butanol	20	15-30	50	10	99	70	
Amberlyst-15	Butanol	20	15-30	60	10	99	74	
Amberlyst-15	Butanol	20	15-30	80	10	99	73	
Pd/Al$_2$O$_3$	2-PrOH	50	30	60	1	96	80	(71)
Cu,CuO-USY	Methanol	5,50	20	90	3	100	68.1	(64)
Cu,CuO-USY	Methanol	5,50	20	100	3	100	74.3	
Cu,CuO-USY	Methanol	5,50	20	110	3	100	84	
Cu,CuO-USY	Methanol	5,50	20	120	3	100	92.2	
Cu,CuO-USY	Methanol	5,50	20	130	3	100	95.3	
Cu,CuO-USY	Ethanol	5,50	20	140	3	100	92.4	
Cu,CuO-USY	1-PrOH	5,50	20	150	3	100	80.2	
Cu,CuO-USY	2-PrOH	5,50	20	150	3	100	81.4	
Co-400	Methanol	16	20	120	1	100	62.3	(72)

Co-400	Methanol	32	20	120	1	100	65	
Co-400	Methanol	16	20	120	6	100	98.2	
Co-400	Methanol	16	20	140	1	100	98.5	

2.5.2. Catalytic Transfer Hydrogenation system

Catalytic transfer hydrogenation (CTH) presents a favorable alternative to the conventional hydrogenation pathway using external molecular H_2. Specifically, CTH offers a method to completely reduce carbonyl compounds, including aldehydes and ketones, to their corresponding alcohols through the Meerwein−Ponndorf−Verley (MPV) reaction, using formic acid and alcohols as hydrogen donors (73–77).

Alcohols like ethanol and isopropanol are particularly advantageous in CTH processes. They are typically in liquid form under ambient conditions, making them practical, safe, and easy to store, transport, and use when compared to gaseous H_2. Additionally, when alcohols are employed as hydrogen donors, the need for additional facilities to handle H_2 transport is eliminated, reducing the complexity of the overall process.

Furthermore, alcohols can serve a dual purpose as both hydrogen donors and reaction media. This eliminates the requirement for additional reaction solvents, contributing to the cost-effectiveness of CTH. If the chosen alcohol is inexpensive, the economic benefits of CTH become even more pronounced.

A crucial advantage of CTH is that after the completion of the reaction, unconverted alcohol can be separated from the reaction mixture and reused as a hydrogen donor and reaction medium. Similarly, the converted alcohol, which is the produced aldehyde or ketone, can be separated and integrated into other reaction steps, such as carbon chain growth via aldol condensation. This not only enhances the sustainability of the process but also reduces waste and increases the overall efficiency of the chemical transformations. By

using CTH method HMF is selectively converted into BHMF through MPV reaction(78–85) and subsequently BHMF converted to various BAMFs. As in case of CTH approach alcohols not only used as solvent but works as etherifying agents also which leads to formation of BAMFs without using molecular H_2. So, based on above mentioned benefits CTH approach has been used by many researchers in recent years for synthesis of BAMFs. Jae et al. (86) has prepared Sn-beta catalyst which is used for reduction as well as etherification reaction in presence of 2-propanol yields 79.5 % BIPMF at 180^oC in 6h reaction time. Similarly, Luo et al.(47) has also prepared same catalyst and checked its activity with same reaction condition and media in 3 h, which leads to yield of BPMF 60.9 %. In 2014 Lewis et al.(26) has tried to prepare more effective Lewis acidic Hf-Beta catalyst which results 81% yield of BBMF by using 1-Butanol as a solvent at 120^oC in 1 h. Preparation of Sn-Beta and Hf-Beta involves long preparation time (> 20 Days) and corrosive and toxic compounds makes them restrictive choice from the Green Chemistry point of view. So, in line with this aspects Shinde and Rode(87) synthesised Zirconium doped montmorillonite clay (Zr-Mont) with Lewis and Bronsted acidic sites using easy method such as impregnation and calcination. Zr-Mont can be used for both reduction and etherification reactions. It was reported that because of combine effect of Zr-Mont catalyst yield of BIPMF (95%) and BBMF (96%) increase as compared to results of Sn-Beta and Hf-Beta catalyst at 150^oC in 1 h. Rana et al.(88) achieved 91.6% selectivity of BPMF using mixed catalyst $Zr(OH)_2$ and Zr-Hβ at 140°C in 4 h through one pot reductive etherification of 5-HMF. He et al. (89) prepared sulfonic acid-functionalized zirconium-based coordination catalyst (Zr-BDC-Sx) using solvo-thermal method with excellent synergetic actions of Bronsted and Lewis acidic sites and reported 100% conversion and 96.9 % yield of BIPMF in 3 h at 120^oC It is noteworthy that the types of alcohol as well as properties of catalyst have pronounced effect on the synthesis of various types of BAMFs. Similar

27

way recently in 2019 Wi et al. (40) has prepared Zirconium modified SBA-15 (Zr-SBA-UH) using simple urea hydrolysis method. They carry out the reactions in reaction media Ethanol and 2-propanol and reaction conditions 150°C in 4 h which leads to formation of BEMF and BIPMF with yield of 87.9 % and 93.9% (Table 2.3). When (Zr-SBA-UH) was used with other solvents like 1-propanol, 1-butanol, 2-butanol and MPrOH which forms BPMF, BBMF, BSBMF and BMPMF with yield of 38.1 %, 17.1%, 4.4% and 54.1% for same reaction conditions respectively. Here it is noteworthy that alcohols with higher reduction potential are not conductive for the formation of BAMFs. The reduction potential (ΔHf°) is defined as the difference between the standard molar enthalpies of formation of an alcohol and its corresponding carbonyl compound, and it represents the complexity of hydrogen abstraction (90–92). Table 2.4, exhibits the reduction potentials of various alcohols decrease in the order methanol > ethanol > 1-butanol > isopropanol ≈ 2-butanol. it was noted that compared with primary alcohols, secondary alcohols, have lower reduction potentials and because of that they are more appropriate as hydrogen donors in the process of CTH, and this may be the reason that isopropanol is widely used for the selective hydrogenation of HMF to DHMF. As isopropanol and 2-butanol have almost similar reduction potential, 2-butanol should also be a superior hydrogen donor.

Table 2.3 Synthesis of BAMFs from HMF using CTH approach

Catalyst	Solvent	Catalyst quantity (g)	Temperature (^{o}C)	Time (h)	Conversion (%)	Yield (%)	Reference
Zr-SBA	2-propanol	0.1	180	4	100	81.2	(40)
Zr-SBA-UH	ethanol	0.1	150	4	97.1	87.9	
Zr-SBA-UH	MPrOH	0.1	150	4	83.4	54.1	
Zr-SBA-UH	1-propanol	0.1	150	4	84.5	38.1	

Zr-SBA-UH	2-propanol	0.1	150	4	98.5	93.9	
Zr-SBA-UH	1-buatanol	0.1	150	4	62.3	17.1	
Zr-SBA-UH	2-Butanol	0.1	150	4	82.3	4.4	
Sn-Beta	ethanol	1	180	6	91.8	64.3	(85)
Sn-Beta	1-propanol	1	180	6	83.5	59.3	
Sn-Beta	2-propanol	1	180	6	91.5	79.6	
Sn-Beta	1-Butanol	1	180	6	88.9	57.8	
Sn-Beta	2-Butanol	1	180	6	85.2	72.4	
Sn-Beta	2-propanol	40	180	3	69.8	60.9	(86)
Sn-Beta	ethanol	3	120	24	69	41	(47)
Sn-Beta	2-Butanol	3	120	1	43	37	
Hf-Beta	ethanol	3	120	24	87	67	
Hf-Beta	1-Butanol	3	120	1	84	22	
Hf-Beta	2-Butanol	3	120	1	93	81	
Zr-Mont	2-propanol	1	150	1	100	90	(87)
Zr-Mont	2-Propanol	1	150	1	100	95	
Zr-Mont	1-Butanol	1	150	3	100	49	
Zr-Mont	2-Butanol	1	150	1	100	96	
ZrO(OH)2+Zr- Hβ	2-Propanol	0.25	140	4	61.62	91	(88)
Zr-BDC-Sx	2-Propanol		120	3	100	96.9	(89)

Table 2.4 Reduction potential of various alcohols

Alcohols	Reduction potential (ΔH_f°),kJ/mol
Methanol	130.1
Ethanol	85.4
Propanol	87.3
Iso-propanol	70.0
1-butanol	79.7
2-Butanol	69.3
MPrOH	-

2.6. Conclusions

In this review, we have explored the recent developments in the synthesis of BAMFs (Bis(alkoxymethyl)furan) from raw materials like BHMF and HMF using various approaches. It's evident from the review that many researchers have made significant progress in this field over the past few years. However, it's important to note that most of these achievements are currently limited to laboratory-scale applications. Scaling up the production of BAMFs for industrial purposes will require further extensive research and development.

To enable the large-scale manufacturing of BAMFs, several critical aspects need to be addressed:

Understanding Reaction Mechanisms and Kinetics: In-depth studies on the reaction mechanisms and kinetics involved in BAMF synthesis are essential. This knowledge will help optimize the process for efficiency and yield.

One-Pot Hydrogenation and Etherification: Developing efficient one-pot processes for both hydrogenation and etherification can simplify and streamline BAMF production.

Exploring High Reduction Potential Alcohols: Investigating the use of alcohols with high reduction potential can potentially enhance BAMF yield, making the process more economically viable.

Dual-Function Catalysts: Developing catalysts with dual properties that can facilitate one-pot reactions to form BAMFs is a promising avenue for research.

Catalyst Stability: Ensuring the stability of catalysts over extended reaction times is crucial for industrial applications, as catalyst degradation can impact the process's efficiency and cost-effectiveness.

Additionally, some researchers have explored the direct conversion of readily available sugars like fructose into BAMFs, which is a promising approach. Exploring other substances such as glucose and various carbohydrates for direct conversion into BAMFs could open up new possibilities and further expand the scope of BAMF production.

In summary, while significant progress has been made in the synthesis of BAMFs, there are still several challenges and areas of research that need to be addressed to enable large-scale and economically viable production of these valuable compounds. Intensive studies and innovative approaches will be crucial in realizing the potential of BAMFs in various applications.

2.7. Characterization methods for catalyst

Catalyst plays crucial role to increase rate of reaction and selectivity of desired product. Physical and chemical properties of the catalyst are responsible for the performance of the catalyst and study of these properties of heterogeneous catalyst is considered as characterization of catalyst. Characterization methods are also useful to determine the reasons of deactivation and minimize it. Catalyst characteristics includes properties such as chemical composition of the surface and bulk of the solid, surface area, porosity, crystal

size, solid structure, surface morphology, acid-base property, particle size, activity, selectivity and stability. Here, a brief introduction to significance of various characterization methods used in present work are discussed.

2.7.1. BET and BJH method to determine Surface area and pore size and its volume

Extent of dispersion of active metal can be studied by knowing the surface area and pore distribution of the catalyst. Higher surface area of the support indicates the higher dispersion of the active metals. Pore is size important to know the accessibility of reactants to active sites and the diffusivity of product back to the bulk fluid. The size and number of pores determine the internal surface area. In this work, The Brunauer–Emmett–Teller (BET) surface area, pore volume, and Barrett–Joyner–Halenda (BJH) pore size distribution of the prepared catalysts were determined by N_2 adsorption-desorption analysis conducted at -196°C. Prior to analysis, the catalysts were degassed under vacuum at $200 \pm 2^{\circ}$C.

Instrument details: Quantachrome Instruments/NOVA/Quantachrome Touch Win v1.2 2.

Analysis details: sample weight: 0.132 g, duration: 220.9 min, firmware: 1.07, void volume mode: He measure, cell type: 9 mm with rod, thermal delay: 600 sec, warm zone: 3.89899 mL, cold zone: 4.12488 mL.

Adsorbate details: nitrogen, Cross Section Area: 16.2 Å²/mol, Bath Temperature:-196°C

Degas information: Time: 6.0 h, Temp: 200°C.

2.7.2. Powder X-ray diffraction (PXRD)

Powder X-ray diffraction is generally used to study information such as crystal size, crystal structure, chemical composition, lattice strain of the material. An X-ray instrument consists of three primary components: an X-ray source, a sample holder, and PXRD detector.

The X-rays generated by the source illuminate the sample, which then diffracts the X-rays toward the detector. By adjusting the position of the tube or the sample and detector to vary the diffraction angle (2θ, the angle between the incident and diffracted beams), the

intensity is measured and diffraction data are collected. Depending on the geometry of the diffractometer and the type of sample, the angle between the incident beam and the sample can be either fixed or variable, typically paired with the angle of the diffracted beam. The relation between the distance between two hkl planes (d) and angle of diffraction (2θ) is given by Bragg's equation as follows:

$$n\lambda = 2d\ Sin\ \theta \dots\dots\dots\dots (2.1)$$

Where, n= an integer order of reflection and λ= wave length of X-rays(93,94). The diffraction pattern provides information such as degree of crystallinity, purity of phase, unit cell parameters and planes of materials(95). Phase can be identify by comparing the set of reflection of sample with the pure reference phases supplied by ICDD (International Center for Diffraction Data). In present work, Powder X-ray diffraction (PXRD) patterns were obtained on a Bruker D8 Advance X-ray diffractometer, using LynxEye Superspeed detector and Cu Kα radiation produced from a PW Bragg–Brentano (BB) goniometer (θ/2θ), operating at 40 kV and 35 mA. The diffractograms were recorded in the 2θ range of 10 - 80° with a 2θ step size of 0.02°.

2.7.3. NH$_3$ Temperature Programmed Desorption (NH$_3$ TPD)

This method measures the desorbed molecules from the catalyst sample surface. In NH$_3$ TPD analysis catalyst is pretreated in situ in oxidative atmosphere at 100-200°C to remove any adsorbed species on the surface. After that sample is equilibrate with an NH$_3$ gas saturated with probe molecule under well-defined condition. Once the surplus gas has been purged from the reactor, the sample undergoes heating within a continuous flow of inert gas. A thermal conductivity detector continuously tracks the concentration of the gas desorbing in the effluent stream. The cumulative area beneath the curve provides the total quantity of probe molecules desorbed. TPD analysis used to study acidic sites on the

surface and gas adsorbed on the surface. Also it gives information about the various peaks correspond to different types and quantities of adsorbed species and the peaks at different temperatures correspond to varying relative bond strengths between the adsorbate and the surface. Higher desorption temperatures indicate stronger bonds and site strength. The quantity of acidic sites is measured by the total number of ammonia molecules adsorbed on the surface, expressed in micromoles per gram of catalyst. The lower temperature peak indicates weaker bond strength and thus weaker acidic sites, whereas the peak at the higher temperature suggests stronger bonds and hence stronger acidic sites. The area under the curve represents the quantity of weaker and stronger sites. In present work, 0.0735 g of catalyst was taken in quartz sample tube. Before measurements, the catalyst was pre-treated in Helium at 30 SCCM and 200°C. A mixture of NH$_3$ in Helium was passed at rate of 30 SCCM and at temperature 50°C for 30 min. The TPD measurements were carried out in the range 50 to 700°C with a ramp rate of 10°C min^{-1}.

2.7.4. Fourier transform infrared spectroscopy (FTIR)

Fourier Transform Infrared (FTIR) spectroscopy examines the vibration of chemical bonds within a molecule, manifesting at various frequencies contingent upon the elements and bond types present. Upon absorption of infrared radiation, the bond's vibration frequency elevates, prompting transitions between the ground state and multiple excited states. These absorption frequencies denote excitations of bond vibrations and are specific to the bond type (stretching or bending) and the atoms engaged in the vibration. The resultant infrared absorption bands, spanning from 400 to 4000 cm^{-1}, characterize the functional groups within the catalyst. The term Fourier Transform (FT) pertains to a mathematical process that converts data from an interference pattern into an infrared absorption spectrum. In this study, Fourier Transform Infrared Spectroscopy (FTIR) spectra of catalyst samples were

collected using Model: Cary630 spectrometer. The instrument was operated in the range of 600-4000 cm^{-1}.

2.7.5. Infrared spectra for pyridine adsorption (Py-IR)

Infrared spectra for pyridine adsorption, were typically referring to the spectroscopic analysis of pyridine molecules adsorbed onto a surface, often a metal oxide or other catalytic material. This type of analysis is crucial in understanding the interaction between pyridine molecules and the surface, which is important in catalysis.

The IR spectra of pyridine adsorbed on a surface can reveal information about the nature of the adsorption process, the binding sites on the surface, and the structural changes in the pyridine molecule upon adsorption. The IR spectrum of pyridine adsorbed on a surface will exhibit shifts and changes compared to the spectrum of free pyridine in the gas phase. These changes are due to interactions between the pyridine molecules and the surface. The absorption bands corresponding to different functional groups in pyridine may shift in frequency upon adsorption. For example, the frequencies of C-H stretching, C=C stretching, and C-N stretching vibrations may shift due to interactions with the surface. In addition to shifts in existing absorption bands, new absorption bands may appear in the spectrum of adsorbed pyridine. These bands can arise from interactions between pyridine and the surface, such as chemisorption or physisorption, as well as from changes in the molecular structure of pyridine upon adsorption. Changes in the intensities of certain absorption bands may also be observed upon adsorption. This can indicate changes in the orientation or conformation of the adsorbed molecules, as well as changes in the electronic environment of specific functional groups. Depending on the nature of the surface, additional features related to the surface structure or composition may be observed in the spectra of adsorbed pyridine. These features can provide valuable information about the surface properties and the nature of the interaction between the adsorbate and the surface.

In present work, Infrared spectra for pyridine adsorption (Py-IR) were recorded using a Cary630 FT-IR Spectrometer. The initial step involved subjecting a self-supporting sample pellet, weighing approximately 20 mg and measuring 10 mm in diameter, to a temperature of 500°C for duration of 2 h under a vacuum. This step was taken to eliminate any moisture and other adsorbed gases from the sample. The subsequent phase consisted of saturating all the acid sites on the sample by exposing it to pyridine at a temperature of 150°C for a period of 1 h. The identification of Lewis and Bronsted acid sites was achieved by analyzing the bands located at 1445 cm^{-1}, 1638 cm^{-1}, and 1543 cm^{-1}.

REFERENCES

1. Zhou CH, Xia X, Lin CX, Tong DS, Beltramini J. Catalytic conversion of lignocellulosic biomass to fine chemicals and fuels. Chem Soc Rev. 2011;40(11):5588.

2. Zhang Z, Song J, Han B. Catalytic Transformation of Lignocellulose into Chemicals and Fuel Products in Ionic Liquids. Chem Rev. 2017 May 24;117(10):6834–80.

3. Hu L, Lin L, Wu Z, Zhou S, Liu S. Recent advances in catalytic transformation of biomass-derived 5-hydroxymethylfurfural into the innovative fuels and chemicals. Renewable and Sustainable Energy Reviews. 2017 Jul;74:230–57.

4. Tollefson J. Can the world kick its fossil-fuel addiction fast enough? Nature. 2018 Apr;556(7702):422–5.

5. Hu L, Zhao G, Hao W, Tang X, Sun Y, Lin L, et al. Catalytic conversion of biomass-derived carbohydrates into fuels and chemicals via furanic aldehydes. RSC Adv. 2012;2(30):11184.

6. Xu C, Arancon RAD, Labidi J, Luque R. Lignin depolymerisation strategies: towards

valuable chemicals and fuels. Chem Soc Rev. 2014;43(22):7485–500.

7. Wang J, Xi J, Wang Y. Recent advances in the catalytic production of glucose from lignocellulosic biomass. Green Chem. 2015;17(2):737–51.

8. Zhang Z, Deng K. Recent Advances in the Catalytic Synthesis of 2,5-Furandicarboxylic Acid and Its Derivatives. ACS Catal. 2015 Nov 6;5(11):6529–44.

9. Liu B, Zhang Z. Catalytic Conversion of Biomass into Chemicals and Fuels over Magnetic Catalysts. ACS Catal. 2016 Jan 4;6(1):326–38.

10. Binder JB, Raines RT. Simple chemical transformation of lignocellulosic biomass into furans for fuels and chemicals. J Am Chem Soc. 2009 Feb 11;131(5):1979–85.

11. Sheldon RA, Arends IWCE, Hanefeld U. Green chemistry and catalysis. Weinheim: Wiley-VCH; 2007.

12. Wang H, Zhu C, Li D, Liu Q, Tan J, Wang C, et al. Recent advances in catalytic conversion of biomass to 5-hydroxymethylfurfural and 2, 5-dimethylfuran. Renewable and Sustainable Energy Reviews. 2019 Apr;103:227–47.

13. Román-Leshkov Y, Barrett CJ, Liu ZY, Dumesic JA. Production of dimethylfuran for liquid fuels from biomass-derived carbohydrates. Nature. 2007 Jun 21;447(7147):982–5.

14. Chidambaram M, Bell AT. A two-step approach for the catalytic conversion of glucose to 2,5-dimethylfuran in ionic liquids. Green Chem. 2010;12(7):1253.

15. Thananatthanachon T, Rauchfuss TB. Efficient Production of the Liquid Fuel 2,5-Dimethylfuran from Fructose Using Formic Acid as a Reagent. Angewandte Chemie

International Edition. 2010 Sep 3;49(37):6616–8.

16. Jae J, Zheng W, Lobo RF, Vlachos DG. Production of dimethylfuran from hydroxymethylfurfural through catalytic transfer hydrogenation with ruthenium supported on carbon. ChemSusChem. 2013 Jul;6(7):1158–62.

17. Huang YB, Chen MY, Yan L, Guo QX, Fu Y. Nickel-tungsten carbide catalysts for the production of 2,5-dimethylfuran from biomass-derived molecules. ChemSusChem. 2014 Apr;7(4):1068–72.

18. Wang GH, Hilgert J, Richter FH, Wang F, Bongard HJ, Spliethoff B, et al. Platinum–cobalt bimetallic nanoparticles in hollow carbon nanospheres for hydrogenolysis of 5-hydroxymethylfurfural. Nature Mater. 2014 Mar;13(3):293–300.

19. Zu Y, Yang P, Wang J, Liu X, Ren J, Lu G, et al. Efficient production of the liquid fuel 2,5-dimethylfuran from 5-hydroxymethylfurfural over Ru/Co3O4 catalyst. Applied Catalysis B: Environmental. 2014 Mar;146:244–8.

20. Liu Y, Mellmer MA, Alonso DM, Dumesic JA. Effects of Water on the Copper-Catalyzed Conversion of Hydroxymethylfurfural in Tetrahydrofuran. ChemSusChem. 2015 Dec 7;8(23):3983–6.

21. Shi J, Wang Y, Yu X, Du W, Hou Z. Production of 2,5-dimethylfuran from 5-hydroxymethylfurfural over reduced graphene oxides supported Pt catalyst under mild conditions. Fuel. 2016 Jan;163:74–9.

22. Hu L, Tang X, Xu J, Wu Z, Lin L, Liu S. Selective Transformation of 5-Hydroxymethylfurfural into the Liquid Fuel 2,5-Dimethylfuran over Carbon-Supported Ruthenium. Ind Eng Chem Res. 2014 Feb 26;53(8):3056–64.

23. Yuan Z, Zhang Z, Zheng J, Lin J. Efficient synthesis of promising liquid fuels 5-ethoxymethylfurfural from carbohydrates. Fuel. 2015 Jun;150:236–42.

24. Yin S, Sun J, Liu B, Zhang Z. Magnetic material grafted cross-linked imidazolium based polyionic liquids: an efficient acid catalyst for the synthesis of promising liquid fuel 5-ethoxymethylfurfural from carbohydrates. J Mater Chem A. 2015;3(9):4992–9.

25. Li H, Saravanamurugan S, Yang S, Riisager A. Direct transformation of carbohydrates to the biofuel 5-ethoxymethylfurfural by solid acid catalysts. Green Chem. 2016;18(3):726–34.

26. Lewis JD, Van de Vyver S, Crisci AJ, Gunther WR, Michaelis VK, Griffin RG, et al. A Continuous Flow Strategy for the Coupled Transfer Hydrogenation and Etherification of 5-(Hydroxymethyl)furfural using Lewis Acid Zeolites. ChemSusChem. 2014 Aug;7(8):2255–65.

27. Wang S, Zhang Z, Liu B, Li J. Silica coated magnetic Fe3O4 nanoparticles supported phosphotungstic acid: a novel environmentally friendly catalyst for the synthesis of 5-ethoxymethylfurfural from 5-hydroxymethylfurfural and fructose. Catal Sci Technol. 2013;3(8):2104.

28. Wang H, Deng T, Wang Y, Cui X, Qi Y, Mu X, et al. Graphene oxide as a facile acid catalyst for the one-pot conversion of carbohydrates into 5-ethoxymethylfurfural. Green Chem. 2013;15(9):2379.

29. Yang Y, Abu-Omar MM, Hu C. Heteropolyacid catalyzed conversion of fructose, sucrose, and inulin to 5-ethoxymethylfurfural, a liquid biofuel candidate. Applied Energy. 2012 Nov;99:80–4.

30. Bing L, Zhang Z, Deng K. Efficient One-Pot Synthesis of 5-(Ethoxymethyl)furfural from Fructose Catalyzed by a Novel Solid Catalyst. Ind Eng Chem Res. 2012 Nov 28;51(47):15331–6.

31. Kraus GA, Guney T. A direct synthesis of 5-alkoxymethylfurfural ethers from fructose via sulfonic acid-functionalized ionic liquids. Green Chem. 2012;14(6):1593.

32. Che P, Lu F, Zhang J, Huang Y, Nie X, Gao J, et al. Catalytic selective etherification of hydroxyl groups in 5-hydroxymethylfurfural over H4SiW12O40/MCM-41 nanospheres for liquid fuel production. Bioresource Technology. 2012 Sep;119:433–6.

33. Dutta S, De S, Alam MdI, Abu-Omar MM, Saha B. Direct conversion of cellulose and lignocellulosic biomass into chemicals and biofuel with metal chloride catalysts. Journal of Catalysis. 2012 Apr;288:8–15.

34. Liu B, Zhang Z, Zhao ZK. Microwave-assisted catalytic conversion of cellulose into 5-hydroxymethylfurfural in ionic liquids. Chemical Engineering Journal. 2013 Jan;215–216:517–21.

35. Cao Q, Liang W, Guan J, Wang L, Qu Q, Zhang X, et al. Catalytic synthesis of 2,5-bis-methoxymethylfuran: A promising cetane number improver for diesel. Applied Catalysis A: General. 2014 Jul;481:49–53.

36. Balakrishnan M, Sacia ER, Bell AT. Etherification and reductive etherification of 5-(hydroxymethyl)furfural: 5-(alkoxymethyl)furfurals and 2,5-bis(alkoxymethyl)furans as potential bio-diesel candidates. Green Chem. 2012;14(6):1626.

37. Han J, Kim YH, Jung B, Hwang S, Jegal J, Kim J, et al. Highly Selective Catalytic Hydrogenation and Etherification of 5-Hydroxymethyl-2-furaldehyde to 2,5-

Bis(alkoxymethyl)furans for Potential Biodiesel Production. Synlett. 2017 Oct;28(17):2299–302.

38. Wei J, Cao X, Wang T, Liu H, Tang X, Zeng X, et al. Catalytic transfer hydrogenation of biomass-derived 5-hydroxymethylfurfural into 2,5-bis(hydroxymethyl)furan over tunable Zr-based bimetallic catalysts. Catal Sci Technol. 2018;8(17):4474–84.

39. Musolino M, Ginés-Molina MJ, Moreno-Tost R, Aricò F. Purolite-Catalyzed Etherification of 2,5-Bis(hydroxymethyl)furan: A Systematic Study. ACS Sustainable Chem Eng. 2019 Jun 17;7(12):10221–6.

40. Wei J, Wang T, Liu H, Li M, Tang X, Sun Y, et al. Highly Efficient Reductive Etherification of 5-Hydroxymethylfurfural to 2,5-Bis(Alkoxymethyl)Furans as Biodiesel Components over Zr-SBA Catalyst. Energy Tech. 2019 May;7(5):1801071.

41. Chen PX, Tang Y, Zhang B, Liu R, Marcone MF, Li X, et al. 5-Hydroxymethyl-2-furfural and Derivatives Formed during Acid Hydrolysis of Conjugated and Bound Phenolics in Plant Foods and the Effects on Phenolic Content and Antioxidant Capacity. J Agric Food Chem. 2014 May 21;62(20):4754–61.

42. Bicker M, Hirth J, Vogel H. Dehydration of fructose to 5-hydroxymethylfurfural in sub- and supercritical acetone. Green Chem. 2003 Apr 8;5(2):280–4.

43. Zhu H, Cao Q, Li C, Mu X. Acidic resin-catalysed conversion of fructose into furan derivatives in low boiling point solvents. Carbohydrate Research. 2011 Sep;346(13):2016–8.

44. Yang F, Zhang S, Zhang ZC, Mao J, Li S, Yin J, et al. A biodiesel additive: etherification of 5-hydroxymethylfurfural with isobutene to tert-butoxymethylfurfural.

Catal Sci Technol. 2015;5(9):4602–12.

45. Sarin R, Kumar R, Srivastav B, Puri SK, Tuli DK, Malhotra RK, et al. Biodiesel surrogates: achieving performance demands. Bioresour Technol. 2009 Jun;100(12):3022–8.

46. Gupta M, Kumar N. Scope and opportunities of using glycerol as an energy source. Renewable and Sustainable Energy Reviews. 2012 Sep;16(7):4551–6.

47. Luo J, Yu J, Gorte RJ, Mahmoud E, Vlachos DG, Smith MA. The effect of oxide acidity on HMF etherification. Catal Sci Technol. 2014;4(9):3074–81.

48. Salminen E, Kumar N, Virtanen P, Tenho M, Mäki-Arvela P, Mikkola JP. Etherification of 5-Hydroxymethylfurfural to a Biodiesel Component Over Ionic Liquid Modified Zeolites. Top Catal. 2013 Jun;56(9–10):765–9.

49. Arias KS, Climent MJ, Corma A, Iborra S. Biomass-derived chemicals: synthesis of biodegradable surfactant ether molecules from hydroxymethylfurfural. ChemSusChem. 2014 Jan;7(1):210–20.

50. Rajoka MI, Malik KA. Cellulase production by Cellulomonas biazotea cultured in media containing different cellulosic substrates. Bioresource Technology. 1997 Jan;59(1):21–7.

51. Jadhav AH, Chinnappan A, Patil RH, Kostjuk SV, Kim H. Green chemical conversion of fructose into 5-hydroxymethylfurfural (HMF) using unsymmetrical dicationic ionic liquids under mild reaction condition. Chemical Engineering Journal. 2014 May;243:92–8.

52. Wang H, Kong Q, Wang Y, Deng T, Chen C, Hou X, et al. Graphene Oxide Catalyzed

Dehydration of Fructose into 5-Hydroxymethylfurfural with Isopropanol as Cosolvent. ChemCatChem. 2014 Mar;6(3):728–32.

53. Yong G, Zhang Y, Ying JY. Efficient catalytic system for the selective production of 5-hydroxymethylfurfural from glucose and fructose. Angew Chem Int Ed Engl. 2008;47(48):9345–8.

54. Hu S, Zhang Z, Song J, Zhou Y, Han B. Efficient conversion of glucose into 5-hydroxymethylfurfural catalyzed by a common Lewis acid SnCl4 in an ionic liquid. Green Chem. 2009;11(11):1746.

55. Zhang X, Murria P, Jiang Y, Xiao W, Kenttämaa HI, Abu-Omar MM, et al. Maleic acid and aluminum chloride catalyzed conversion of glucose to 5-(hydroxymethyl) furfural and levulinic acid in aqueous media. Green Chem. 2016;18(19):5219–29.

56. Jadhav AH, Kim H, Hwang IT. An efficient and heterogeneous recyclable silicotungstic acid with modified acid sites as a catalyst for conversion of fructose and sucrose into 5-hydroxymethylfurfural in superheated water. Bioresour Technol. 2013 Mar;132:342–50.

57. Kreissl HT, Nakagawa K, Peng YK, Koito Y, Zheng J, Tsang SCE. Niobium oxides: Correlation of acidity with structure and catalytic performance in sucrose conversion to 5-hydroxymethylfurfural. Journal of Catalysis. 2016 Jun;338:329–39.

58. Hu L, Wu Z, Xu J, Sun Y, Lin L, Liu S. Zeolite-promoted transformation of glucose into 5-hydroxymethylfurfural in ionic liquid. Chemical Engineering Journal. 2014 May;244:137–44.

59. Nikolla E, Román-Leshkov Y, Moliner M, Davis ME. "One-Pot" Synthesis of 5-

(Hydroxymethyl)furfural from Carbohydrates using Tin-Beta Zeolite. ACS Catal. 2011 Apr 1;1(4):408–10.

60. Yang Y, Xiang X, Tong D, Hu C, Abu-Omar MM. One-pot synthesis of 5-hydroxymethylfurfural directly from starch over SO(4)(2-)/ZrO2-Al2O3 solid catalyst. Bioresour Technol. 2012 Jul;116:302–6.

61. Roy Goswami S, Dumont MJ, Raghavan V. Microwave Assisted Synthesis of 5-Hydroxymethylfurfural from Starch in AlCl $_3$ ·6H $_2$ O/DMSO/[BMIM]Cl System. Ind Eng Chem Res. 2016 Apr 27;55(16):4473–81.

62. Zhi Z, Li N, Qiao Y, Zheng X, Wang H, Lu X. Kinetic study of levulinic acid production from corn stalk at relatively high temperature using FeCl3 as catalyst: A simplified model evaluated. Industrial Crops and Products. 2015 Dec;76:672–80.

63. Liu H, Tang X, Hao W, Zeng X, Sun Y, Lei T, et al. One-pot tandem conversion of fructose into biofuel components with in-situ generated catalyst system. Journal of Energy Chemistry. 2018 Mar;27(2):375–80.

64. Wei J, Wang T, Cao X, Liu H, Tang X, Sun Y, et al. A flexible Cu-based catalyst system for the transformation of fructose to furanyl ethers as potential bio-fuels. Applied Catalysis B: Environmental. 2019 Dec;258:117793.

65. Nguyen H, Xiao N, Daniels S, Marcella N, Timoshenko J, Frenkel A, et al. Role of Lewis and Brønsted Acidity in Metal Chloride Catalysis in Organic Media: Reductive Etherification of Furanics. ACS Catal. 2017 Oct 6;7(10):7363–70.

66. Sacia ER, Balakrishnan M, Bell AT. Biomass conversion to diesel via the etherification of furanyl alcohols catalyzed by Amberlyst-15. Journal of Catalysis.

2014 May;313:70–9.

67. Fang W, Hu H, Ma Z, Wang L, Zhang Y. Two Possible Side Reaction Pathways during Furanic Etherification. Catalysts. 2018 Sep 8;8(9):383.

68. Hu H, Hu D, Jin H, Zhang P, Li G, Zhou H, et al. Efficient Production of Furanic Diether in a Continuous Fixed Bed Reactor. ChemCatChem. 2019 Apr 18;11(8):2179–86.

69. Gupta D, Saha B. Dual acidic titania carbocatalyst for cascade reaction of sugar to etherified fuel additives. Catalysis Communications. 2018 May;110:46–50.

70. Fang W, Hu H, Dong P, Ma Z, He Y, Wang L, et al. Improvement of furanic diether selectivity by adjusting Brønsted and Lewis acidity. Applied Catalysis A: General. 2018 Sep;565:146–51.

71. Wu D, Hernández WY, Zhang S, Vovk EI, Zhou X, Yang Y, et al. In Situ Generation of Brønsted Acidity in the Pd-I Bifunctional Catalysts for Selective Reductive Etherification of Carbonyl Compounds under Mild Conditions. ACS Catal. 2019 Apr 5;9(4):2940–8.

72. Li XL, Zhang K, Chen SY, Li C, Li F, Xu HJ, et al. A cobalt catalyst for reductive etherification of 5-hydroxymethyl-furfural to 2,5-bis(methoxymethyl)furan under mild conditions. Green Chem. 2018;20(5):1095–105.

73. Noyori R, Hashiguchi S. Asymmetric Transfer Hydrogenation Catalyzed by Chiral Ruthenium Complexes. Acc Chem Res. 1997 Feb 1;30(2):97–102.

74. Ikariya T, Blacker AJ. Asymmetric Transfer Hydrogenation of Ketones with Bifunctional Transition Metal-Based Molecular Catalysts. Acc Chem Res. 2007 Dec

1;40(12):1300–8.

75. Wang D, Astruc D. The golden age of transfer hydrogenation. Chem Rev. 2015 Jul 8;115(13):6621–86.

76. Osatiashtiani A, Lee AF, Wilson K. Recent advances in the production of γ-valerolactone from biomass-derived feedstocks via heterogeneous catalytic transfer hydrogenation: Recent advances in γ-valerolactone production. J Chem Technol Biotechnol. 2017 Jun;92(6):1125–35.

77. Xue Z, Jiang J, Li G, Zhao W, Wang J, Mu T. Zirconium–cyanuric acid coordination polymer: highly efficient catalyst for conversion of levulinic acid to γ-valerolactone. Catal Sci Technol. 2016;6(14):5374–9.

78. Leng Y, Shi L, Du S, Jiang J, Jiang P. A tannin-derived zirconium-containing porous hybrid for efficient Meerwein–Ponndorf–Verley reduction under mild conditions. Green Chem. 2020;22(1):180–6.

79. Zhou S, Dai F, Xiang Z, Song T, Liu D, Lu F, et al. Zirconium–lignosulfonate polyphenolic polymer for highly efficient hydrogen transfer of biomass-derived oxygenates under mild conditions. Applied Catalysis B: Environmental. 2019 Jul;248:31–43.

80. Rojas-Buzo S, García-García P, Corma A. Catalytic Transfer Hydrogenation of Biomass-Derived Carbonyls over Hafnium-Based Metal-Organic Frameworks. ChemSusChem. 2018 Jan 23;11(2):432–8.

81. Li H, He J, Riisager A, Saravanamurugan S, Song B, Yang S. Acid–Base Bifunctional Zirconium *N* -Alkyltriphosphate Nanohybrid for Hydrogen Transfer of Biomass-

Derived Carboxides. ACS Catal. 2016 Nov 4;6(11):7722–7.

82. Hu L, Li N, Dai X, Guo Y, Jiang Y, He A, et al. Highly efficient production of 2,5-dihydroxymethylfuran from biomass-derived 5-hydroxymethylfurfural over an amorphous and mesoporous zirconium phosphonate catalyst. Journal of Energy Chemistry. 2019 Oct;37:82–92.

83. Hu L, Dai X, Li N, Tang X, Jiang Y. Highly selective hydrogenation of biomass-derived 5-hydroxymethylfurfural into 2,5-bis(hydroxymethyl)furan over an acid–base bifunctional hafnium-based coordination polymer catalyst. Sustainable Energy Fuels. 2019;3(4):1033–41.

84. Hu L, Li T, Xu J, He A, Tang X, Chu X, et al. Catalytic transfer hydrogenation of biomass-derived 5-hydroxymethylfurfural into 2,5-dihydroxymethylfuran over magnetic zirconium-based coordination polymer. Chemical Engineering Journal. 2018 Nov;352:110–9.

85. Hu D, Hu H, Jin H, Zhang P, Hu Y, Ying S, et al. Building hierarchical zeolite structure by post-synthesis treatment to promote the conversion of furanic molecules into biofuels. Applied Catalysis A: General. 2020 Jan;590:117338.

86. Jae J, Mahmoud E, Lobo RF, Vlachos DG. Cascade of Liquid-Phase Catalytic Transfer Hydrogenation and Etherification of 5-Hydroxymethylfurfural to Potential Biodiesel Components over Lewis Acid Zeolites. ChemCatChem. 2014 Feb;6(2):508–13.

87. Shinde S, Rode C. Cascade Reductive Etherification of Bioderived Aldehydes over Zr-Based Catalysts. ChemSusChem. 2017 Oct 23;10(20):4090–101.

88. Rana SP, Rana PH. One-pot reductive etherification of 5-hydroxymethylfurfural into

biofuel (2,5-bis(propoxymethyl) furan (BPMF)) using mixed catalyst $ZrO(OH)_2$ and Zr-Hβ. New J Chem. 2023;47(2):891–9.

89. He A, Gu Q, Shen X, Zheng J, Hu L, Wang X, et al. One-pot reductive etherification of biomass-derived 5-hydroxymethylfurfural to 2,5-bis(isopropoxymethyl)furan over a sulfonic acid-functionalized zirconium-based coordination catalyst. Green Chem. 2023;25(6):2349–60.

90. Van Der Waal JC, Kunkeler PJ, Tan K, Van Bekkum H. Zeolite Titanium Beta. Journal of Catalysis. 1998 Jan;173(1):74–83.

91. Tang X, Wei J, Ding N, Sun Y, Zeng X, Hu L, et al. Chemoselective hydrogenation of biomass derived 5-hydroxymethylfurfural to diols: Key intermediates for sustainable chemicals, materials and fuels. Renewable and Sustainable Energy Reviews. 2017 Sep;77:287–96.

92. Hu L, Yang M, Xu N, Xu J, Zhou S, Chu X, et al. Selective transformation of biomass-derived 5-hydroxymethylfurfural into 2,5-dihydroxymethylfuran via catalytic transfer hydrogenation over magnetic zirconium hydroxides. Korean J Chem Eng. 2018 Jan;35(1):99–109.

93. Lawrance Bragg. The crystalline state. New York: McMillan; 1949.

94. S.R. Stock, B.D. Cullity. Elements of X-Ray Diffraction. 3rd edition. Pentice Hall; 2001.

95. Biz S, Occelli ML. Synthesis and Characterization of Mesostructured Materials. Catalysis Reviews. 1998 Aug;40(3):329–407.

CHAPTER – 3

Catalytic conversion of 5-HydroxyMethylFurfural (5-HMF) into valuable chemicals

3.1. Introduction

Petroleum refinery and petrochemical industry is having significant role in human life as it plays vital role to provide energy and food and affect the environment. As the population of the world increases it is expected that demand will increase significantly by next decade (1–4). The massive use of fossil fuel resources has resulted in a slew of issues such as reserve depletion, price volatility, and environmental concerns (5–7). In this regard, exploration of renewable resources as an alternative of fossil fuel has been become urgent needs(8–10). Biomass is a renewable carbon resource obtained from plants, crop wastes, and industrial residues. It can be converted into valuable compounds like 5-hydroxymethylfurfural (HMF) through chemical or biocatalytic processes. HMF, derived from various hexoses, is a key platform molecule for producing numerous high-value derivatives used in pharmaceuticals, materials, and fuels, which makes them important source for sustainable development of valuable chemicals(11–13). Hence, conversion of biomass derived platform molecules into valuable chemical and derivatives is the most attractive approach(14,15). Bio refinery is emerged as viable route to maximize the use of biomass. Biomass-derived chemicals, such as 5-hydroxymethylfurfural (5-HMF), levulinic acid, furfurals, sugar alcohols, lactic acid, succinic acid, and phenols, are considered platform chemicals. These platform chemicals can be further used for the production of a variety of important chemicals on an industrial scale(16–18). Various transformation method of lignocellulosic biomass to platform chemicals such as 5-hydroxymethylfurfural (HMF), which can be converted further to polymer building blocks and potential biofuel

49

candidates, have been reported recently. The U.S. Department of Energy has identified 12 representative biomass platform molecules, including HMF. So, manufacturing of biofuels from HMF is particularly gaining thrust. Biomass-derived furans, like 2-furfuraldehyde (furfural) and 5-hydroxymethyl-2-furfural (HMF), can be produced efficiently via acid-catalyzed dehydration of pentose and hexose, respectively. Due to the reactive side chains (–CHO and/or –CH$_2$OH) on the furan ring, these compounds can be further processed into valuable chemicals, including 2,5-furandicarboxylic acid (FDCA), 2-furoic acid, levulinic acid (LA), various ketones and diketones, 1,6-hexanediol (1,6-HDO), 1-hydroxyhexane-2,5-dione (1-HHD), cyclopentanone (CPO), adipic acid, maleic anhydride (MA), caprolactam, caprolactone, γ-valerolactone, 2,5-dimethylfuran (DMF), and various alkanes. These chemicals have extensive applications in pharmaceutical and polymer industries and in fuel production. 2, 5-dihydroxymethylfuran (DHMF) is formed *via* hydrogenation of aldehyde group present in 5-HMF. The catalytic transfer hydrogenation (CTH) is favourable alternative to conventional hydrogenation pathway with external molecular H$_2$. Specifically, carbonyl compounds, including aldehydes and ketones can be completely reduced to corresponding alcohols through the Meerwein−Ponndorf− Verley (MPV) reaction by using formic acid and alcohols as hydrogen donors (19–23). Beside the various biomass derived liquid fuel such as 2, 5-dimethylfuran (DMF) (24–33) and AMFs (MMF and 5-ethoxymethylfurfural (EMF)) (34–43) 2, 5 Bis-alkoxymethyl furans (BAMFs) are specifically draw more attention because of its superior properties as biofuel. In comparison with 5- alkoxymethyl furfurals (AMFs) and bioethanol, BAMFs hold properties such as higher energy density (more than 31 MJ/L), higher boiling point, stronger chemical stability, lower water solubility, higher flashing point , lower cold filter plugging point and higher cetane number to the ordinary commercial diesels (44,45). As cetane number (80) of 2, 5 Bis-alkoxymethyl furans are higher than commercial diesel

(45), it can be mix with diesels in different propositions which enhance the combustion and reduce the emissions. So, BAMFs are widely considered as potential biodiesel candidates or fuel additives with great application prospects. Since 2,5-bis(alkoxymethyl)furan (BAMF) exhibits properties like higher energy density, higher cetane number, higher miscibility, and stronger stability, it has been assessed as a more attractive diesel additive than 5- alkoxymethylfurfural (AMF)(37,46–50). Similar to the preparation of AMF from HMF(35,51–60), BAMF can be produced by the etherification of DHMF with the corresponding alcohols in the presence of various heterogeneous catalysts for this conversion (Table 3.1).

Table 3.1 Transformation of HMF to BAMF using various alcohols

Catalyst	Alcohol	Temperature (°C)	Time ,h	HMF Conversion (%)	BAMF Yield (%)	Reference
HZSM-5 (Si/Al=25)	Methanol	100	3	100	70	(61)
HZSM-5 (Si/Al=38)	Methanol	100	3	100	68	
HZSM-5 (Si/Al=300)	Methanol	100	3	100	69	
HZSM-5 (Si/Al=25)	Methanol	120	12	-	68	
HZSM-5 (Si/Al=25)	Methanol	140	8	-	59	
Amberlyst-15	Methanol	60	10	99	57	(47)

Amberlyst-15	Methanol	60	10	-	50	
Amberlyst-15	Ethanol	40	16	-	80	(62)
Amberlyst-15	Ethanol	60	5	-	74	
Amberlyst-15	Ethanol	60	18	-	64	(47)
Amberlyst-15	Ethanol	60	10	99	70	
Sn-Beta	Ethanol	60	10	-	70	
Hf-Beta	Ethanol	180	6	-	68	(50)
Amberlyst-15	Propanol	120	24	-	67	(63)
Amberlyst-15	Propanol	60	10	-	74	(47)
Sn-Beta	Isopropanol	60	10	-	72	
Sn-Beta	Isopropanol	180	6	-	61	(50)
Zr-Mont	Isopropanol	180	3	-	82.5	(48)
Sn-Beta	Isopropanol	150	1	-	95	(49)
Amberlyst-15	1-butabol	180	3	-	85.6	(50)
Amberlyst-15	1-butanol	180	6	-	79.6	

Zr-Mont	1-butanol	60	10	-	74	(47)
Sn-Beta	1-butanol	60	10	-	71	
Zr-Mont	2-butanol	150	3	-	49	(49)
Sn-Beta	2-butanol	180	6	-	60.5	(50)
Hf-Beta	2-butanol	120	1	-	96	(49)

Balakrishnan et al.(62) first reported the etherification of DHMF with ethanol. The results demonstrated that among various acid catalysts, such as H_2SO_4, Amberlyst-15, Amberlite IR120, Dowex 50WX8, and Dowex DR2030, Amberlyst-15 showed an outstanding catalytic performance with an 80% yield of 2,5- bis(ethoxymethyl)furan (BEMF) at a low reaction temperature of 40 °C for 16 h, which was in harmony with the results of Sacia et al.(46). More significantly, Amberlyst-15 could also be employed for the efficient preparation of 2,5 bis- (propoxymethyl)furan (BPMF) and 2,5-bis(butoxymethyl)-furan (BBMF) via the etherification of DHMF with propanol and 1-butanol, respectively. However, when methanol is used for etherification of DHMF, the catalytic performance of Amberlyst-15 was not satisfactory, and the yield of 2,5-bis(methoxymethyl)furan (BMMF) was only 57% at 60 °C in 10 h, which might be attributed to the high polarity of methanol, leading to the formation of many by-products (47). By this instant, Cao et al. (61) used acidic zeolites to obtain a satisfactory yield of BMMF. It was found that amongst various acidic zeolites, HZSM-5 with a Si/Al ratio of 25 was the most effective for the etherification of DHMF with methanol. After 3 h at 100 °C, a BMMF yield of 70% could be achieved, this was higher than that over HZSM-5 with a Si/Al ratio of 38 or 300. Lower Si/Al ratio of the zeolite means more acidic sites and stronger hydrophilicities, which facilitated the etherification reaction between DHMF and methanol on the surface of the catalyst (61). Above results conclude that the types of alcohol as well as properties of

catalyst have pronounced effect on the etherification of DHMF into BAMF. In addition, it should be particularly noted that various BAMFs could also be directly produced from HMF in the corresponding alcohols (Table 3.1)(46–50,63) in which two successive steps were involved in the same reactor: the selective hydrogenation of HMF into DHMF over a hydrogenation catalyst and the subsequent etherification of DHMF into BAMF over an acid catalyst. The yield of BAMF did not decrease, according to the results. Therefore, from the perspective of practical manufacturing, this one-pot, two-step method was more suitable for the preparation of BAMF. It is clear from the research cited above that the catalytic conversion of 5-HMF into useful compounds also depends on the supports in the catalytic system. A key factor in improving the conversion of 5-HMF and the selectivity of the intended products is the adjustment of acidic sites like Lewis and Bronsted.

Investigating the effects of different zeolites as a support for Zr metal particles in the catalytic conversion of 5-HMF and the variables influencing it is the goal of the current work. 5-HMF and 2-propanol are used in the tests, along with the impact of temperature, reaction time, and catalyst loading.

3.2. Materials and Methods

3.2.1. Materials

The chemicals obtained were used as received. 5- (hydroxymethyl) furfural (98%), were purchased from SRL(Sisco Research Laboratories Pvt. Ltd.) India. All the alcohols and solvents, Aq. ammonia (30%), $ZrOCl_2.8H_2O$ and metal precursors such as Zirconyl Nitrate Hydrate (99.5%) were purchased from Loba Chemie, Mumbai, India., Hβ zeolite, Hγ zeolite and ZSM-5 was purchased from the Sud-cheme India Private Limited, Vadodara, Gujarat.

3.2.2. Catalyst Preparation

3.2.2.1. Preparation of ZrO(OH)$_2$

The hydroxide of Zr was prepared by precipitation process as described elsewhere(64). In a typical preparation, 10 g of metal chloride precursors were precipitated to respective hydroxide by adding of aq. NH$_3$ upto pH of the solution was 9-10. Mixture was aged in 24 h, filtered and washed residue with plenty of distilled water until pH of the filtrate was neutral. Residue was subsequently dried at 110 °C in 12 h, followed by being ground to powder in a mortar with a pestle and stored in a glass bottle.

3.2.2.2. Preparation of Zr supported on zeolite

Zirconium (IV) nitrate hydrate metals were impregnated into the structure of zeoltie using a typical wet impregnation method(65). To prepare Zr-impregnated zeolite, 4.05 g zirconium (IV) oxynitrate hydrate was dissolved into 20 mL deionised water. After all zirconium (IV) nitrate salt dissolved, 16 g of zeolite was added to the aqueous solution. The mixture was then kept at room temperature overnight for impregnation. After impregnation, the dried solid particles dried at 120°C in 4 h before being calcined at 550°C in 6h with heating rate of 10°C min^{-1}.

3.2.3. Catalyst Characterization

Powder X-ray diffraction (PXRD) patterns were obtained on a Bruker D8 Advance X-ray diffractometer, using LynxEye Superspeed detector and Cu Kα radiation produced from a PW Bragg–Brentano (BB) goniometer (θ/2θ), operating at 40 kV and 35 mA. The diffractograms were recorded in the 2θ range of 10 - 80° with a 2θ step size of 0.02°.

The Brunauer–Emmett–Teller (BET) surface area, pore volume, and Barrett–Joyner–Halenda (BJH) pore size distribution of the prepared catalysts were determined by N$_2$ adsorption-desorption analysis conducted at −196°C. Prior to analysis, the catalysts were degassed under vacuum at 200 ± 2^oC.

Fourier Transform Infrared Spectroscopy (FTIR) spectra of catalyst samples were collected using Model: Cary630 spectrometer. The instrument was operated in the range of 600-4000 cm^{-1}.

3.3. Catalytic Reaction

The experiment was conducted in 100 mL stainless steel autoclave reactor. The autoclave was charged with 1 g HMF, 0.1- 0.25g catalyst, and 50 mL of 2-propanol. The autoclave was closed then heated to the desired reaction temperature of 120-140°C under stirring conditions in 4 h reaction time. Stirring was kept constant (550 rpm) for the reactions. After each reaction, the autoclave was cooled. At the end of each run, the product mixture was separated from the catalyst by centrifuge and then analyzed by GC MS (make: Shimadzu, model: QP2020 NX) equipped using DB-1701 column (60M x 0.32mm x 1.µm film thickness).Cyanopropylphenyl (14%), Dimethylpolysiloxane (86%).

Column temperatures:	
Initial temperature	: 50°C
Initial hold time	: 0 minute
Heating rate-I	: 10°C/minute
Temperature-II	: 180°C
Hold time-II	: 0 minute
Heating rate -II	: 20°C/ minute
Final temperature	: 280°C
Final hold	: 17.0 minute
Injection port temperature	: 250°C
Carrier gas	: Helium
Pressure programme	
Initial Head pressure	: 5Kpa
Initial Hold time	: 11.0 minute
Pressure rate	: 10Kpa/minute
Final pressure	: 80Kpa/minute
Final Hold time	: 16.5 minute
Split ratio	: 1:10
Run time	: 35.0 minute
GCMS Programme:	
Source	: Electron Ionization (EI)
Mode	: Scan (TIC)
Ion source temperature	: 230°C
Interface temperature	: 290°C

Filament of time	: 0.0minute
Filament on time	: 8.5 minute
Start m/z	: 30
End m/z	: 500
Detector gain mode	: Absolute
Start time	: 8.5 minute
End time	: 35.0 minute

To find the performance of the catalytic systems, conversions of 5-HMF ($X_{5\text{-HMF}}$, %) and selectivity to products (Si) are defined as follow: 5-HMF conversion ($X_{5\text{-HMF}}$) was calculated from ratio of the amount of 5-HMF converted and initial amount of 5-HMF. The selectivities for reaction products like BHMF, HPMF, and BPMF (Si) were calculated by dividing the amount of products formed by the amount of 5-HMF converted.

$$\text{conversion (\%)} = \frac{(I.N.)_i - (I.N.)_f}{(I.N.)_i} * 100 \ ,$$

where (I.N.)i = Initial moles of 5-HMF & (I.N.)f = Final moles of 5-HMF

$$\text{Selectivity (\%)} = \frac{\text{moles of product formed}}{\text{moles of 5-HMF converted}} * \ 100$$

3.4. Results and discussion

3.4.1. Physical and chemical properties of catalyst

3.4.1.1. Powder X-ray diffraction (PXRD) analysis

Figure 3.1 (a) shows PXRD patterns of $ZrO(OH)_2$. The wide and weak PXRD pattern (diffraction angle at 2θ = 21.7°, 26.69°, 27.81°, 31.26°,39.63°,41.20°,44.23°,50°) of $ZrO(OH)_2$ is indicating the amorphous nature of $ZrO(OH)_2$. From Figure 3.1 (c) , it can be seen that the PXRD peaks for the Zr-Hβ catalysts were very similar to those of Hβ (Figure 3.1 (b)) as indicated by the diffraction angle at 2θ = 22.6°, 25.98°, 28.08°,31.26° and, 50°. No new diffraction peak was observed which suggested that the MFI structure of Hβ catalyst was intact and no new phase was produced after the modification of Hβ catalyst

and Zr were nicely dispersed(66). The diffractions at 31.26 and 50, due to tetragonal zirconia phase (67,68) were clearly observed on the Zr-Hβ catalyst sample.
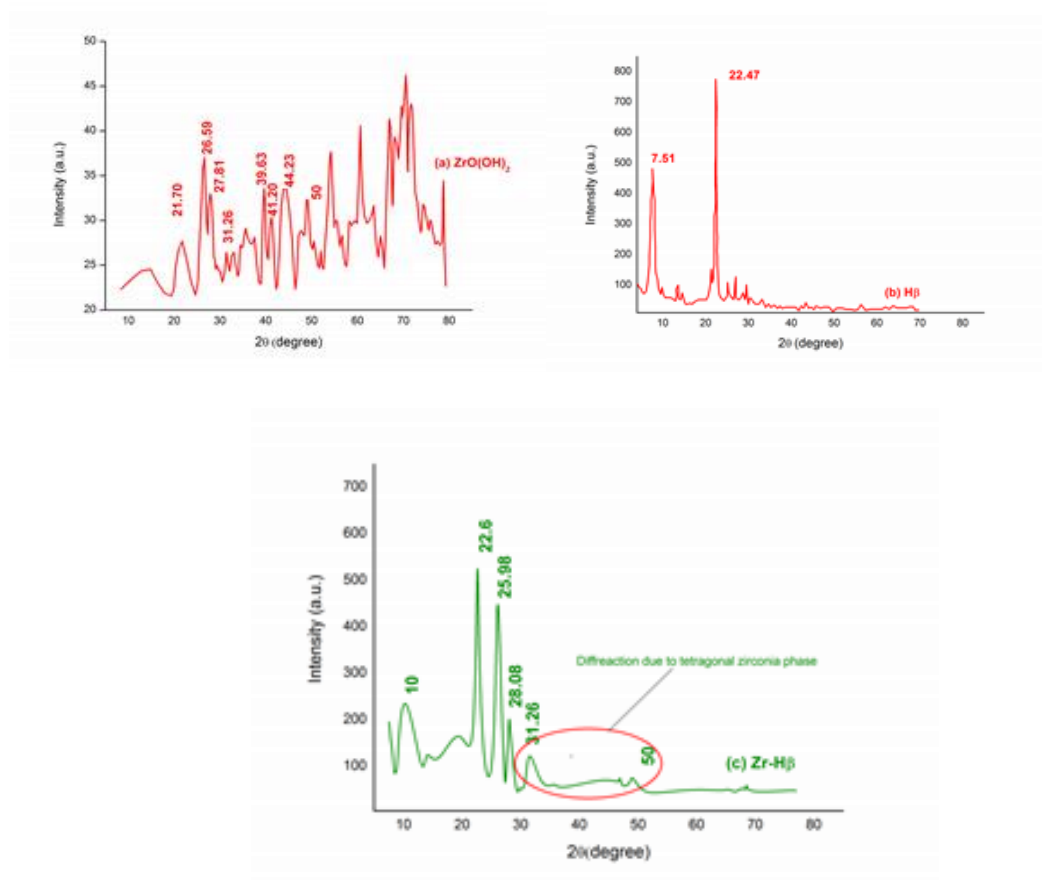
Figure 3.1 PXRD patterns of (a) ZrO(OH)$_2$ (b) Hβ and (c) Zr-Hβ catalysts

The PXRD patterns of Zr-Y catalysts (Figure 3.2) shows similar pattern to that of the parent HY(69–71) as indicated by the diffraction angle at $2\theta = 15.8°$ and $23.1°$. This indicates the framework structure has been retained after Zr impregnation.
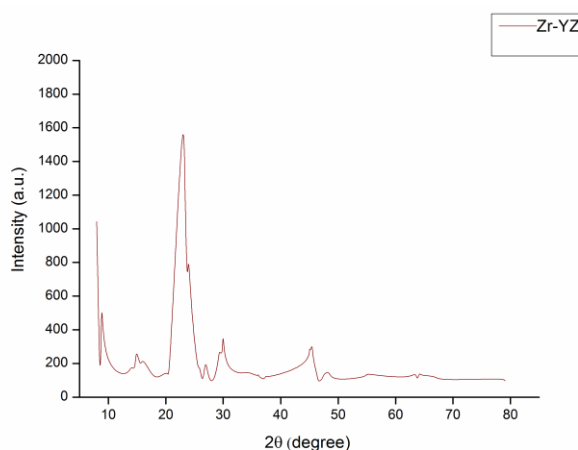
Figure 3.2 PXRD patterns of Zr-HY catalyst

The PXRD patterns of Zr-HZSM5 catalysts (Figure 3.3) shows similar pattern to that of the parent HZSM5(70) as indicated by the diffraction angle at 2θ = 14.2°,23.94°,26.16°,27.36°,29.94°and 31.74°.This indicates the framework structure has been retained after Zr impregnation.
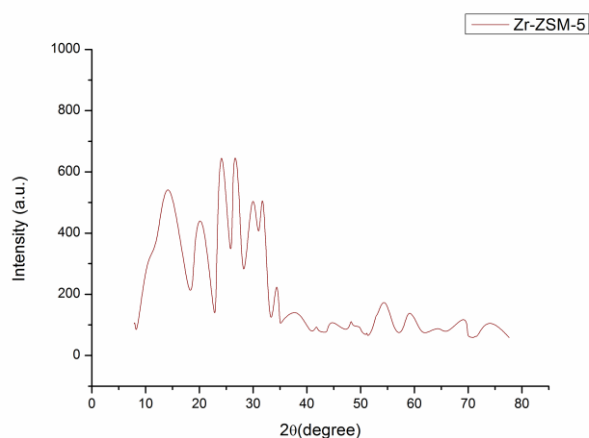
Figure 3.3 PXRD patterns of Zr-HZSM-5 catalyst

3.4.1.2. Fourier transforms infrared spectroscopy (FTIR)

Fourier transform infrared (FTIR) spectrum of $ZrO(OH)_2$ in the range of 400–4000 cm^{-1} is studied and shown in Figure 3.4 (a). The very broad absorption band at 3141 cm^{-1} is attributed to the stretching vibrations of OH groups on the surface of the catalyst. In the spectrum of $ZrO(OH)_2$, a sharp peak at 1441 cm^{-1} are assignable to Zr-OH vibrations. The

59

peak at 1634 cm^{-1} is due to OH vibration of ZrO(OH)$_2$. Zr-Hβ spectra (Figure 3.4 (b & c)) exhibit band in the region of 3735, 3641, 1625, 1229, 1083 and 562 cm^{-1} are due to bending of isolated terminal Si-OH groups, bending of bridging hydroxyl Si-OH-Al bending vibration of OH groups, asymmetrical stretching vibration, symmetric and asymmetric stretching vibrations of the Si–O–Si linkages of the zeolite framework and double ring opening vibration of external linkages, respectively. Zr precursor, causes a decrease in the intensity of OH bands at 3735 cm^{-1}, suggesting that Zr species could react with silanols located in the vacant sites and thus be incorporated into the Hβ zeolite framework (72). IR spectra of Zr-Y in Figure 3.5 shows Band at 1621 cm^{-1} reveals to bending vibration of water molecules in zeolite structure. bands around 1062 cm^{-1} indicates presence of Si-O and assigned to external asymmetrical stretching while the band at about 793 cm^{-1} associated with symmetric stretching modes of external linkages(69,73). Fourier transform infrared (FTIR) spectrum in Figure 3.6 of Zr-HZSM-5 shows IR bands around 734 and 1021 cm^{-1} can be allocated to the symmetric and asymmetric stretching vibrations of the Si–O–Si linkages of the zeolite framework, respectively. Vibration modes of 1021 and 734 cm^{-1} are consigned to the internal vibration of SiO$_4$ and AlO$_4$ tetrahedra and a small IR band near 1220 and 1632 cm^{-1} is attributed to their asymmetric stretching vibration and H-OH bending vibration of adsorbed water respectively .
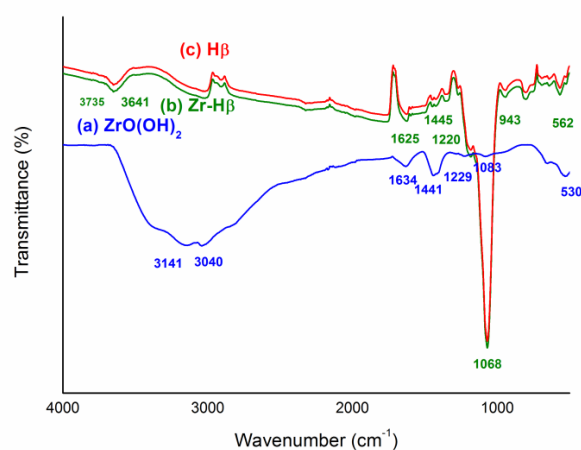
Figure 3.4 (a) FTIR spectra of ZrO(OH)$_2$ catalyst and (b) Zr-Hβ catalyst (c) Hβ catalyst
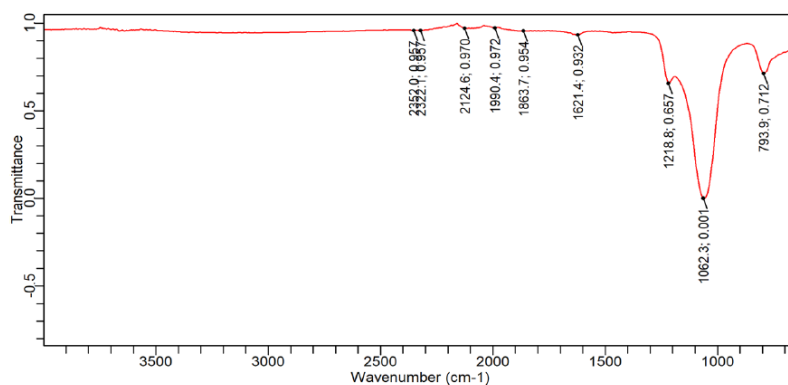
Figure 3.5 FTIR spectra of Zr-HY
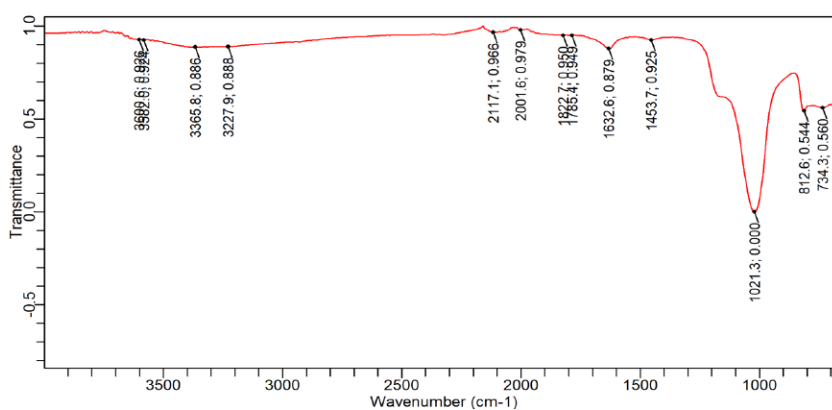
Figure 3.6 FTIR spectra of Zr-HSM-5

3.4.2. Study of catalyst activity

3.4.2.1. Effect of temperature and catalyst loading

Catalytic conversion of HMF was carried out at different temperatures (120°C, 130°C, and 140°C), time (2 h & 4 h), and catalyst loading (0.1 g) over a ZrO(OH)$_2$ (0.1 g) and mixture of Zr-Hβ (0.1 g, 0.15g, 0.2g, 0.25g), and the results are shown in Table 3.2. Conversion of the 5-HMF was found to be 23.53% and selectivity of BHMF and HPMF was found to be 83.55 and 17.67%, respectively, at 120°C (entry1) in 2 h and no BPMF was observed. By increasing the temperature to 130°C and 140°C (entry 2 and 3) and keeping all other reaction conditions the same, it was observed that the conversion of 5-HMF was increased to 29.42% and 57.12% respectively and the selectivity of BHMF was decreased to 76.43%

61

and 68.04%, respectively. Whereas the selectivity of HPMF increased and there was no generation of BPMF. The higher conversion of 5-HMF was achieved by increasing reaction time to 4 h and keeping all other parameters constant (entry 4, 5 and 6) and reaching a maximum of 71.32 % (entry 6). At a higher reaction time (4 h), a significant change in the selectivity of BHMF, HPMF and BPMF was observed (entry 4, 5, and 6). BHMF selectivity decreased to 9.89% (entry 6) from 21.98% (entry 4), and HPMF selectivity decreased to 37.60% (entry 6) from 68.57% (entry 4), while BPMF selectivity increased and was around 20.82% at higher reaction temperature of $140^{\circ}C$ (entry 6). This may be due to the conversion of HPMF to BPMF at higher reaction temperature and time. Shinde and Rode(49) reported a similar observation of higher reaction temperature for the production of BPMF using $ZrO(OH)_2$ as a catalyst. The lower yield and selectivity of BPMF, on the other hand, may be due to $ZrO(OH)_2$, which acts as a charge transfer hydrogenation catalyst. Further, to enhance the yield and selectivity of the desired product, Hβ and Zr-Hβ catalysts were tested at reaction conditions (entry 7 and 8), but the obtained results were not encouraging. However, the presence of BPMF in the product mixture indicated the impact of Zr-Hβ during the etherification step.

The results showed that $ZrO(OH)_2$ acts as a hydrogenation catalyst, whereas Zr-Hβ acts as an etherification catalyst in the reductive etherification of 5-HMF to BPMF. Hence, it was decided to carry out the reaction with a combined $ZrO(OH)_2$ and Zr-Hβ catalyst.

Alcohols can also be used as etherifying agents which leads to formation of BAMFs without using molecular H_2 (23-30). In present work, 2-propanol used as both hydrogen donors as well as substrate for the etherification. To check the effect of combined catalyst on 5-HMF conversion and BPMF selectivity, reaction was performed with equal weight of both catalysts (entry 9) at $120^{\circ}C$ in 4 h. It was observed that both 5-HMF conversion and

BPMF selectivity increased to 79.41 % and 38.50 % respectively, and this was higher than their individual results (entry 6 and 8).

We also tested the Zr-HY and Zr-HSM-5 (entry-10 & 11) with ZrO(OH)$_2$ (T=120°C in 4 h) with catalyst loading (0.1 g each) and found conversion of 5-HMF 64.76 % and 60.88% respectively. BPMF selectivity was measured at 35.40 % and 54.09 %respectively.

Also it was noted that using only ZrO(OH)$_2$ for etherification was ineffective because BPMF (targeted product) was not produced at all at different temperatures with a reaction time of 2 h. upon increase in reaction time to 4 h, results show that the selectivity of BPMF increases. In general, Lewis acid sites are mainly accountable to transfer hydrogenation through the Meerwein−Ponndorf−Verley (MPV) reaction, although Bronsted acid sites are responsible for the etherification step. Luo et al.(48) reported that the etherification reaction also can be recognized to excessive Lewis acid sites. Based on the product analysis (Table 3.2) in the reaction pathway of the one pot reductive etherification, the carbonyl in 5-HMF is initially hydrogenated to form BHMF in the presence of Lewis acid sites. Afterward BHMF can be etherified to HPMF and BPMF in 2-propanol over excessive Lewis or Bronsted acid sites.

Table 3.2 Catalytic activity of different Catalyst (Reaction conditions: 5-HMF – 1g, 2-propanol- 50 ml)

Entry	Catalyst	Catalyst quantity (g)	Temp (^{o}C)	Time (h)	Conv. %	Selectivity%		
						BHMF	HPMF	BPMF
1	ZrO(OH)$_2$	0.1	120	2	23.53	83.55	17.67	-
2		0.1	130	2	29.42	76.43	23.57	-
3		0.1	140	2	57.12	68.04	31.96	-
4		0.1	120	4	37.89	21.98	68.57	9.45

5		0.1	130	4	54.32	32.52	53.96	13.52
6		0.1	140	4	71.32	9.89	37.60	20.82
7	Hβ	0.1	120	2	10.00	-	3.04	6.86
8	Zr-Hβ	0.1	120	2	25.39	-	-	15.55
9	ZrO(OH)$_2$+ Zr-Hβ	0.1+0.1	120	4	79.41	0.46	7.25	38.50
10	ZrO(OH)$_2$+ Zr-HY	0.1+0.1	120	4	64.76	8.72	48.99	35.40
11	ZrO(OH)$_2$+ Zr-HZSM-5	0.1+0.1	120	4	60.88	-	45.90	54.09

3.5. Conclusions

Various catalysts Zr over different zeolite and ZrO(OH)$_2$ were synthesized by wet impregnation method and characterized by PXRD and FTIR. The characterization result indicates that no significant change was observed in structure of HZSM5, HY and Hβ. It remains intact after the impregnation of metal over zeolites. Presence of metal has also been confirmed by their characteristic peaks observed in the characterization. The lower yield and selectivity of BPMF, on the may be due to ZrO(OH)$_2$, which acts as a charge transfer hydrogenation catalyst. Higher conversion 79.41% of 5-HMF was achieved with Zr-Hβ catalyst, while 64.76% and 60.88% conversion towards 5-HMF was observed with Zr-HY and Zr-HSM-5 respectively.

In product distribution 2,5-bis(isopropoxymethyl)furan (BPMF) was remain main reaction product with selectivity 38.50 % for Zr-Hβ catalyst, while 35.4% and 54.09% selectivity towards BPMF was observed and with Zr-HY and Zr-HSM-5 respectively.

3.6. References

1. Huber GW, Iborra S, Corma A. Synthesis of Transportation Fuels from Biomass: Chemistry, Catalysts, and Engineering. Chem Rev. 2006 Sep 1;106(9):4044–98.

2. Alonso DM, Wettstein SG, Dumesic JA. Gamma-valerolactone, a sustainable platform molecule derived from lignocellulosic biomass. Green Chem. 2013;15(3):584.

3. Rorrer JE, Bell AT, Toste FD. Synthesis of Biomass-Derived Ethers for Use as Fuels and Lubricants. ChemSusChem. 2019 Jul 5;12(13):2835–58.

4. Serrano-Ruiz JC, Dumesic JA. Catalytic routes for the conversion of biomass into liquid hydrocarbon transportation fuels. Energy Environ Sci. 2011;4(1):83–99.

5. Zhou CH, Xia X, Lin CX, Tong DS, Beltramini J. Catalytic conversion of lignocellulosic biomass to fine chemicals and fuels. Chem Soc Rev. 2011;40(11):5588.

6. Zhang Z, Song J, Han B. Catalytic Transformation of Lignocellulose into Chemicals and Fuel Products in Ionic Liquids. Chem Rev. 2017 May 24;117(10):6834–80.

7. Hu L, Lin L, Wu Z, Zhou S, Liu S. Recent advances in catalytic transformation of biomass-derived 5-hydroxymethylfurfural into the innovative fuels and chemicals. Renewable and Sustainable Energy Reviews. 2017 Jul;74:230–57.

8. Tollefson J. Can the world kick its fossil-fuel addiction fast enough? Nature. 2018 Apr;556(7702):422–5.

9. Hu L, Zhao G, Hao W, Tang X, Sun Y, Lin L, et al. Catalytic conversion of biomass-derived carbohydrates into fuels and chemicals via furanic aldehydes. RSC Adv. 2012;2(30):11184.

10. Xu C, Arancon RAD, Labidi J, Luque R. Lignin depolymerisation strategies: towards valuable chemicals and fuels. Chem Soc Rev. 2014;43(22):7485–500.

11. Wang J, Xi J, Wang Y. Recent advances in the catalytic production of glucose from lignocellulosic biomass. Green Chem. 2015;17(2):737–51.

12. Zhang Z, Deng K. Recent Advances in the Catalytic Synthesis of 2,5-Furandicarboxylic Acid and Its Derivatives. ACS Catal. 2015 Nov 6;5(11):6529–44.

13. Liu B, Zhang Z. Catalytic Conversion of Biomass into Chemicals and Fuels over Magnetic Catalysts. ACS Catal. 2016 Jan 4;6(1):326–38.

14. Binder JB, Raines RT. Simple Chemical Transformation of Lignocellulosic Biomass into Furans for Fuels and Chemicals. J Am Chem Soc. 2009 Feb 11;131(5):1979–85.

15. Sheldon RA, Arends IWCE, Hanefeld U. Green Chemistry and Catalysis [Internet]. 1st ed. Wiley; 2007 [cited 2024 Feb 8]. Available from: https://onlinelibrary.wiley.com/doi/book/10.1002/9783527611003

16. Bozell JJ, Petersen GR. Technology development for the production of biobased products from biorefinery carbohydrates—the US Department of Energy's "Top 10" revisited. Green Chem. 2010;12(4):539.

17. Mika LT, Cséfalvay E, Németh Á. Catalytic Conversion of Carbohydrates to Initial Platform Chemicals: Chemistry and Sustainability. Chem Rev. 2018 Jan 24;118(2):505–613.

18. Mascal M, Dutta S. Chemical-Catalytic Approaches to the Production of Furfurals and Levulinates from Biomass. In: Nicholas KM, editor. Selective Catalysis for Renewable Feedstocks and Chemicals [Internet]. Cham: Springer International Publishing; 2014

[cited 2024 May 27]. p. 41–83. (Topics in Current Chemistry; vol. 353). Available from: https://link.springer.com/10.1007/128_2014_536

19. Noyori R, Hashiguchi S. Asymmetric Transfer Hydrogenation Catalyzed by Chiral Ruthenium Complexes. Acc Chem Res. 1997 Feb 1;30(2):97–102.

20. Ikariya T, Blacker AJ. Asymmetric Transfer Hydrogenation of Ketones with Bifunctional Transition Metal-Based Molecular Catalysts. Acc Chem Res. 2007 Dec 1;40(12):1300–8.

21. Wang D, Astruc D. The Golden Age of Transfer Hydrogenation. Chem Rev. 2015 Jul 8;115(13):6621–86.

22. Osatiashtiani A, Lee AF, Wilson K. Recent advances in the production of γ-valerolactone from biomass-derived feedstocks via heterogeneous catalytic transfer hydrogenation. J of Chemical Tech & Biotech. 2017 Jun;92(6):1125–35.

23. Xue Z, Jiang J, Li G, Zhao W, Wang J, Mu T. Zirconium–cyanuric acid coordination polymer: highly efficient catalyst for conversion of levulinic acid to γ-valerolactone. Catal Sci Technol. 2016;6(14):5374–9.

24. Román-Leshkov Y, Barrett CJ, Liu ZY, Dumesic JA. Production of dimethylfuran for liquid fuels from biomass-derived carbohydrates. Nature. 2007 Jun 21;447(7147):982–5.

25. Chidambaram M, Bell AT. A two-step approach for the catalytic conversion of glucose to 2,5-dimethylfuran in ionic liquids. Green Chem. 2010;12(7):1253.

26. Thananatthanachon T, Rauchfuss TB. Efficient Production of the Liquid Fuel 2,5-Dimethylfuran from Fructose Using Formic Acid as a Reagent. Angewandte Chemie

International Edition. 2010 Sep 3;49(37):6616–8.

27. Jae J, Zheng W, Lobo RF, Vlachos DG. Production of dimethylfuran from hydroxymethylfurfural through catalytic transfer hydrogenation with ruthenium supported on carbon. ChemSusChem. 2013 Jul;6(7):1158–62.

28. Huang YB, Chen MY, Yan L, Guo QX, Fu Y. Nickel-tungsten carbide catalysts for the production of 2,5-dimethylfuran from biomass-derived molecules. ChemSusChem. 2014 Apr;7(4):1068–72.

29. Wang GH, Hilgert J, Richter FH, Wang F, Bongard HJ, Spliethoff B, et al. Platinum–cobalt bimetallic nanoparticles in hollow carbon nanospheres for hydrogenolysis of 5-hydroxymethylfurfural. Nature Mater. 2014 Mar;13(3):293–300.

30. Zu Y, Yang P, Wang J, Liu X, Ren J, Lu G, et al. Efficient production of the liquid fuel 2,5-dimethylfuran from 5-hydroxymethylfurfural over Ru/Co3O4 catalyst. Applied Catalysis B: Environmental. 2014 Mar;146:244–8.

31. Liu Y, Mellmer MA, Alonso DM, Dumesic JA. Effects of Water on the Copper-Catalyzed Conversion of Hydroxymethylfurfural in Tetrahydrofuran. ChemSusChem. 2015 Dec 7;8(23):3983–6.

32. Shi J, Wang Y, Yu X, Du W, Hou Z. Production of 2,5-dimethylfuran from 5-hydroxymethylfurfural over reduced graphene oxides supported Pt catalyst under mild conditions. Fuel. 2016 Jan;163:74–9.

33. Hu L, Tang X, Xu J, Wu Z, Lin L, Liu S. Selective Transformation of 5-Hydroxymethylfurfural into the Liquid Fuel 2,5-Dimethylfuran over Carbon-Supported Ruthenium. Ind Eng Chem Res. 2014 Feb 26;53(8):3056–64.

34. Yuan Z, Zhang Z, Zheng J, Lin J. Efficient synthesis of promising liquid fuels 5-ethoxymethylfurfural from carbohydrates. Fuel. 2015 Jun;150:236–42.

35. Yin S, Sun J, Liu B, Zhang Z. Magnetic material grafted cross-linked imidazolium based polyionic liquids: an efficient acid catalyst for the synthesis of promising liquid fuel 5-ethoxymethylfurfural from carbohydrates. J Mater Chem A. 2015;3(9):4992–9.

36. Li H, Saravanamurugan S, Yang S, Riisager A. Direct transformation of carbohydrates to the biofuel 5-ethoxymethylfurfural by solid acid catalysts. Green Chem. 2016;18(3):726–34.

37. Lewis JD, Van de Vyver S, Crisci AJ, Gunther WR, Michaelis VK, Griffin RG, et al. A Continuous Flow Strategy for the Coupled Transfer Hydrogenation and Etherification of 5-(Hydroxymethyl)furfural using Lewis Acid Zeolites. ChemSusChem. 2014 Aug;7(8):2255–65.

38. Wang S, Zhang Z, Liu B, Li J. Silica coated magnetic Fe3O4 nanoparticles supported phosphotungstic acid: a novel environmentally friendly catalyst for the synthesis of 5-ethoxymethylfurfural from 5-hydroxymethylfurfural and fructose. Catal Sci Technol. 2013;3(8):2104.

39. Wang H, Deng T, Wang Y, Cui X, Qi Y, Mu X, et al. Graphene oxide as a facile acid catalyst for the one-pot conversion of carbohydrates into 5-ethoxymethylfurfural. Green Chem. 2013;15(9):2379.

40. Yang Y, Abu-Omar MM, Hu C. Heteropolyacid catalyzed conversion of fructose, sucrose, and inulin to 5-ethoxymethylfurfural, a liquid biofuel candidate. Applied Energy. 2012 Nov;99:80–4.

41. Bing L, Zhang Z, Deng K. Efficient One-Pot Synthesis of 5-(Ethoxymethyl)furfural from Fructose Catalyzed by a Novel Solid Catalyst. Ind Eng Chem Res. 2012 Nov 28;51(47):15331–6.

42. Kraus GA, Guney T. A direct synthesis of 5-alkoxymethylfurfural ethers from fructose via sulfonic acid-functionalized ionic liquids. Green Chem. 2012;14(6):1593.

43. Che P, Lu F, Zhang J, Huang Y, Nie X, Gao J, et al. Catalytic selective etherification of hydroxyl groups in 5-hydroxymethylfurfural over H4SiW12O40/MCM-41 nanospheres for liquid fuel production. Bioresource Technology. 2012 Sep;119:433–6.

44. Dutta S, De S, Alam MdI, Abu-Omar MM, Saha B. Direct conversion of cellulose and lignocellulosic biomass into chemicals and biofuel with metal chloride catalysts. Journal of Catalysis. 2012 Apr;288:8–15.

45. Liu B, Zhang Z, Zhao ZK. Microwave-assisted catalytic conversion of cellulose into 5-hydroxymethylfurfural in ionic liquids. Chemical Engineering Journal. 2013 Jan;215–216:517–21.

46. Sacia ER, Balakrishnan M, Bell AT. Biomass conversion to diesel via the etherification of furanyl alcohols catalyzed by Amberlyst-15. Journal of Catalysis. 2014 May;313:70–9.

47. Han J, Kim YH, Jung B, Hwang S, Jegal J, Kim J, et al. Highly Selective Catalytic Hydrogenation and Etherification of 5-Hydroxymethyl-2-furaldehyde to 2,5-Bis(alkoxymethyl)furans for Potential Biodiesel Production. Synlett. 2017 Oct;28(17):2299–302.

48. Luo J, Yu J, Gorte RJ, Mahmoud E, Vlachos DG, Smith MA. The effect of oxide

acidity on HMF etherification. Catal Sci Technol. 2014;4(9):3074–81.

49. Shinde S, Rode C. Cascade Reductive Etherification of Bioderived Aldehydes over Zr-Based Catalysts. ChemSusChem. 2017 Oct 23;10(20):4090–101.

50. Jae J, Mahmoud E, Lobo RF, Vlachos DG. Cascade of Liquid-Phase Catalytic Transfer Hydrogenation and Etherification of 5-Hydroxymethylfurfural to Potential Biodiesel Components over Lewis Acid Zeolites. ChemCatChem. 2014 Feb;6(2):508–13.

51. Chen PX, Tang Y, Zhang B, Liu R, Marcone MF, Li X, et al. 5-Hydroxymethyl-2-furfural and Derivatives Formed during Acid Hydrolysis of Conjugated and Bound Phenolics in Plant Foods and the Effects on Phenolic Content and Antioxidant Capacity. J Agric Food Chem. 2014 May 21;62(20):4754–61.

52. Bicker M, Kaiser D, Ott L, Vogel H. Dehydration of d-fructose to hydroxymethylfurfural in sub- and supercritical fluids. The Journal of Supercritical Fluids. 2005 Dec;36(2):118–26.

53. Zhu H, Cao Q, Li C, Mu X. Acidic resin-catalysed conversion of fructose into furan derivatives in low boiling point solvents. Carbohydrate Research. 2011 Sep;346(13):2016–8.

54. Liu R, Chen J, Huang X, Chen L, Ma L, Li X. Conversion of fructose into 5-hydroxymethylfurfural and alkyl levulinates catalyzed by sulfonic acid-functionalized carbon materials. Green Chem. 2013;15(10):2895.

55. Li H, Govind KS, Kotni R, Shunmugavel S, Riisager A, Yang S. Direct catalytic transformation of carbohydrates into 5-ethoxymethylfurfural with acid–base bifunctional hybrid nanospheres. Energy Conversion and Management. 2014

Dec;88:1245–51.

56. Wang Z, Chen Q. Conversion of 5-hydroxymethylfurfural into 5-ethoxymethylfurfural and ethyl levulinate catalyzed by MOF-based heteropolyacid materials. Green Chem. 2016;18(21):5884–9.

57. Xiang B, Wang Y, Qi T, Yang HQ, Hu CW. Promotion catalytic role of ethanol on Brønsted acid for the sequential dehydration-etherification of fructose to 5-ethoxymethylfurfural. Journal of Catalysis. 2017 Aug;352:586–98.

58. Salminen E, Kumar N, Virtanen P, Tenho M, Mäki-Arvela P, Mikkola JP. Etherification of 5-Hydroxymethylfurfural to a Biodiesel Component Over Ionic Liquid Modified Zeolites. Top Catal. 2013 Jun;56(9–10):765–9.

59. Arias KS, Climent MJ, Corma A, Iborra S. Biomass-Derived Chemicals: Synthesis of Biodegradable Surfactant Ether Molecules from Hydroxymethylfurfural. ChemSusChem. 2014 Jan;7(1):210–20.

60. Yang F, Zhang S, Zhang ZC, Mao J, Li S, Yin J, et al. A biodiesel additive: etherification of 5-hydroxymethylfurfural with isobutene to tert-butoxymethylfurfural. Catal Sci Technol. 2015;5(9):4602–12.

61. Cao Q, Liang W, Guan J, Wang L, Qu Q, Zhang X, et al. Catalytic synthesis of 2,5-bis-methoxymethylfuran: A promising cetane number improver for diesel. Applied Catalysis A: General. 2014 Jul;481:49–53.

62. Balakrishnan M, Sacia ER, Bell AT. Etherification and reductive etherification of 5-(hydroxymethyl)furfural: 5-(alkoxymethyl)furfurals and 2,5-bis(alkoxymethyl)furans as potential bio-diesel candidates. Green Chem. 2012;14(6):1626.

63. Lewis JD, Van de Vyver S, Crisci AJ, Gunther WR, Michaelis VK, Griffin RG, et al. A Continuous Flow Strategy for the Coupled Transfer Hydrogenation and Etherification of 5-(Hydroxymethyl)furfural using Lewis Acid Zeolites. ChemSusChem. 2014 Aug;7(8):2255–65.

64. Li H, Saravanamurugan S, Yang S, Riisager A. Direct transformation of carbohydrates to the biofuel 5-ethoxymethylfurfural by solid acid catalysts. Green Chem. 2016;18(3):726–34.

65. Güleç F, Sher F, Karaduman A. Catalytic performance of Cu- and Zr-modified beta zeolite catalysts in the methylation of 2-methylnaphthalene. Pet Sci. 2019 Feb;16(1):161–72.

66. Perez-Pariente J, A. Martens J, A. Jacobs P. Crystallization mechanism of zeolite beta from (TEA)2O, Na2O and K2O containing aluminosilicate gels. Applied Catalysis. 1987 Jan;31(1):35–64.

67. Córdoba LF, Sachtler WMH, Montes De Correa C. NO reduction by CH4 over Pd/Co-sulfated zirconia catalysts. Applied Catalysis B: Environmental. 2005 Apr;56(4):269–77.

68. He D, Ding Y, Luo H, Li C. Effects of zirconia phase on the synthesis of higher alcohols over zirconia and modified zirconia. Journal of Molecular Catalysis A: Chemical. 2004 Feb;208(1–2):267–71.

69. Nor Aishah,Nor Aishah Saidina Amin,Didi Dwi Anggoro. Characterization and Activity of Cr, Cu and Ga Modified ZSM-5 for Direct Conversion of Methane to Liquid Hydrocarbons. Journal of Natural Gas Chem. 12:123–34.

70. M.M.J. Treacy, J.B. Higgins. Collection of Simulated PXRD Powder Patterns for Zeolites.

71. Shameli K, Mansor Bin Ahmad M, Mohsen Z, Yunis WZ, Ibrahim NA. Fabrication of silver nanoparticles doped in the zeolite framework and antibacterial activity. IJN. 2011 Feb;331.

72. Shanjiao K, Yanjun G, Tao D, Ying Z, Yanying Z. Preparation and characterization of zeolite beta with low SiO2/Al2O3 ratio. Pet Sci. 2007 Mar;4(1):70–4.

73. Zhang X, Ke X, Zhu H. Zeolite-Supported Gold Nanoparticles for Selective Photooxidation of Aromatic Alcohols under Visible-Light Irradiation. Chemistry A European J. 2012 Jun 25;18(26):8048–56.

3.7. GC-MS data of products

2, 5 bis Propoxymethyl furan

GC-MS data: 212(BPMF), 153, 139, 111, 97, 83, 69, 43, 31

170 (HPMF), 153, 139, 127, 97, 81, 69, 55, 41, 30

128 (BHMF), 111, 97, 69, 55, 41, 30
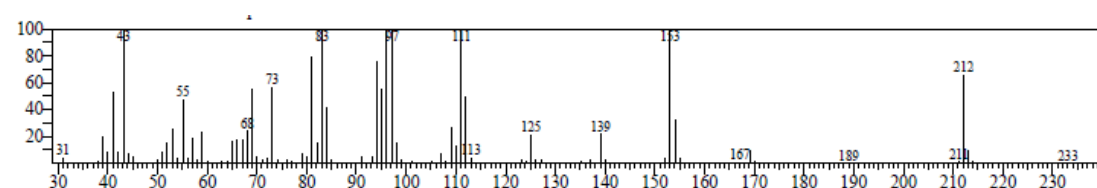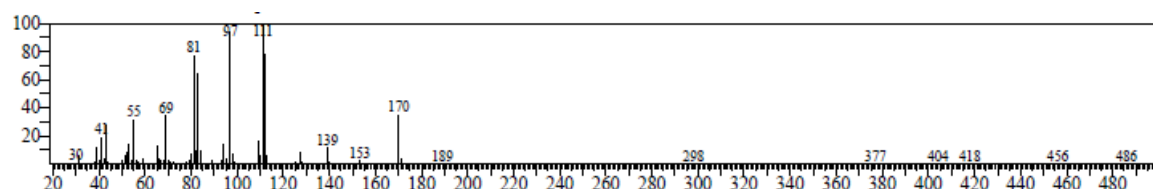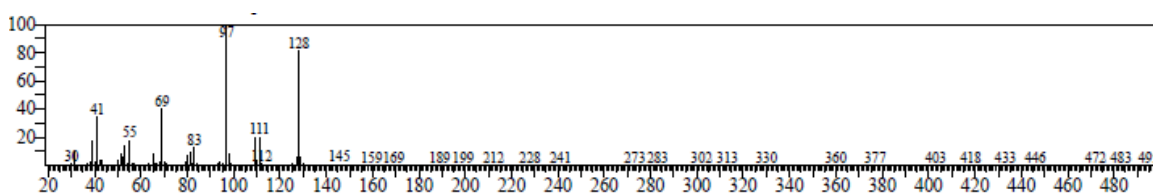
CHAPTER – 4

One pot reductive etherification of 5-HydroxyMethylFurfural into biofuel (2, 5-Bis (Propoxymethyl) Furan (BPMF)) using mixed catalyst ZrO(OH)$_2$ and Zr-Hβ.
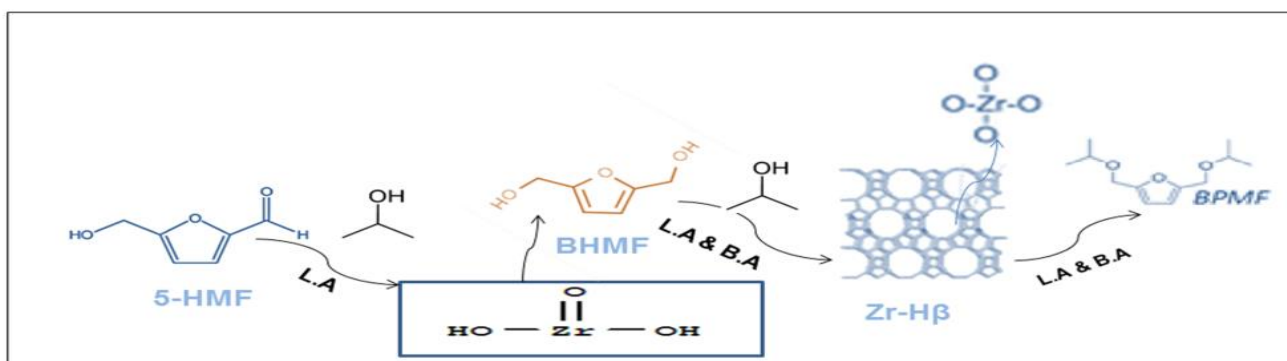
In previous chapter 3 catalytic conversion of 5-HMF was carried out using $ZrO(OH)_2$, Zr supported on Hβ, HY, HZSM-5 and mixed catalyst $ZrO(OH)_2$ + Zr-Hβ. Obtained results revels that mixed catalyst have given encouraging results in terms of conversion of 5-HMF and selectivity of BPMF. Hence it is decided to study the activity of mixed catalyst by varying temperature, time and catalyst loading. One pot synthesis of 2,5-bis(propoxymethyl)furan (BPMF) from 5-hydroxymethylfurfural (5-HMF) is essential and simultaneously difficult. In this chapter, mixed heterogenous catalyst ($ZrO(OH)_2$ and Zr-Hβ) was used to study the conversion of 5-HMF to BPMF using 2-propanol as a hydrogen donor in a one-pot process. The Prepared catalysts were characterized by temperature-programmed desorption of ammonia (NH_3-TPD), powder X-ray diffraction, transmission electron microscopy, BET surface area, and Fourier transform infrared spectroscopy. The Bronsted acid sites and Lewis acid sites of catalyst played a vital role in the selectivity of BPMF. At the optimized reaction conditions (temperature 140^oC, catalyst loading (0.25 g), reaction time 4 h and 5-HMF concentration (1 g)), 61.6 % 5-HMF conversion and 91.23 % BPMF selectivity was achieved.

4.1. Introduction

Human life is significantly affected by energy derived from fossil fuels. The massive use of fossil fuel resources has resulted in a slew of issues such as reserve depletion, price volatility, and environmental concerns (1–3). In this regards, exploration of renewable resources as an alternative of fossil fuel has been become urgent needs(4–6). Biomass is a carbon based renewable resource having many advantages like, low cost, environmental friendly and availability, which makes them important source for sustainable development of valuable chemicals(7–9). Hence, conversion of biomass derived platform molecules into valuable chemical and derivatives is the most attractive approach(10,11). Bio refinery is emerged as viable route to maximize the use of biomass. Biomass-derived chemicals, such

as 5-hydroxymethylfurfural (5-HMF), levulinic acid, furfurals, sugar alcohols, lactic acid, succinic acid, and phenols, are considered platform chemicals. These platform chemicals can be further used for the production of a variety of important chemicals on an industrial scale(12–14). Various transformation method of lignocellulosic biomass to platform chemicals such as 5-hydroxymethylfurfural (HMF), which can be converted further to polymer building blocks and potential biofuel candidates, have been reported recently. So, manufacturing of biofuels from HMF is particularly gaining thrust. For instance, 5-ethoxymethylfurfural (EMF) produced by the etherification of HMF with ethanol is consider as a promising bio-diesel or additive, because of its high energy density 30.3 MJ/L, which is very near to that of commercial available gasoline (31.1 MJ/L) or diesel (33.6 MJ/L)(15). Gruter et al.(16) reported that the aldehyde group of the EMF affects stability of the molecules when it is blended with regular diesel as phase separation occurs. On other hand products such as di-ethers and 2,5-bis(alkoxymethyl)furans (BAMFs) exhibits higher energy densities and good blending properties with diesel(17). Cao et al.(18) also reported complete miscibility of 2,5-bismethoxymethylfuran(BMMF) with diesel. For the synthesis of BAMFs from HMF two type of catalytic system are reported in literature (i) Using H2 gas directly as hydrogen source (Conventional Hydrogenation), and (ii) Catalytic Transfer Hydrogenation (CTH). As compared to conventional hydrogenation with molecular H2, the CTH is favourable alternative because carbonyl compounds, including aldehydes and ketones can be completely reduced to corresponding alcohols through the Meerwein−Ponndorf−Verley (MPV) reaction by using formic acid and alcohols as hydrogen donor(19–22). Many researchers have reported the combination of hydrogenation and subsequently its etherification to produce BAMFs from HMF. This approach can be considered as economically viable due to reduced production cost of BAMFs and process becomes more simple as the numbers of unit operation are reduced.

By using CTH method HMF is selectively converted into 2,5bis (hydroxymethyl) furan BHMF through MPV reaction(23–30) and subsequently BHMF converted to various BAMFs. In this approach alcohols not only used as solvent but works as etherifying agents also which leads to formation of BAMFs without using molecular H_2. Jae et al.(31) used Sn-beta catalyst for reduction as well as etherification reaction in presence of 2-propanol and obtained 79.5 % BIPMF after 6h at 180°C. Luo et al.(32) reported a 60.9% yield of BPMF with same reaction condition and media in 3 h using Sn-beta catalyst. Lewis et al.(33) tuned the Lewis acidity of Hf-Beta catalyst which resulted in a higher yield of BBMF (81%), by using 1-Butanol as solvent at 120°C in 1 h. Shinde and Rode(34) synthesized Zr-Mont catalyst by impregnation method and showed that prepared catalyst effectively worked for both reduction and etherification reactions, respectively. The strong interaction between Zr and Mont increases the Lewis acidity of Zr-Mont catalyst and results in a higher yield of BIPMF (95%) and BBMF (96%) as compared to Sn-Beta and Hf-Beta catalyst at 150°C. Similarly, Wi et al.(35) prepared Zr-SBA-UH and carried out the reactions with ethanol and 2-propanol at 150°C in 4 h, which leads to formation of BEMF and BIPMF with a yield of 87.9 % and 93.9% respectively. When Zr-SBA-UH was used with other solvents such as 1-propanol, 1-butanol, 2-butanol and MPrOH, it formed BPMF, BBMF, BSBMF and BMPMF with a yield of 38.1 %, 17.1%, 4.4% and 54.1% for same reaction conditions respectively. The reason for higher selectivity of BAMF with 2-propanol as compared to other alcohol is the effect of stearic hindrance and reduction potential of alcohol. It was reported that a lower value of reduction potential shows easy removal of hydrogen for alcohols which encourage the MPV reduction and 2-propnaol has a lower value of reduction potential as compared to other alcohols.

Although the higher conversion of 5-HMF and selectivity towards desired product is reported in the literature, but they are based on the combination of hydrogenation and

etherification processes. Hence, It is important to develop a one-pot process for the catalytic conversion 5-HMF to BPMF in the present scenario. As the current processes are carried out separately, such as hydrogenation of 5-HMF to BHMF and etherification of BHMF to BPMF, which increases the production cost, energy consumption, and number of unit operations. Even they cannot give a high selectivity of BPMF due to the formation of by-products. Herein, we propose a mixed heterogeneous catalyst (ZrO(OH)$_2$+Zr-Hβ) for the synthesis of BPMF from 5-HMF by using 2-propanol as a hydrogen donor in a one-pot process. In this work mixed catalyst (ZrO(OH)$_2$+Zr-Hβ) was synthesized and used as a catalyst for the conversion of 5-HMF to BPMF. For the reductive etherification of 5-HMF to BPMF, ZrO(OH)$_2$ acts as a hydrogenation catalyst, while Zr-Hβ acts as an etherification step. Zr-Hβ holds plenty of strong Lewis acid sites with a sufficient number of Brønsted acid sites, which favours reductive etherification of 5-HMF to BPMF. Most previous research focused on the synthesis of BPMF from 5-HMF via hydrogenation to form BHMF and then BHMF etherification at high temperatures. In present study the reduction and etherification steps were carried out together using mixed catalyst (ZrO(OH)$_2$+Zr-Hβ) and 2-propanol as a hydrogen donor. The reaction mechanism for reductive etherification of 5-HMF in 2-propanol over mixed catalyst shows that the carbonyl group in 5-HMF is hydrogenated to form BHMF in the presence of Lewis acid sites. After that BHMF etherified to HPMF and BPMF in 2-propanol in the presence of excessive Lewis acid sites or Brønsted acid sites. Here we report one pot catalytic conversion of 5-HMF to BPMF at 140°C in 4 h with > 90% selectivity using a mix catalyst (ZrO(OH)$_2$+Zr-Hβ).

4.2. Materials and Methods

4.2.1. Materials

The chemicals obtained were used as received. SRL (Sisco Research Laboratories Pvt. Ltd.) in India supplied the 5-(hydroxymethyl) furfural (98%). All the alcohols and

solvents, aq. ammonia (30%), $ZrOCl_2.8H_2O$ and metal precursors such as Zirconyl Nitrate Hydrate (99.5%) were purchased from LobaChemie, Mumbai, India. Hβ was purchased from Sud-cheme India Private Limited, Vadodara, Gujarat.

4.2.2. Catalyst Preparation

Preparation of $ZrO(OH)_2$

The hydroxide of Zr was prepared by precipitation process as described elsewhere(36). In a typical preparation, 10 g of metal chloride precursors were precipitated to respective hydroxide by adding of aq. NH_3 upto pH of the solution was 9-10. Mixture was aged in 24 h, filtered and washed residue with plenty of distilled water until pH of the filtrate was neutral. Residue was subsequently dried at 110 °C in 12 h, followed by being ground to powder in a mortar with a pestle and stored in a glass bottle.

Preparation of Zr- Hβ

Zirconium (IV) nitrate hydrate metals were impregnated into the structure of Hβ using a typical wet impregnation method(37). To prepare Zr-impregnated Hβ, 4.05 g zirconium (IV) oxynitrate hydrate was dissolved into 20 mL deionised water. After all zirconium (IV) nitrate salt dissolved, 16 g of Hβ was added to the aqueous solution. The mixture was then kept at room temperature overnight for impregnation. After impregnation, the dried solid particles dried at 120°C in 4 h before being calcined at 550°C in 6h.

4.2.3. Catalyst Characterization

Powder X-ray diffraction (PXRD) patterns were obtained on a Bruker D8 Advance X-ray diffractometer, using LynxEye Superspeed detector and Cu Kα radiation produced from a PW Bragg–Brentano (BB) goniometer (θ/2θ), operating at 40 kV and 35 mA. The diffractograms were recorded in the 2θ range of 10 - 80° with a 2θ step size of 0.02°.

The Brunauer–Emmett–Teller (BET) surface area, pore volume, and Barrett–Joyner–Halenda (BJH) pore size distribution of the prepared catalysts were determined by

N2adsorption-desorption analysis conducted at -196°C. Prior to analysis, the catalysts were degassed under vacuum at $200 \pm 2^{\circ}$C.

Fourier Transform Infrared Spectroscopy (FTIR) spectra of catalyst samples were collected using Model: Cary630 spectrometer. The instrument was operated in the range of 600-4000 cm^{-1}.

Transmissions electron microscopy (TEM) images of the catalyst were recorded on a JEOL JEM2100 microscope.

Total acidity of Hβ was measured by using n-butyl amine titration method(38).1 In this method 0.25 g support/catalyst was suspended in 25mL of 0.025N n-butyl amine solution in toluene. Keep the solution for 24 h to neutralize the surface acidic sites. Titrate it against 0.025 N tri-chloroacetic acid solutions in toluene by using neutral red indicator. This gives the catalyst's total acidity.

Temperature-programmed desorption of ammonia (NH$_3$-TPD) was used to measure total acidity, strong and weak acid site of catalyst. In a process of NH$_3$-TPD, 0.0735 g of catalyst was taken in quartz sample tube. Before measurements, the catalyst was pre-treated in Helium at 30 SCCM and 200°C. A mixture of NH$_3$ in Helium was passed at rate of 30 SCCM and at temperature 50 $^{\circ}$C for 30 min. The TPD measurements were carried out in the range 50 to 700°C with a ramp rate of 10°C min^{-1}.

4.3. Catalytic Reaction

The experiment was conducted in 100 mL stainless steel autoclave reactor. The autoclave was charged with 1 g HMF, 0.25g catalyst, and 50 mL of 2-propanol. The autoclave was closed then heated to the desired reaction temperature of 140°C under stirring conditions for a 4 h reaction time. Stirring was kept constant (550 rpm) for the reactions. After each reaction, the autoclave was cooled. At the end of each run, the product mixture was separated from the catalyst by centrifuge and then analyzed by GC MS equipped using

DB-1701 column (60M x 0.32mm x 1.µm film thickness).Cyanopropylphenyl (14%), Dimethylpolysiloxane (86%).

To find the performance of the catalytic systems, conversions of 5-HMF (X5-HMF, %) and selectivity to products (Si) are defined as follow: 5-HMF conversion (X5-HMF) was calculated from ratio of the amount of 5-HMF converted and initial amount of 5-HMF. The selectivities for reaction products like BHMF, HPMF, and BPMF (Si) were calculated by dividing the amount of products formed by the amount of 5-HMF converted.

$$\text{conversion (\%)} = \frac{(I.N.)_i - (I.N.)_f}{(I.N.)_i} * 100 \ ,$$

Where, $(I.N.)i$ = Initial moles of 5-HMF & $(I.N.)f$ = Final moles of 5-HMF

$$\text{Selectivity (\%)} = \frac{\text{moles of product formed}}{\text{moles of 5-HMF converted}} * \ 100$$

4.4. Results and discussion

4.4.1. Physical and chemical properties of catalyst

4.4.1.1. Transmission electron microscopy (TEM)

TEM measurements were carried out in order to obtain the particle size and morphology of catalysts. TEM images (Figure 4.1) showed that the samples consisted of crystallites with a size of about 30 nm. However, metal particles were not easily recognized due to aggregation of particle during impregnation method for catalyst preparation. The average size of metal particle and d-spacing was around 14 nm and 0.327 nm, respectively.
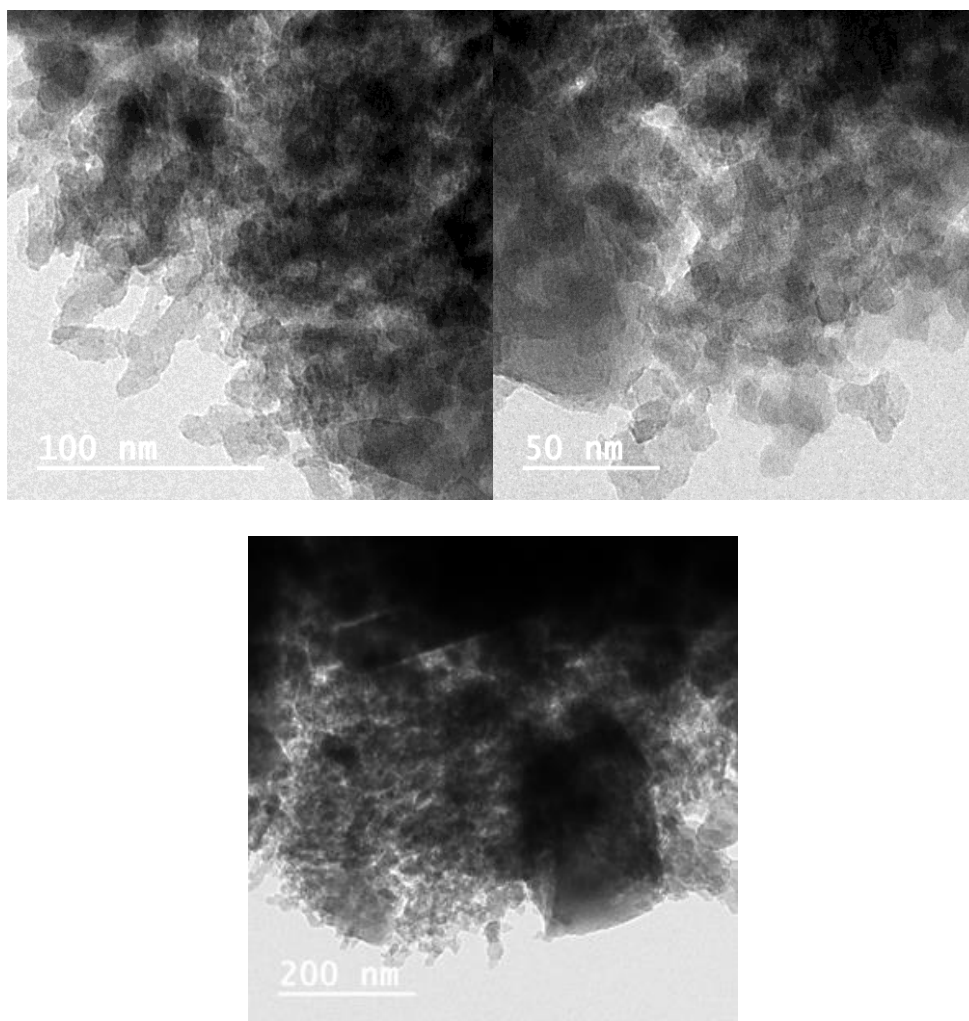
Figure 4.1 TEM images of ZrHβ

4.4.1.2. Powder X-ray diffraction (PXRD) analysis

Figure 4.2 (a) shows PXRD patterns of ZrO(OH)2 . The wide and weak PXRD pattern (diffraction angle at $2\theta = 21.7°$, $26.69°$, $27.81°$, $31.26°,39.63°,41.20°,44.23°,50°$) of $ZrO(OH)_2$ is indicating the amorphous nature of $ZrO(OH)_2$. From Figure 4.2 (c) , it can be seen that the PXRD peaks for the Zr-Hβ catalysts were very similar to those of Hβ (Figure 4.2 (b)) as indicated by the diffraction angle at $2\theta = 22.6°$, $25.98°$, $28.08°,31.26°$ and, $50°$. No new diffraction peak was observed which suggested that the MFI structure of Hβ catalyst was intact and no new phase was produced after the modification of Hβ catalyst and Zr were nicely dispersed(39). The diffractions at 31.26 and 50, due to tetragonal zirconia phase (40,41) were clearly observed on the Zr-Hβ catalyst sample.

83
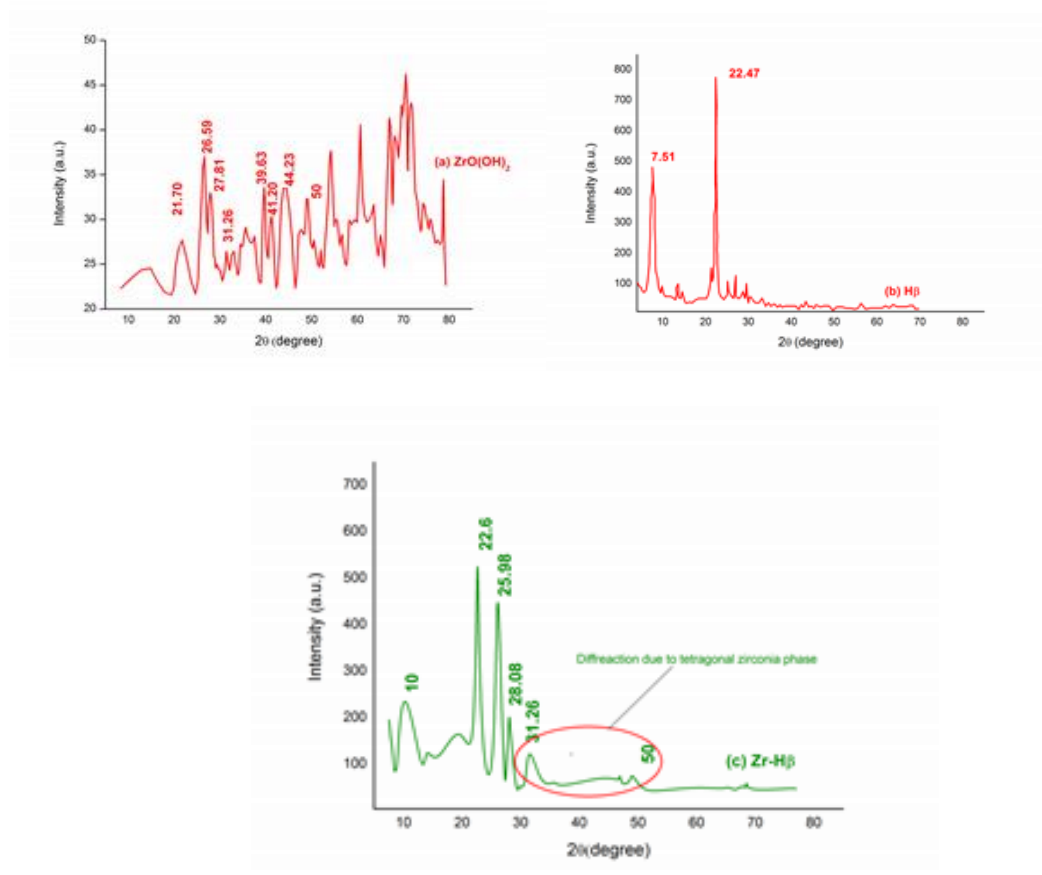
Figure 4.2 PXRD patterns of (a) ZrO(OH)₂ (b) Hβ and (c) Zr-Hβ catalysts

4.4.1.3. Fourier transforms infrared spectroscopy (FTIR)

Fourier transform infrared (FTIR) spectrum of $ZrO(OH)_2$ in the range of 400–4000 cm^{-1} is studied and shown in Figure 4.3 (a). The very broad absorption band at 3141 cm^{-1} is attributed to the stretching vibrations of OH groups on the surface of the catalyst. In the spectrum of $ZrO(OH)_2$, a sharp peak at 1441 cm^{-1} are assignable to Zr-OH vibrations. The peak at 1634 cm^{-1} is due to OH vibration of $ZrO(OH)_2$. Zr-Hβ spectra (Figure 4.3 (b & c)) exhibit band in the region of 3735, 3641, 1625, 1229, 1083 and 562 cm^{-1} are due to bending of isolated terminal Si-OH groups, bending of bridging hydroxyl Si-OH-Al bending vibration of OH groups, asymmetrical stretching vibration, symmetric and asymmetric stretching vibrations of the Si–O–Si linkages of the zeolite framework and double ring opening vibration of external linkages, respectively. Zr precursor, causes a

decrease in the intensity of OH bands at 3735 cm^{-1}, suggesting that Zr species could react with silanols located in the vacant sites and thus be incorporated into the Hβ zeolite framework (42).
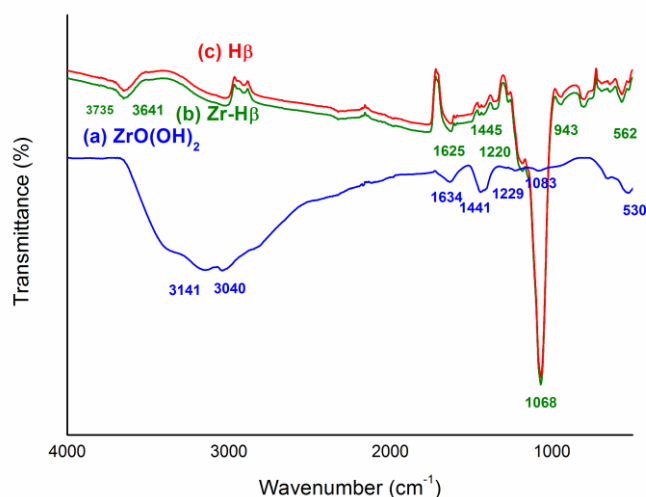
Figure 4.3 (a) FTIR spectra of ZrO(OH)$_2$ catalyst and (b) Zr-Hβ catalyst (c) Hβ catalyst

4.4.1.4. Surface area and pore volume (BET)

The results of N$_2$ adsorption of the catalysts are listed in Table 4.1. From Table 4.1, it can be seen that no significant effect observed on the surface are and pore volume of the Zr-Hβ catalyst. The Zr impregnation on Hβ did not seem to affect the specific surface area and the pore volume to a greater extent compared to that of the Hβ catalyst. Whereas ZrO(OH)$_2$ has the lower surface area of 274.09m^2/g and the smallest pore volume of 0.27 cm^3/g.

Table 4.1 Textures of ZrO (OH)$_2$, Hβ and Zr-Hβ catalysts

Sample	Surface area, m^2/g	Pore volume, cm^3/g			Pore size, nm
	S.A^a	V$_{pore}$^{b}	V$_{micro}$^{c}	V$_{meso}$	D$_{pore}$^{d}
ZrO(OH)$_2$	274.09	0.27	0.037	0.24	3.44
Hβ	415.25	0.45	0.15	0.30	-
Zr-Hβ	412.71	0.44	0.15	0.29	4.37

a-S.A- BET surface area, b-Total pore volume measured at P/P0= 0.9999,c-t-plot method, V$_{meso}$=V$_{pore}$- V$_{micro}$, d-Average pore width calculated by BJH method.

4.4.1.5. Acidity of catalysts

Both Brønsted acid and Lewis acid have significant effects on the high product selectivity and reduction in undesired reactions. According to the literature, Lewis acid increases the catalytic activity of MPV reduction, etherification rate increases with density of Lewis acid sites, and undesired products decrease with decreases in Brønsted acid sites(31). So, it is necessary to prepare Lewis acid catalysts with limited Brønsted acid for the etherification of HMF to BPMF. Figure 4.4 shows the amount and strength of acid sites on ZrO(OH)$_2$ and Zr-Hβ catalysts were determined by NH$_3$-TPD. The acidity of Hβ was determined by the n-butylamine titration method. The NH$_3$-TPD profile of ZrO(OH)$_2$ and Zr-Hβ catalysts are depicted in Figure 4.4. The TPD peaks can be defined based on lower temperature region (<250°C), middle temperature region (250°C to 500°C) and higher temperature region (>500°C). Three typical desorption peaks for the ZrO(OH)$_2$ catalyst are observed at 178°C, 497.3^{o}C, and 594.4^{o}C, and for the Zr-Hβ catalyst at around 156°C, 475.6^{o}C, and 498.6^{o}C, respectively, and are recognized as NH$_3$ desorption from weak, medium, and strong acid sites. Higher temperature region could be assigned to desorption of NH$_3$ from strong acidic sites. Whereas, lower temperature region peaks assigned to release of NH$_3$

from weak acidic sites. Results indicate the presence of both weak as well as strong acidic sites in catalyst. The high-temperature peak was observed around 594.4^{o}C for ZrO(OH)$_2$ and 498.6^{o}C for Zr-Hβ, respectively. Higher temperature peaks represents desorption of NH$_3$ from Lewis acid sites(43,44). From Table 4.2, it can be said that the impregnation of Zr on Hβ reduced the total acidity. It can be observed that the amount of total acid sites on Zr-Hβ was reduced to 1.28 mmol/g from 2.14 mmol/g. Hence, the nature of acid sites changes with the impregnation of Zr species. The impregnation of Zr on Hβ sharply increased Lewis acid sites and decreased Brønsted acid sites, which can be observed from the values of weak, medium, and strong acid sites in Table 4.2. The change in Brønsted acid sites and Lewis acid sites is endorsed by the strong interaction between the intrinsic acid sites and the Zr species due to which few Brønsted acid sites are converted into Zr-Lewis acid sites. As reported in the literature, Zr-Lewis acid sites have the ability to accelerate the process of etherification(34).
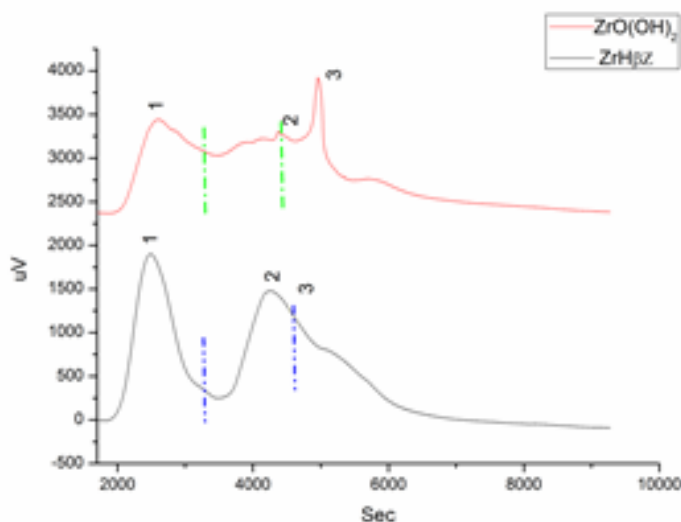
Figure 4.4 NH$_3$-TPD profiles of Zr-Hβ and ZrO(OH)$_2$

Table 4.2 Acidity information of catalysts by NH$_3$-TPD & Titration method

Sample	Amount of acid sites, (mmol/g)			
	Total	Weak (<250°C)	Medium (250-500°C)	Strong (>500°C)
Hβ*	2.14	-	-	-
ZrO(OH)2**	1.27	0.42	0.43	0.42
Zr-Hβ**	1.28	0.51	0.34	0.43

* n-butyl-amine titration method, ** NH$_3$-TPD

4.4.2. Study of catalyst activity

4.4.2.1. Effect of temperature and catalyst loading

This sequential reductive etherification of HMF was carried out at different temperatures (120°C, 130°C, and 140°C), time (2 h & 4 h), and catalyst loading (0.1 g) over a ZrO(OH)$_2$ (0.1 g) and mixture of Zr-Hβ (0.1 g, 0.15g, 0.2g, 0.25g), and the results are shown in Table 4.3. Conversion of the 5-HMF was found to be 23.53% and selectivity of BHMF and HPMF was found to be 83.55 and 17.67%, respectively, at 120°C (entry1) for 2 h and no BPMF was observed. By increasing the temperature to 130°C and 140°C (entry 2 and 3) and keeping all other reaction conditions the same, it was observed that the conversion of 5-HMF was increased to 29.42% and 57.12% and the selectivity of BHMF was decreased to 76.43% and 68.04%, respectively. Whereas the selectivity of HPMF increased and there was no generation of BPMF. The higher conversion of 5-HMF was achieved by increasing reaction time to 4 h and keeping all other parameters constant (entry 4, 5 and 6) and reaching a maximum of 71.32 % (entry 6). At a higher reaction time (4 h), a significant change in the selectivity of BHMF, HPMF and BPMF was observed (entry 4, 5, and 6). BHMF selectivity decreased to 9.89% (entry 6) from 21.98% (entry 4), and HPMF selectivity decreased to 37.60% (entry 6) from 68.57% (entry 4), while BPMF selectivity

increased and was around 20.82% at higher reaction temperature of 140°C (entry 6). This may be due to the conversion of HPMF to BPMF at higher reaction temperature and time. Shinde and Rode(34) reported a similar observation of higher reaction temperature for the production of BPMF using ZrO(OH)$_2$ as a catalyst. The lower yield and selectivity of BPMF, on the other hand, may be due to ZrO(OH)$_2$, which acts as a charge transfer hydrogenation catalyst. Further, to enhance the yield and selectivity of the desired product, Hβ and Zr-Hβ catalysts were tested at reaction conditions (entry 7 and 8), but the obtained results were not encouraging. However, the presence of BPMF in the product mixture indicated the impact of Zr-Hβ during the etherification step.

The results show that ZrO(OH)$_2$ acts as a hydrogenation catalyst, whereas Zr-Hβ acts as an etherification catalyst in the reductive etherification of 5-HMF to BPMF. Hence, it was decided to carry out the reaction with a combined ZrO(OH)$_2$ and Zr-Hβ catalyst.

Alcohols can also be used as etherifying agents which leads to formation of BAMFs without using molecular H$_2$ (23-30). In present work, 2-propanol used as both hydrogen donors as well as substrate for the etherification. To check the effect of combined catalyst on 5-HMF conversion and BPMF selectivity, reaction was performed with equal weight of both catalysts (entry 9) at 120°C in 4 h. It was observed that both 5-HMF conversion and BPMF selectivity increased to 70.36 % and 50.28 % respectively, and this was higher than their individual results (entry 6 and 8). Furthermore, a changed the loading of ZrO(OH)$_2$ from 0.25g to 0.1g resulted in a higher conversion of 5-HMF and reaching to 75.09 % (entry 10). However, a decreased in the selectivity of BPMF (35.63 %) was observed. This can be due to reduction in the Lewis acid sites on the catalyst which favors the ring opening reaction and side reactions. Keeping all the parameters constant, reaction was carried out at 130°C (entry 11) and surprisingly the conversion was reduced to 64.05 % but

selectivity was enhanced to 73.41 % which confirms earlier assumption that high temperature is desired for BPMF.

To better understand the role of Zr-Hβ in combined catalysts, the reaction was run at various catalyst loadings while keeping $ZrO(OH)_2$ (0.1g) constant at 140^oC in 4 h (entry 12-15). It was observed that at lower loading of Zr-Hβ (entry 12 and 13), higher conversion of 84.83 % and 85.05 %, respectively, was achieved. Selectivity, on the other hand, was around 75.20% and 80.81%, respectively. The higher selectivity confirms the role of the Zr-Hβ catalyst. This can be due to an increase in reaction temperature, which favours the conversion of HPMF to BPMF. It was observed that on increasing the loading of Zr-Hβ (entry 14), the conversion was reduced to 61.62 % but selectivity was enhanced to 91.23 %. This can be due to an increase in Lewis acid sites and a reduction in the Brønsted acid sites on the catalyst, which favours the etherification. However, further reduction in the loading of Zr-H (entry 15) shows a similar trend as entries 12 and 13, which confirms that the catalytic activity of etherification is enhanced with high Lewis acid sites.

Similarly, we repeated experiments 12-15 (T=140^oC in 4 h) by changing the loading of Zr-Hβ only and leaving all other parameters constant, and found conversion of HMF to be 84.83%, 85.05%, 61.62%, and 79.41%, respectively. BPMF selectivity was measured at 60.02%, 80.81%, 91.23%, and 38.50%, respectively.

Figure 4.5 shows that using only $ZrO(OH)_2$ for etherification was ineffective because BPMF (targeted product) was not produced at all at different temperatures with a reaction time of 2 h. increase in reaction time to 4 h, results show that the selectivity of BPMF increases. Low surface area and pore volume may be reasons for $ZrO(OH)_2$'s inactivity in the etherification reaction. Other hand, it can be seen from the results that $ZrO(OH)_2$ favours the MPV/catalytic transfer hydrogenation (34).Good results were obtained when

ZrO(OH)$_2$ was used in combination with Zr-Hβ in which conversion of 5-HMF was also increased with a high selectivity of 91.2% to BPMF because of hydrogenation of 5-HMF followed by etherification of 2-hydroxymethyl-5-isopropoxymethylfuran (HPMF) and BPMF with 2-propanol in the same reactor. Figure 4.6 shows that an increase in temperature also favours the increase in the conversion of 5-HMF and the selectivity of BPMF. From Figure 4.7, it is clear that with a change in the loading of catalyst Zr-Hβ, the selectivity of BPMF changes. The Table 4.3 shows that at lower (0.1 g) catalyst loading, selectivity of BPMF is 38.50% and it will increase to 91.2% at higher catalyst loading (0.25g). In general, Lewis acid sites are mainly accountable to transfer hydrogenation through the Meerwein−Ponndorf−Verley (MPV) reaction, although Bronsted acid sites are responsible for the etherification step. Luo et al.(32) reported that the etherification reaction also can be recognized to excessive Lewis acid sites. Based the product analysis (Table 4.3) in the reaction pathway of the one pot reductive etherification, the carbonyl in 5-HMF is initially hydrogenated to form BHMF in the presence of Lewis acid sites. Afterward BHMF can be etherified to HPMF and BPMF in 2-propanol over excessive Lewis or Bronsted acid sites.

Table 4.3 Catalytic activity of different Catalyst (Reaction conditions: 5-HMF – 1g, 2-propanol- 50 ml)

Entry	Catalyst	Catalyst quantity (g)	Temp (^{o}C)	Time (h)	Conv. %	Selectivity%		
						BHMF	HPMF	BPMF
1	ZrO(OH)$_2$	0.1	120	2	23.53	83.55	17.67	-
2		0.1	130	2	29.42	76.43	23.57	-
3		0.1	140	2	57.12	68.04	31.96	-
4		0.1	120	4	37.89	21.98	68.57	9.45

5		0.1	130	4	54.32	32.52	53.96	13.52
6		0.1	140	4	71.32	9.89	37.60	20.82
7	Hβ	0.1	120	2	10.00	-	3.04	6.86
8	Zr-Hβ	0.1	120	2	25.39	-	-	15.55
9	ZrO(OH)$_2$+ Zr-Hβ	0.25+0.25	120	4	70.36	2.40	38.30	50.28
10	ZrO(OH)$_2$+ Zr-Hβ	0.1+0.25	120	4	75.09	9.43	42.92	35.63
11	ZrO(OH)$_2$+ Zr-Hβ	0.1 +0.25	130	4	64.05	1.64	16.50	73.41
12	ZrO(OH)$_2$+ Zr-Hβ	0.1+0.15	140	4	84.83	0.7	24.79	75.20
13	ZrO(OH)$_2$+ Zr-Hβ	0.1+0.20	140	4	85.05	0.95	17.83	80.81
14	ZrO(OH)$_2$+ Zr-Hβ	0.1+0.25	140	4	61.62	0.17	7.04	91.23
15	ZrO(OH)$_2$+ Zr-Hβ	0.1+0.1	140	4	79.41	0.46	7.25	38.50
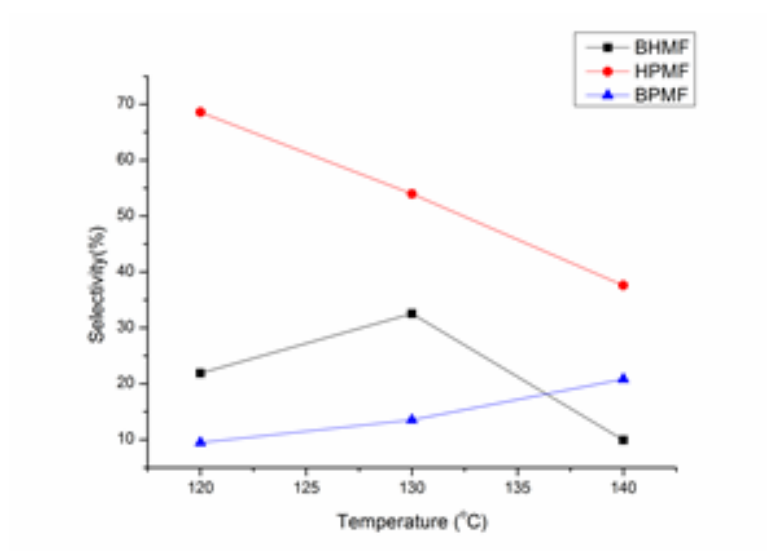
Figure 4.5 Effect of temperature on BHMF, HPMF and BPMF selectivity (Catalyst
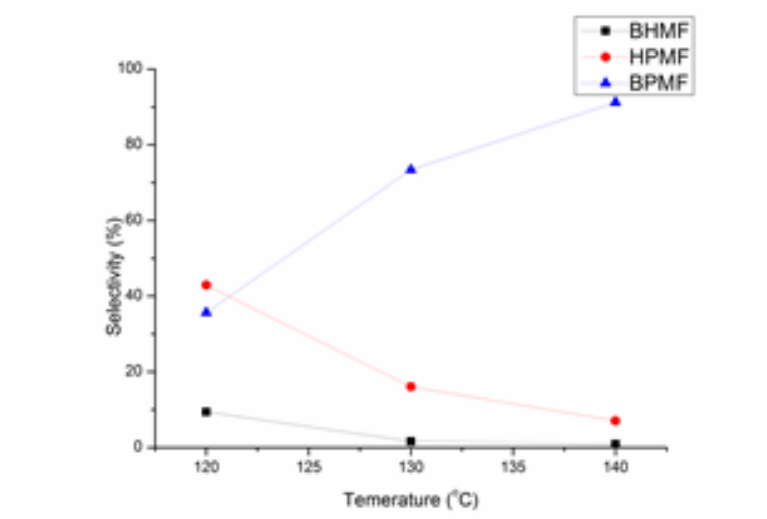
(ZrO(OH)$_2$)

Figure 4.6 Effect of temperature on BHMF, HPMF and BPMF selectivity (Catalyst

(ZrO(OH)$_2$+ Zr-Hβ)
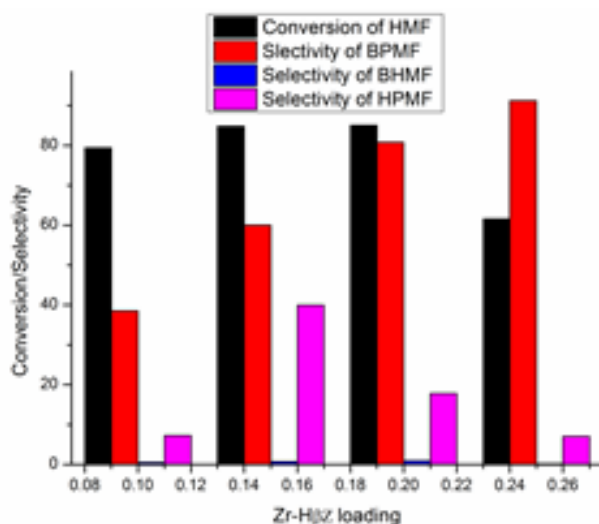
Figure 4.7 Effect of Catalyst loading on BHMF, HPMF & BPMF selectivity (reaction

condition- 140°C at 4 h)

4.4.3. Comparison of various supported metal catalyst from literature and present work

According to the literature, very few studies were conducted using a mix catalyst for the conversion of 5-HMF into BPMF. Table 4.4 compares the activity of the catalyst studied in this work with the catalytic system used in previous studies. At reaction temperatures and times of 140°C and 4 h, respectively, the mixed catalyst system ZrO (OH)$_2$ + Zr-Hβ can provide 61.62% conversion and 91.2% selectivity. Shinde and Rode(34) reported high selectivity for BPMF (95%) because of the combined effect of the Zr-Mont catalyst. However, this high selectivity requires higher temperatures of 150°C and 160°C. Jae et al.(31) have prepared Sn-beta and Zr-Hβ catalysts which are used for reduction as well as etherification reactions in the presence of 2-propanol and give selectivity of BPMF of 87% and 77%, respectively, at 180°C in 6 h reaction time. When the reaction was carried out at 120°C, it required 24 h to achieve the selectivity of 66% and 67%. Lewis et al.(33) have tried to prepare a more effective Lewis acidic Hf-Beta catalyst which results in 77% selectivity of BBMF by using 1-Butanol as solvent at 120°C in 24 h. It was reported by Wi

et al.(35) by using Zr-SBA-UH as a catalyst and 2-propanol as a solvent, When Zr-SBA-UH was combined with other solvents such as 1-propanol, 1-butanol, 2-butanol, and M-PrOH, it formed BPMF, BBMF, BSBMF, and BMPMF with yields of 38.1%, 17.1%, 4.4%, and 54.1% for the same reaction conditions. The catalyst used in this work exhibited good catalytic activity in terms of selectivity of BPMF at a lower temperature and less reaction time as compared to reported catalysts. In addition to this, as BPMF is produced by one pot process which decreases the production cost, energy consumption, and number of unit operations and exhibits promising aspects with respect to commercialization of this process.

Table 4.4 Comparison of various supported metal catalyst from literature and present work

Catalyst	Alcohol	Temperature ($^{\circ}$C)	Time ,h	X_{HMF} (%)	S_{BAMF} Yield (%)	$S_{BMMF}/_{BEMF}/_{BPMF}$ (%)	Reference
HZSM-5 (Si/Al=25)	Methanol	100	3	100.00	70.00	70.00	(18)
HZSM-5 (Si/Al=38)	Methanol	100	3	100.00	68.00	68.00	
HZSM-5 (Si/Al=300)	Methanol	100	3	100.00	69.00	69.00	
HZSM-5 (Si/Al=25)	Methanol	120	12	-	68.00	68.00	
HZSM-5 (Si/Al=25)	Methanol	140	8	-	59.00	59.00	

Cu-HZSM-5	Methanol	120	12	100.00	68.00	68.00	(18)
Hf-Hβ	Ethanol	120	24	87.00		77.00	(31)
Zr-Hβ	2-Propanol	180	6	100.00	77.00	77.00	(33)
Sn- Hβ	2-Propanol	180	6	91.50		87.00	
Zr-Hβ	Ethanol	120	24	81.00		66.00	(31)
Sn- Hβ	Ethanol	120	24	69.00		67.00	
ZrO(OH)$_2$+Zr-Mont	2-Propanol	160	1	100.00	94.00	94.00	(34)
ZrO(OH)$_2$+Zr-Mont	2-Propanol	150	1	100.00	95.00	95.00	
Zr-SBA-UH	2-Propanol	150	4	98.50		93.90	(45)
iUSY@ZrCP	2-Propanol	120	3	78.90		86.90	
ZrO(OH)$_2$+Zr- Hβ	2-Propanol	140	4	61.62		91.00	This work

4.5. Conclusions

We discussed the catalytic conversion of 5-HMF into 2,5-bis(isopropoxymethyl)furan (BPMF) in a single reactor using a mixed catalysts such as ZrO(OH)$_2$ and Zr-Hβ in this work. It was found that the catalyst is capable of converting 5-HMF to BPMF with good selectivity. BHMF and HPMF were mainly produced, with HPMF selectivity much higher

96

than BHMF selectivity. The high selectivity of HPMF may be due to hydrogen transfer promoted by the combined effect of Brønsted and Lewis acidic sties found on $ZrO(OH)_2$. By using a mixed catalytic system, the number of Lewis acid sites is increased and the Brønsted acid sites are reduced, which results in an increase in the selectivity of BPMF. The Zr-Lewis acid sites are found to promote etherification more strongly than hydrogen transfer. The reaction is carried out in a single pot because of the combination of catalytic transfer hydrogenation and subsequently its etherification to produce BPMF from HMF. This reduces the production cost of BPMF and also the process becomes more simpler as the numbers of unit operations are reduced.

4.6. References

1. Zhou CH, Xia X, Lin CX, Tong DS, Beltramini J. Catalytic conversion of lignocellulosic biomass to fine chemicals and fuels. Chem Soc Rev. 2011;40(11):5588.

2. Zhang Z, Song J, Han B. Catalytic Transformation of Lignocellulose into Chemicals and Fuel Products in Ionic Liquids. Chem Rev. 2017 May 24;117(10):6834–80.

3. Hu L, Lin L, Wu Z, Zhou S, Liu S. Recent advances in catalytic transformation of biomass-derived 5-hydroxymethylfurfural into the innovative fuels and chemicals. Renewable and Sustainable Energy Reviews. 2017 Jul;74:230–57.

4. Tollefson J. Can the world kick its fossil-fuel addiction fast enough? Nature. 2018 Apr;556(7702):422–5.

5. Hu L, Zhao G, Hao W, Tang X, Sun Y, Lin L, et al. Catalytic conversion of biomass-derived carbohydrates into fuels and chemicals via furanic aldehydes. RSC Adv. 2012;2(30):11184.

6. Xu C, Arancon RAD, Labidi J, Luque R. Lignin depolymerisation strategies: towards

valuable chemicals and fuels. Chem Soc Rev. 2014;43(22):7485–500.

7. Wang J, Xi J, Wang Y. Recent advances in the catalytic production of glucose from lignocellulosic biomass. Green Chem. 2015;17(2):737–51.

8. Zhang Z, Deng K. Recent Advances in the Catalytic Synthesis of 2,5-Furandicarboxylic Acid and Its Derivatives. ACS Catal. 2015 Nov 6;5(11):6529–44.

9. Liu B, Zhang Z. Catalytic Conversion of Biomass into Chemicals and Fuels over Magnetic Catalysts. ACS Catal. 2016 Jan 4;6(1):326–38.

10. Binder JB, Raines RT. Simple Chemical Transformation of Lignocellulosic Biomass into Furans for Fuels and Chemicals. J Am Chem Soc. 2009 Feb 11;131(5):1979–85.

11. Sheldon RA, Arends IWCE, Hanefeld U. Green Chemistry and Catalysis [Internet]. 1st ed. Wiley; 2007 [cited 2024 Feb 8]. Available from: https://onlinelibrary.wiley.com/doi/book/10.1002/9783527611003

12. Bozell JJ, Petersen GR. Technology development for the production of biobased products from biorefinery carbohydrates—the US Department of Energy's "Top 10" revisited. Green Chem. 2010;12(4):539.

13. Mika LT, Cséfalvay E, Németh Á. Catalytic Conversion of Carbohydrates to Initial Platform Chemicals: Chemistry and Sustainability. Chem Rev. 2018 Jan 24;118(2):505–613.

14. Mascal M, Dutta S. Chemical-Catalytic Approaches to the Production of Furfurals and Levulinates from Biomass. In: Nicholas KM, editor. Selective Catalysis for Renewable Feedstocks and Chemicals [Internet]. Cham: Springer International Publishing; 2014 [cited 2024 May 27]. p. 41–83. (Topics in Current Chemistry; vol. 353). Available

from: https://link.springer.com/10.1007/128_2014_536

15. Ras E, Maisuls S, Haesakkers P, Gruter G, Rothenberg G. Selective Hydrogenation of 5-Ethoxymethylfurfural over Alumina-Supported Heterogeneous Catalysts. Adv Synth Catal. 2009 Dec;351(18):3175–85.

16. Gerardus Johannes Maria Gruter. 5-SUBSTITUTED 2-(ALKOXYMETHYL)FURANS. US 8,231,693 B2, 2012.

17. De Jong E, Vijlbrief T, Hijkoop R, Gruter GJM, Van Der Waal JC. Promising results with YXY Diesel components in an ESC test cycle using a PACCAR Diesel engine. Biomass and Bioenergy. 2012 Jan;36:151–9.

18. Cao Q, Liang W, Guan J, Wang L, Qu Q, Zhang X, et al. Catalytic synthesis of 2,5-bis-methoxymethylfuran: A promising cetane number improver for diesel. Applied Catalysis A: General. 2014 Jul;481:49–53.

19. Ikariya T, Blacker AJ. Asymmetric Transfer Hydrogenation of Ketones with Bifunctional Transition Metal-Based Molecular Catalysts. Acc Chem Res. 2007 Dec 1;40(12):1300–8.

20. Wang D, Astruc D. The Golden Age of Transfer Hydrogenation. Chem Rev. 2015 Jul 8;115(13):6621–86.

21. Osatiashtiani A, Lee AF, Wilson K. Recent advances in the production of γ-valerolactone from biomass-derived feedstocks via heterogeneous catalytic transfer hydrogenation. J of Chemical Tech & Biotech. 2017 Jun;92(6):1125–35.

22. Xue Z, Jiang J, Li G, Zhao W, Wang J, Mu T. Zirconium–cyanuric acid coordination polymer: highly efficient catalyst for conversion of levulinic acid to γ-valerolactone.

Catal Sci Technol. 2016;6(14):5374–9.

23. Leng Y, Shi L, Du S, Jiang J, Jiang P. A tannin-derived zirconium-containing porous hybrid for efficient Meerwein–Ponndorf–Verley reduction under mild conditions. Green Chem. 2020;22(1):180–6.

24. Zhou S, Dai F, Xiang Z, Song T, Liu D, Lu F, et al. Zirconium–lignosulfonate polyphenolic polymer for highly efficient hydrogen transfer of biomass-derived oxygenates under mild conditions. Applied Catalysis B: Environmental. 2019 Jul;248:31–43.

25. Rojas-Buzo S, García-García P, Corma A. Hf-based metal–organic frameworks as acid–base catalysts for the transformation of biomass-derived furanic compounds into chemicals. Green Chem. 2018;20(13):3081–91.

26. Li H, He J, Riisager A, Saravanamurugan S, Song B, Yang S. Acid–Base Bifunctional Zirconium *N* -Alkyltriphosphate Nanohybrid for Hydrogen Transfer of Biomass-Derived Carboxides. ACS Catal. 2016 Nov 4;6(11):7722–7.

27. Hu L, Li N, Dai X, Guo Y, Jiang Y, He A, et al. Highly efficient production of 2,5-dihydroxymethylfuran from biomass-derived 5-hydroxymethylfurfural over an amorphous and mesoporous zirconium phosphonate catalyst. Journal of Energy Chemistry. 2019 Oct;37:82–92.

28. Hu L, Dai X, Li N, Tang X, Jiang Y. Highly selective hydrogenation of biomass-derived 5-hydroxymethylfurfural into 2,5-bis(hydroxymethyl)furan over an acid–base bifunctional hafnium-based coordination polymer catalyst. Sustainable Energy Fuels. 2019;3(4):1033–41.

29. Hu L, Li T, Xu J, He A, Tang X, Chu X, et al. Catalytic transfer hydrogenation of biomass-derived 5-hydroxymethylfurfural into 2,5-dihydroxymethylfuran over magnetic zirconium-based coordination polymer. Chemical Engineering Journal. 2018 Nov;352:110–9.

30. Hu D, Hu H, Jin H, Zhang P, Hu Y, Ying S, et al. Building hierarchical zeolite structure by post-synthesis treatment to promote the conversion of furanic molecules into biofuels. Applied Catalysis A: General. 2020 Jan;590:117338.

31. Jae J, Mahmoud E, Lobo RF, Vlachos DG. Cascade of Liquid-Phase Catalytic Transfer Hydrogenation and Etherification of 5-Hydroxymethylfurfural to Potential Biodiesel Components over Lewis Acid Zeolites. ChemCatChem. 2014 Feb;6(2):508–13.

32. Luo J, Yu J, Gorte RJ, Mahmoud E, Vlachos DG, Smith MA. The effect of oxide acidity on HMF etherification. Catal Sci Technol. 2014;4(9):3074–81.

33. Lewis JD, Van de Vyver S, Crisci AJ, Gunther WR, Michaelis VK, Griffin RG, et al. A Continuous Flow Strategy for the Coupled Transfer Hydrogenation and Etherification of 5-(Hydroxymethyl)furfural using Lewis Acid Zeolites. ChemSusChem. 2014 Aug;7(8):2255–65.

34. Shinde S, Rode C. Cascade Reductive Etherification of Bioderived Aldehydes over Zr-Based Catalysts. ChemSusChem. 2017 Oct 23;10(20):4090–101.

35. Wei J, Wang T, Liu H, Li M, Tang X, Sun Y, et al. Highly Efficient Reductive Etherification of 5-Hydroxymethylfurfural to 2,5-Bis(Alkoxymethyl)Furans as Biodiesel Components over Zr-SBA Catalyst. Energy Tech. 2019 May;7(5):1801071.

36. Li H, Saravanamurugan S, Yang S, Riisager A. Direct transformation of carbohydrates

to the biofuel 5-ethoxymethylfurfural by solid acid catalysts. Green Chem. 2016;18(3):726–34.

37. Güleç F, Sher F, Karaduman A. Catalytic performance of Cu- and Zr-modified beta zeolite catalysts in the methylation of 2-methylnaphthalene. Pet Sci. 2019 Feb;16(1):161–72.

38. Ranjan Sahu H, Ranga Rao G. Characterization of combustion synthesized zirconia powder by UV-vis, IR and other techniques. Bull Mater Sci. 2000 Oct;23(5):349–54.

39. Perez-Pariente J, A. Martens J, A. Jacobs P. Crystallization mechanism of zeolite beta from (TEA)2O, Na2O and K2O containing aluminosilicate gels. Applied Catalysis. 1987 Jan;31(1):35–64.

40. Córdoba LF, Sachtler WMH, Montes De Correa C. NO reduction by CH4 over Pd/Co-sulfated zirconia catalysts. Applied Catalysis B: Environmental. 2005 Apr;56(4):269–77.

41. He D, Ding Y, Luo H, Li C. Effects of zirconia phase on the synthesis of higher alcohols over zirconia and modified zirconia. Journal of Molecular Catalysis A: Chemical. 2004 Feb;208(1–2):267–71.

42. Shanjiao K, Yanjun G, Tao D, Ying Z, Yanying Z. Preparation and characterization of zeolite beta with low SiO2/Al2O3 ratio. Pet Sci. 2007 Mar;4(1):70–4.

43. Ma X, Gong J, Wang S, He F, Yang X, Wang G, et al. Characterization and reactivity of silica-supported bimetallic molybdenum and stannic oxides for the transesterification of dimethyl oxalate with phenol. Journal of Molecular Catalysis A: Chemical. 2004 Aug;218(2):253–9.

44. Kovalenko V, Zhukova A, Rumyantseva M, Gaskov A, Yushchenko V, Ivanova I, et al. Surface chemistry of nanocrystalline SnO2: Effect of thermal treatment and additives. Sensors and Actuators B: Chemical. 2007 Sep 20;126(1):52–5.

45. Wei J, Wang T, Liu H, Liu Y, Tang X, Sun Y, et al. Assembly of Zr-based coordination polymer over USY zeolite as a highly efficient and robust acid catalyst for one-pot transformation of fructose into 2,5-bis(isopropoxymethyl)furan. Journal of Catalysis. 2020 Sep;389:87–98.

4.7. GC-MS data of synthesized product

2, 5 bis Propoxymethyl furan (BPMF)

GC-MS data: 212(BPMF), 153, 139, 111, 97, 83, 69, 43, 31

170 (HPMF), 153, 139, 127, 97, 81, 69, 55, 41, 30
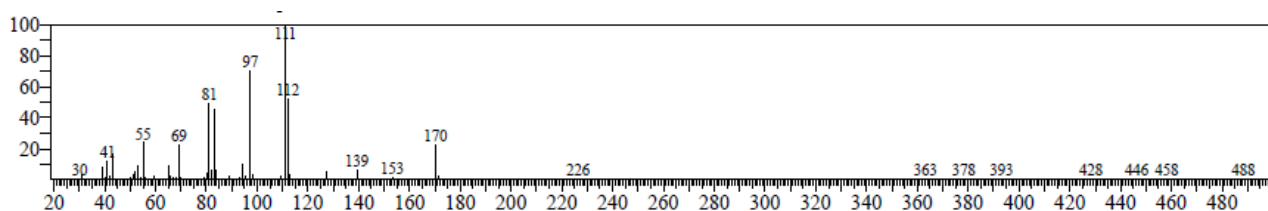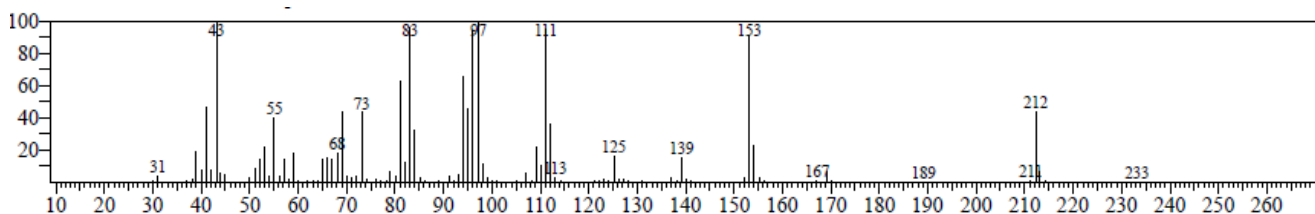
CHAPTER – 5

Effect of tunable acidic properties on the selectivity of biofuel candidate 2, 5-Bis (PropoxyMethyl) Furan (BPMF) using Sn- Hβ and Sn-dAlHβ catalysts
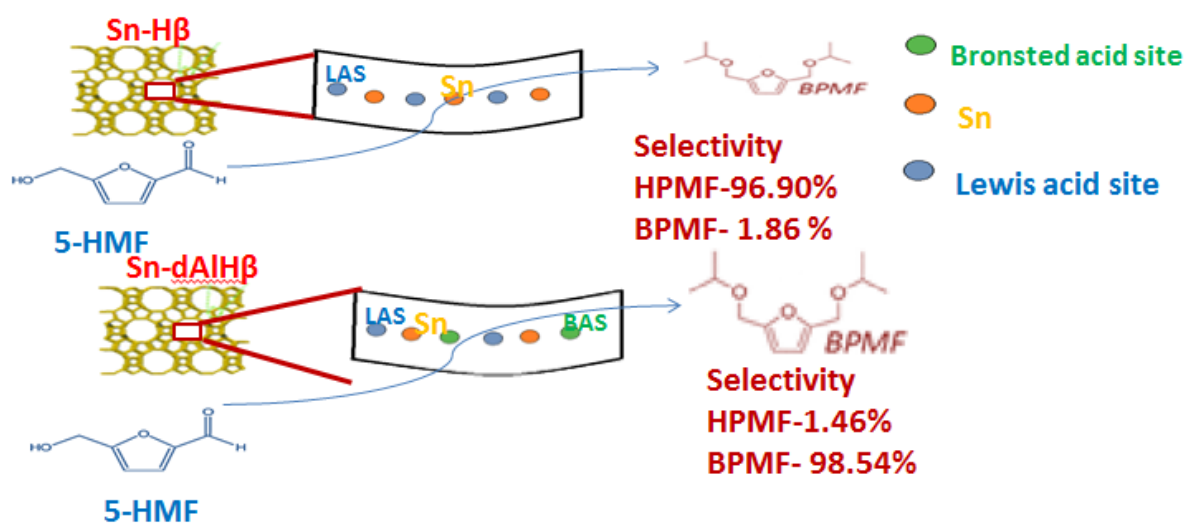
Results obtained from the work discussed in the Chapter 4 shows that, the Zr-Lewis acid sites are found to promote etherification more strongly than hydrogen transfer. By using a mixed catalytic system, the number of Lewis acid sites is increased and the Brønsted acid sites are reduced, which results in an increase in the selectivity of BPMF. Which conclude that that the Lewis acidic sites and Bronsted acidic sites of the catalyst play a key role in the selectivity of BPMF. Sn metal based is also Lewis acid and shows higher Lewis acidity than Zr metal based catalyst. With aim to achieve higher selectivity of 2,5-bis(propoxymethyl) furan (BPMF) which is a potential biofuel candidate, In the present work, the effect of tunable acidic properties such as Lewis and Bronsted acidity of Sn- Hβ and Sn-dAlβ (Sn in dealuminated Hβ) catalysts on the selectivity of 2,5-bis(propoxymethyl)furan (BPMF) was studied by carrying out one-pot reductive etherification of 5-hydroxymethylfurfural (5-HMF) using 2-propanol as a hydrogen donor.

The catalysts that were readied underwent analysis using techniques such as temperature-programmed desorption of ammonia (NH$_3$-TPD), powder X-ray diffraction, transmission electron microscopy, Pyridine-IR spectroscopy, BET surface area measurement, and Fourier transform infrared spectroscopy. Under the optimized reaction conditions, which included a temperature of 150°C, a catalyst loading of 0.25 g, a reaction time of 4 h, and a concentration of 1 g of 5-HMF, impressive results were obtained: a 93.57% conversion of 5-HMF and a 98.54% selectivity towards BPMF.

It was observed the catalysts remains active up to 5 cycles and slight/moderate change was observed in the conversion of 5-HMF, while selectivity of BPMF remains intact.

5.1. Introduction

The exhaustive usage of petroleum products and petrochemicals resulted into deterioration of environment, depletion of fossil fuels resources(1–6). In this regards, transformation of sustainable lignocellulosic biomass, which is abundantly available renewable carbon resources on the earth as an alternative of fossil fuel has been become needs of today(7–12). Biomass represents an unconventional energy reservoir that offers numerous advantages, including reduced environmental impact, renewability, cost-effectiveness, and widespread availability. These attributes establish biomass as a significant contributor to the sustainable advancement of valuable chemical production(13–15). Hence, transformation of bio-derived platform molecules into valuable chemical and derivatives has drawn the more attention nowadays(16–19). Numerous bio-derived compounds, including 5-hydroxymethylfurfural (5-HMF), levulinic acid, furfurals, sugar alcohols, lactic acid, succinic acid, and phenols, are categorized as foundational chemicals. These substances serve as a cornerstone for the industrial-scale synthesis of various essential compounds(20–22). Over the recent years, there has been a notable surge in the popularity and promise of 5-hydroxymethylfurfural (5-HMF) as a biomass-derived molecule. This

compound holds the potential for conversion into a diverse array of valuable chemicals, including key components for polymers and promising candidates for biofuels. Consequently, the focus on developing methods to manufacture biofuels from 5-HMF has been on the rise. For instance, 2,5-bis (hydroxymethyl) furan (BHMF) reductive derivative of 5-HMF, which can be transformed into the di ethers which are considered as potential biofuel compounds(23) and so, previous studies have reported the etherification of BHMF(24–27). For instance 5-ethoxymethylfurfural (EMF) is considered as a promising bio-diesel or additive, because of its similar energy density (30.3 MJ/L) to that of commercial available gasoline (31.1 MJ/L) or diesel (33.6 MJ/L)(28). Recent findings indicate(29) that the presence of the aldehyde group in the context of 5-ethoxymethylfurfural (EMF) has a discernible impact on the stability of the molecules. Specifically, when EMF is combined with conventional diesel fuel, issues of phase separation arise. In contrast, di ethers and 2,5-bis(alkoxymethyl)furans (BAMFs) demonstrate superior energy densities and exhibit favorable compatibility with diesel fuel during blending processes(30). Jong et al.(30), reported that when 2,5-bisethoxymethylfuran (BEMF) was blended with diesel in different blending ratios there was no significant change in engine operation and also exhibits reduction in emissions of polluting gases. Cao et al.(31), also documented the complete compatibility between 2,5-bismethoxymethylfuran (BMMF) and diesel fuel. Typically, the direct use of H_2 gas serves as the hydrogen source for converting HMF into BAMFs. However, due to the cost and safety considerations associated with producing and handling H_2 gas, it is preferable to minimize its usage to ensure economic viability and safety. In this context, catalytic transfer hydrogenation (CTH) presents an attractive alternative. This approach is advantageous as it allows for the thorough reduction of carbonyl compounds, including aldehydes and ketones, to their corresponding alcohols through the

Meerwein−Ponndorf−Verley (MPV) reaction. This transformation employs formic acid and alcohols as hydrogen donors and is being explored as a more efficient and safer method compared to conventional hydrogenation using molecular hydrogen(32–35). Numerous researchers have documented the sequential process of hydrogenation followed by etherification as a means to generate BAMFs from HMF. This strategy proves economically advantageous, as it lowers the overall production costs of BAMFs and streamlines the process by reducing the number of required unit operations. Consequently, a wide array of catalysts and reaction conditions(36–43) have been investigated to achieve the reductive etherification of 5-HMF. These studies have been unveiled varying levels of selectivity in BAMF formation. A notable feature of this approach is the dual role played by alcohol- they not only serve as a solvent but also function as etherifying agents. This multifunctional role obviates the need for molecular hydrogen, leading to formation of BAMFs. For example, Cao et al.(31), employed an HZSM-5 catalyst with a Si/Al ratio of 25 for hydrogenation using H_2 gas and the etherification of BHMF with methanol to synthesize BMMF, resulting in a maximum yield of 70%. Another investigation by Balakrishnan et al.(44) detailed a one-pot reductive etherification process converting 5-HMF to BAMFs. This was achieved using various catalysts, including Amberlyst-15 and Dowex DR-2030, along with alcohols like ethanol and butanol, yielding up to 80% product. Similarly, Han et al.(45) utilized an Amberlyst-15 catalyst for the etherification of BHMF into BAMFs using different solvents (methanol, ethanol, propanol, and butanol), leading to yields of 50%, 70%, 74%, and 71% for BMMF, BEMF, BPMF, and BBMF, respectively. Likewise, Wi et al.(46) synthesized Zr-SBA-UH, conducting reactions with ethanol and 2-propanol at 150°C in 4 h, resulting in the formation of BEMF and BIPMF with yields of 87.9% and 93.9%, respectively. When Zr-SBA-UH was combined with alternative solvents such as 1-propanol, 1-butanol, 2-butanol, and MPrOH, it generated

BPMF, BBMF, BSBMF, and BMPMF with corresponding yields of 38.1%, 17.1%, 4.4%, and 54.1%, under the same reaction conditions. The reason for higher selectivity of BAMF with 2-propanol as compared to other alcohol is the effect of stearic hindrance and reduction potential of alcohol. It was reported that a lower value of reduction potential shows easy removal of hydrogen for alcohols which encourage the MPV reduction and 2-propnaol has a lower value of reduction potential as compared to other alcohols. Wei et al.(47) prepared Zr-SBA to synthesized BPMF by reductive etherification of 5-HMF and obtained 81.2% selectivity of BPMF after 4 h at 180°C. Jae et al.(48) employed a Sn-beta catalyst to carry out reduction and etherification reactions in the presence of 2-propanol, leading to a 79.5% yield of BIPMF after a 6-hour period at 180°C. In a similar vein, Luo et al.(49) achieved a 60.9% BPMF yield using the same reaction conditions and catalyst (Sn-beta) in 3 h duration. Lewis et al.(50) manipulated the Lewis acidity of an Hf-Beta catalyst, resulting in an elevated 81% yield of BBMF. This was accomplished by utilizing 1-butanol as a solvent and conducting the reaction at 120°C in 1 h. Shinde and Rode(51) synthesized a Zr-Mont catalyst through an impregnation method, demonstrating its efficacy in both reduction and etherification reactions. The robust interaction between Zr and Mont imbued the Zr-Mont catalyst with enhanced Lewis acidity, culminating in superior yields of 95% BIPMF and 96% BBMF at 150°C, surpassing the performance of Sn-Beta and Hf-Beta catalysts. Rana et al.(52) synthesized BPMF by one-pot reductive etherification using mixed catalyst Zr-Hβ + ZrO(OH)$_2$ and obtained 91.23 % selectivity of BPMF. It was noted that competitive reactions reduces the selectivity of BAMFs. So, highly selective and efficient catalysts are necessary to achieve high selectivity of BAMFs. As indicated in recent literature, the presence of Lewis and Brønsted acidic sites has been highlighted for their significant influence on achieving heightened product selectivity and minimizing undesirable secondary reactions. Certain studies have suggested that the process of

etherifying 5-HMF with alcohol is primarily governed by the presence of Lewis acid, while concurrent competitive reactions are primarily regulated by the presence of Brønsted acid(23). Lanzafam et al.(53) showed that strong Bronsted acidity was responsible for the furan ring opening reaction, whereas Lewis acidity led to formation of EMF. On other hand, Barbera at el.(54) used sulphated zirconia and reported that formation of EMF was suppressed due to increased Bronsted acidity and decreased Lewis acidity. However, Luo et at.(49) concluded that both Lewis and Bronsted acid were necessary for the etherification of 5-HMF.

In this study, Sn-Hβ and Sn-dAlHβ catalysts were synthesized through wet impregnation and post-synthesis methods, respectively. These catalysts were then employed to facilitate the conversion of 5-HMF to 2,5-bis(isopropoxymethyl)furan (BPMF) using 2-propanol. The aim was to investigate the impacts of acidity and preparation techniques on the etherification of 5-HMF. A comprehensive examination of the pore structures and acidity of Sn-Hβ and Sn-dAlHβ was conducted. It was observed that Sn-dAlHβ exhibited a substantial quantity of potent Lewis acid sites alongside an ample number of Brønsted acid sites, setting the stage for the reductive etherification of 5-HMF into BPMF. While previous studies primarily concentrated on synthesizing BPMF from 5-HMF under elevated temperatures, the current research delved into the mechanism of the reductive etherification process using a catalyst in the presence of 2-propanol. This revealed that 5-HMF underwent etherification into both HPMF and BPMF in the presence of an excess of Lewis acid sites and a sufficient amount of Bronsted acid sites. Notably, the study presented herein showcases the accomplishment of one-pot reductive etherification of 5-HMF into BPMF at 150°C over a 4h timeframe, achieving an impressive selectivity of 98.54% using the Sn-dAlHβ catalyst.

5.2. Materials and methods

5.2.1. Materials

The chemicals acquired were utilized without further modification. In India, 5-(hydroxymethyl) furfural (98% purity) was provided by SRL (Sisco Research Laboratories Pvt. Ltd.). All alcohols, solvents, aqueous ammonia (30%), and metal precursors including Tin Chloride pentahydrate ($SnCl_4.5H_2O$) were procured from Sigma-Aldrich, India. Hβ was bought from Sud-cheme India Private Limited, located in Vadodara, Gujarat.

5.2.2. Catalyst Preparation

5.2.2.1 Preparation of Sn-Hβ

The modification of Hβ with Sn was carried out using the conventional wet impregnation(55) method as outlined below: Initially, a specific quantity of $SnCl_4 \bullet 5H_2O$ was dissolved in 100 mL of deionized water, yielding solutions of 0.3 M and 0.05 M. Subsequently, 10 g of Hβ was introduced into the solution. The mixture underwent treatment at 353 K in 4 h under atmospheric pressure. Afterward, it was filtered and subjected to rinsing with deionized water until the wash water no longer contained chloride ions. The resulting filter cake was then dried at 373 K in duration of 2 h. Following the drying process, the modified zeolite was subjected to calcination in a muffle furnace at 823 K in 6 h.

5.2.2.2. Preparation of Sn-dAl Hβ

Sn-Hβ catalysts were prepared using a two-step post-synthesis procedure(56), involving the de-alumination of the initial Hβ catalyst and subsequent integration of Sn species into the framework of the de-aluminated Si-Beta using dry impregnation and calcination. To elaborate, commercial Hβ with a nominal nSi/nAl ratio of 2.6 was stirred in a 13 mol L^{-1} nitric acid aqueous solution (20 mL per gram of zeolite) at 373 K for an overnight period, resulting in the formation of a de-aluminated Beta (Si-Beta). The resultant powder was

filtered, meticulously washed with deionized water, and then dried at 353 K overnight. Prior to the incorporation of Sn, the sample underwent a pre-treatment phase at 473 K overnight under vacuum conditions to eliminate physisorbed water. The resulting solid mixture was introduced into a reactor, sealed, and gradually heated to 823 K over a span of 6 h (with a heating rate of 5 K/min) under a vacuum. Following this, the material was subjected to calcination under a stream of flowing air at 823 K in 6 h.

5.3. Catalyst Characterization

5.3.1. Powder X-ray diffraction measurements

Powder X-ray diffraction (PXRD) profiles were acquired utilizing a Bruker D8 Advance X-ray diffractometer. The LynxEye Superspeed detector and Cu Kα radiation sourced from a PW Bragg–Brentano (BB) goniometer ($\theta/2\theta$) were employed for this purpose, with operational settings at 40 kV and 35 mA. The recorded diffractograms spanned the 2θ range of 5° to 90°, employing a 2θ step increment of 0.02°.

5.3.2. BET measurements

The surface areas according to the Brunauer–Emmett–Teller (BET) method, along with pore volume and pore size distribution using Barrett–Joyner–Halenda (BJH) analysis, were evaluated for the catalysts under investigation. This assessment involved N_2 adsorption-desorption analysis performed at a temperature of -196°C. Prior to the analysis, the catalysts were subjected to vacuum degassing at a temperature of 200 ± 2°C.

5.3.3. TEM

Images of the catalyst were captured using a JEOL JEM2100 transmission electron microscope (TEM).

5.3.4. Temperature Programmed Desorption of NH_3 (NH_3-TPD)

The acidity strength and quantity of acid sites located on the catalyst's surface were ascertained via Temperature Programmed Desorption (TPD), utilizing the Belcat-II instrument from BEL Japan. In a standard protocol, a 75 mg catalyst sample underwent pretreatment at 300°C with a continuous flow of helium in 2 h within a quartz U-tube, preceding the chemisorption step. Subsequently, the temperature was lowered to 50°C, and a mixture of 10% NH_3 in helium was directed through the catalyst in duration of 30 min. Following this, any physically adsorbed NH_3 gas was purged out by flowing helium for 15 min at 50°C. Subsequent to this, the TPD analysis of NH_3 adsorbed onto the acidic sites was conducted. The temperature was raised at a rate of 10°C per min, elevating the samples up to 800°C within a helium environment, while utilizing a Thermal Conductivity Detector (TCD) to quantify the quantity of desorbed gas.

5.3.5. Acidity measurement by titration method pyridine FTIR

Total acidity of Hβ was determined employing the n-butyl amine titration technique(57). In this approach, 0.25 g of support/catalyst was suspended within 25 mL of a 0.025N n-butyl amine solution in toluene. The mixture was allowed to stand in 24 h to neutralize the acidic sites present on the surface. Following this, titration was performed using 0.025N tri-chloroacetic acid solutions in toluene, utilizing neutral red indicator. The outcome of this process yields the total acidity measurement for the catalyst.

Infrared spectra for pyridine adsorption (Py-IR) were recorded using a Cary630 FT-IR Spectrometer. The initial step involved degassing of a self-supporting sample pellet, weighing approximately 20 mg and measuring 10 mm in diameter, to a temperature of 500°C in duration of 2 h under a vacuum. This step was taken to eliminate any moisture and other adsorbed gases from the sample. The subsequent phase consisted of saturating all the acid sites on the sample by exposing it to pyridine at a temperature of 150°C for a

period of 1 h. The identification of Lewis and Bronsted acid sites was achieved by analyzing the bands located at 1445 cm^{-1}, 1638 cm^{-1}, and 1543 cm^{-1}.

5.4. Catalytic Activity

The experiment was executed within a 100 mL stainless steel autoclave reactor. The autoclave was loaded with 1 g of hydroxymethylfurfural (HMF), 0.2 and 0.25 g of the catalyst, and 50 mL of 2-propanol. After sealing the autoclave, it was heated to the desired reaction temperature of 140°C-170°C under continuous stirring at 550 rpm for reaction duration of 4 h. Following each reaction, the autoclave was cooled. At the conclusion of each run, the mixture of products was separated from the catalyst through centrifugation and subsequently subjected to analysis using Gas Chromatography-Mass Spectrometry (GC-MS). The GC-MS was equipped with a DB-1701 column (60M x 0.32mm x 1μm film thickness), consisting of a 14% cyanopropylphenyl phase and an 86% dimethylpolysiloxane phase.

To assess the performance of the catalytic systems, two metrics were defined: conversion of 5-HMF ($X_{5\text{-HMF}}$, %) and selectivity to products (Si). The calculation of 5-HMF conversion ($X_{5\text{-HMF}}$) involved determining the ratio of the amount of 5-HMF converted to the initial amount of 5-HMF. Selectivity values for reaction products such as BHMF, HPMF, and BPMF (Si) were calculated by dividing the quantity of formed products by the amount of 5-HMF that underwent conversion. The reaction for the reductive etherification of 5-HMF to BPMF is as shown in Figure 5.1.

$$\text{conversion } (\%) = \frac{(I.N.)_i - (I.N.)_f}{(I.N.)_i} * 100 \quad ,$$

Where, (I.N.)i = Initial moles of 5-HMF   & (I.N.)f = Final moles of 5-HMF

$$\text{selectivity } (\%) = \frac{\text{moles of product formed}}{\text{moles of 5-HMF converted}} * 100$$
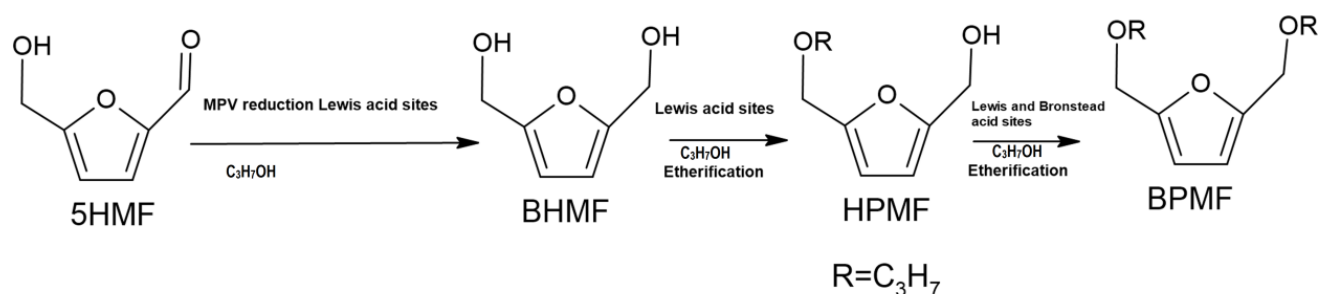
Figure 5.1 Reductive etherification of 5-HMF to BPMF

5.5. Results and discussions

5.5.1. Physical and chemical properties of catalysts

5.5.1.1. Transmission Electron Microscopy

Transmission Electron Microscopy (TEM) analysis was performed to acquire information about the particle size and morphology of the catalysts. The TEM images, displayed in Figure 5.2 (a & b), revealed that the samples contained crystallites with dimensions of approximately 31 nm and 24 nm for Sn-Hβ and Sn-dAl Hβ, respectively. However, the identification of metal particles proved challenging due to their tendency to aggregate during the ion exchange method used for catalyst preparation. The mean size of the metal particles and the d-spacing were estimated at around 13 nm (Figure 5.2 (c)) and 0.327 nm, respectively.
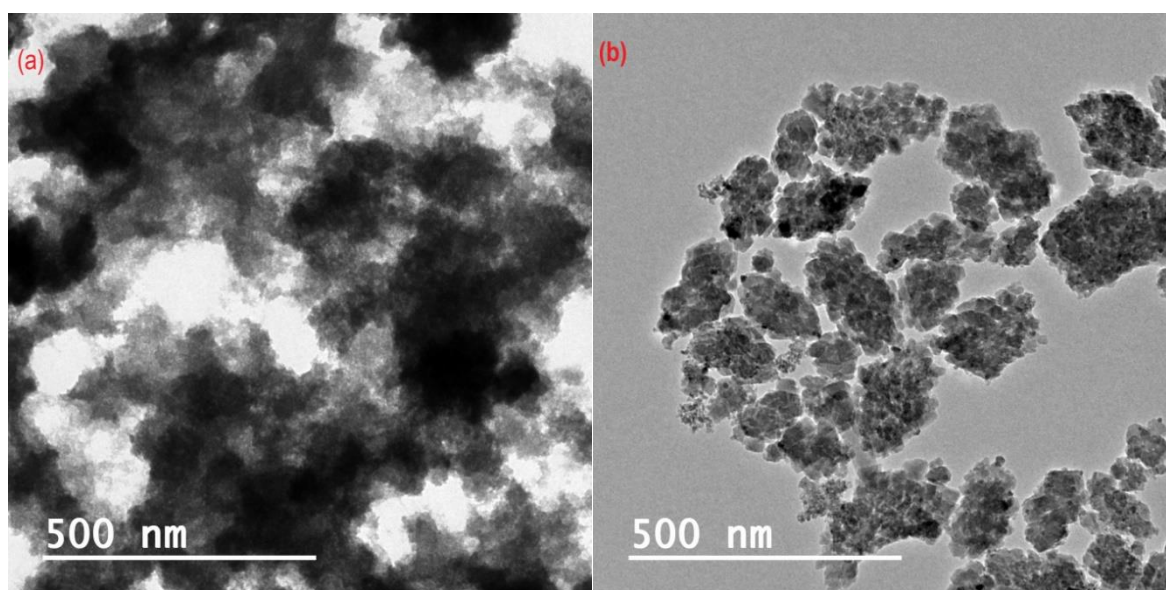
Figure 5.2 TEM Images and particle size (a) Sn-Hβ (b) Sn-dAlHβ (c) particle size

distribution

5.5.1.2. Powder X-ray diffraction (PXRD) analysis

In Figure 5.3(a), the PXRD patterns of the Hβ catalysts exhibit distinctive peaks at

diffraction angles of $2\theta = 7.61°$ and $22.45°$. Moving on to Figure 5.3(b & c), the PXRD

patterns of the Sn-Hβ and Sn-dAlHβ catalysts display a pattern that closely resembles that

of the parent Hβ, with evident peaks at $2\theta = 22.7°$, $26.94°$, $34.07°$, $38.17°$, and $52.04°$.

Following the incorporation of Sn, the zeolite sample's spacing becomes larger, indicating

an expansion of the BEA framework. This expansion serves as clear evidence of the successful integration of Sn species into the Hβ framework (Hβ, 2θ=22.45° / Sn-Hβ and Sn-dAlHβ = 2θ=22.70°).

Notably, no novel diffraction peaks emerged, underscoring the preservation of the MFI structure of the Hβ catalyst and the absence of new phases post-modification. This demonstrates that the introduction of Sn was well-dispersed and did not induce the formation of new phases. The presence of distinct diffraction peaks at 34.07°, attributed to Sn (JCPDS file No.-00-004-0673)(58,59) was distinctly observed in the Sn-Hβ and Sn-dAlHβ catalyst samples.
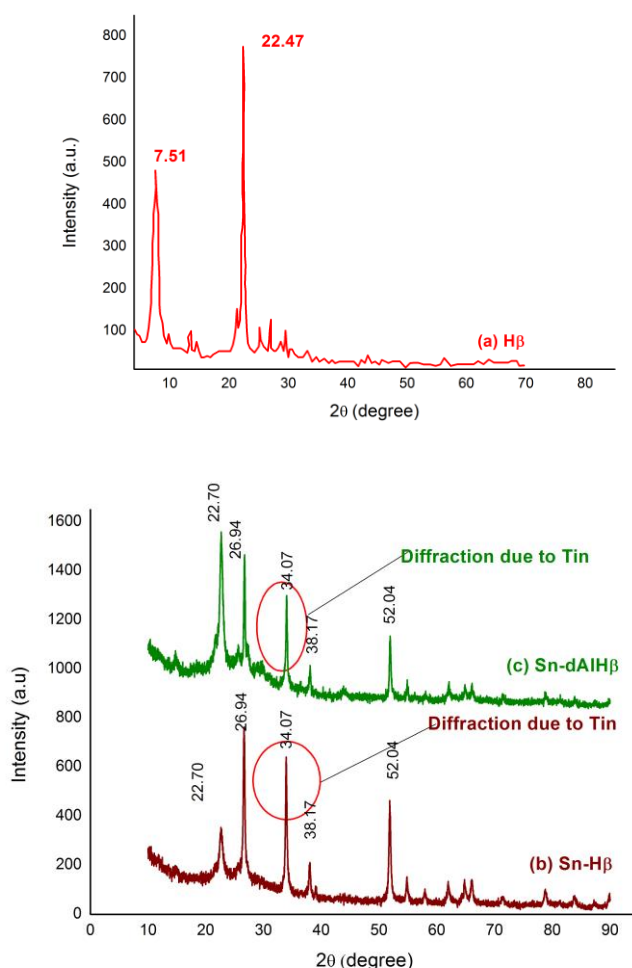
Figure 5.3 PXRD patterns of (a)Hβ and (b) 1 Sn-Hβ (c) Sn-dAl Hβ catalysts.

5.5.1.3. Surface areas, external surface area and pore volumes

The N_2 adsorption results for the catalysts are outlined in Table 5.1. Observing Table 5.1, it's apparent that the specific surface area has decreased for the Sn-Hβ and Sn-dAlHβ catalysts. The introduction of Sn to Hβ doesn't appear to significantly impact the specific surface area and micro pore volume when compared to the Hβ catalyst. An increase in mesopore volume has been noted, potentially attributed to the extraction of Al atoms from the zeolites. The Sn-dAlHβ sample exhibits a notably larger external surface area and mesopore volume in contrast to the Sn-Hβ prepared via the wet impregnation method. The greater mesopore volume in the Sn-dAlHβ sample aids in enhancing mass transfer during heterogeneous catalytic reactions, consequently leading to heightened intrinsic site activity.

Table 5.5. Textures of Hβ, Sn-Hβ and Sn-dAl Hβ catalyst

Sample	Surface area, m^2/g	Pore volume, cm^3/g			External surface area, m^2/g
	$S.A^a$	$V_{pore,}^b$	V_{micro}^c	V_{meso}	S_{meso}^c
Hβ	622	0.45	0.15	0.30	-
Sn-Hβ	429	0.28	0.18	0.10	110
Sn-dAl Hβ	580	0.62	0.16	0.46	156

a-S.A- BET surface area, b-Total pore volume measured at P/P0= 0.9999,c-t-plot method, V_{meso}= V_{pore}- V_{micro}, External surface area.

5.5.1.4. Acidity of catalysts

The NH_3-TPD analysis was utilized to determine the quantity and strength of acidic sites in the Sn-Hβ and Sn-dAlHβ catalysts. The efficacy of product selectivity and the rate of undesired reactions are significantly influenced by both Bronsted and Lewis acids. Literature suggests that Lewis acid sites enhance the catalytic activity for MPV reduction, and increased Lewis acid sites correspond to higher etherification, while reduced Bronsted

acid sites lead to decreased production of undesired byproducts(48). Consequently, the preparation of catalysts with limited Bronsted acid and ample Lewis acid is crucial for efficient HMF to BPMF etherification. The NH_3-TPD results for Sn-Hβ and Sn-dAlHβ catalysts are presented in Figure 5.4, and the acidity of Hβ was determined via the n-butylamine titration technique. The NH_3-TPD profiles of Sn-Hβ and Sn-dAlHβ catalysts, shown in Figure 5.4, display distinct peaks in the lower temperature region (<250°C), middle temperature range (250°C to 550°C), and higher temperature range (>550°C). The Sn-Hβ catalyst exhibits three characteristic desorption peaks at 130.7°C, 488.3°C, and 548.7°C, while the Sn-dAlHβ catalyst presents peaks at approximately 173°C, 484.5°C, and 549.4°C. These peaks are identified as NH_3 desorption from weak, medium, and strong acid sites. The middle and higher temperature peaks correspond to desorption from strong acidic sites, while the lower temperature peaks are attributed to the release of NH_3 from weak acidic sites.

The data indicates the presence of both weak and strong acidic sites in the catalyst. The middle and high-temperature peaks around 488.3°C and 548.7°C for Sn-Hβ, and 484.5°C and 549.4°C for Sn-dAlHβ, respectively, are representative of desorption from Lewis acid sites(60,61). Table 5.2 reveals that the impregnation of Sn onto Hβ resulted in a reduction in total acidity. Specifically, the total acid sites on Sn-Hβ and Sn-dAlHβ decreased to 1.34 and 2.77 mmol/g from 2.85 mmol/g. This alteration in acidity nature is linked to the introduction of Sn species. The Sn impregnation led to a significant increase in Lewis acid sites and a decrease in Bronsted acid sites, as evidenced by the values of weak, medium, and strong acid sites in Table 5.2. Notably, the Sn-dAlHβ catalyst displayed a higher value of medium acidic sites (1.86 mmol/g) compared to Sn-Hβ (0.42 mmol/g). This shift in Bronsted and Lewis acid sites is attributed to the robust interaction between intrinsic acid sites and Sn species, which resulted in the conversion of some Bronsted acid sites into Sn-

118

Lewis acid sites. These Sn-Lewis acid sites, known from literature, have the capacity to accelerate the etherification process(49). To support this conclusion, Py-IR analysis was conducted to differentiate between Lewis and Bronsted acid sites. Pyridine, acting as a Lewis base, can interact with Bronsted acid sites to form pyridinium ions, evident from the FTIR bands between 1512 and 1567 cm^{-1}. It can also adsorb on the surface of Lewis acid sites, indicated by FTIR bands at 1445 and 1638 cm^{-1}. Figure 5.5 displays the Pyridine spectra of Sn-Hβ and Sn-dAlHβ catalysts, showing the presence of both Lewis and Bronsted acid sites. The quantities of these acid sites are detailed in Table 5.3. Remarkably, the impregnation of Sn onto Hβ increased the Lewis acid sites while reducing Bronsted acid sites. Table 5.3 provides a quantitative analysis of Bronsted and Lewis acid sites for both catalysts, demonstrating that Sn-dAlHβ possesses a higher quantity of Lewis acid sites compared to Sn-Hβ, possibly attributed to variations in their preparation methods and the quality of Sn impregnation on Hβ and dAlHβ.
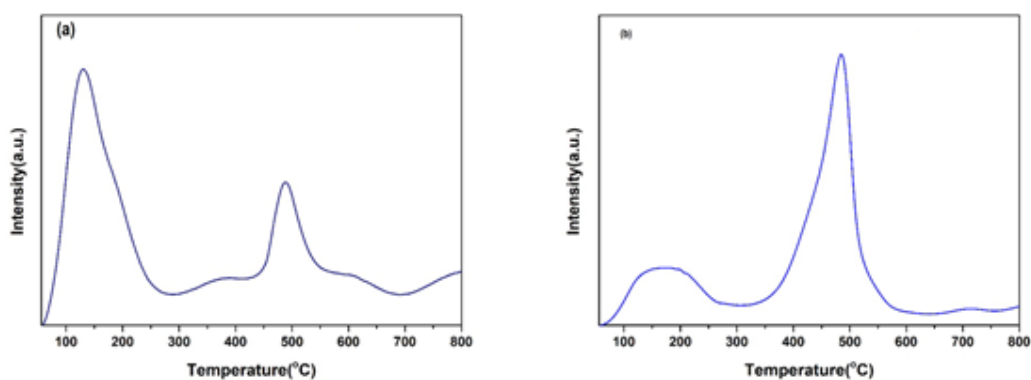
Figure 5.4 NH$_3$-TPD profiles of (a) Sn-Hβ (b) Sn-DAl Hβ**.**
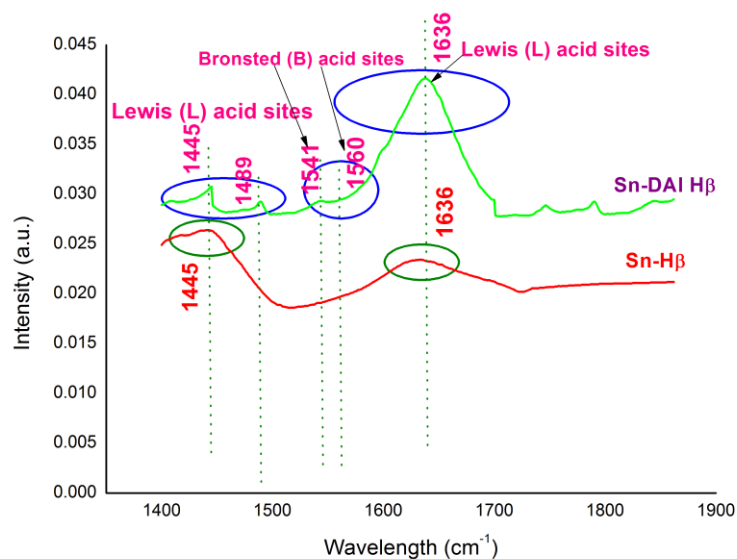
Figure 5.5 Py-FTIR of Sn-dAl Hβ and Sn-Hβ.

Table 5. 6. Acidity information of catalysts by NH$_3$-TPD & Titration method

Sample	Amount of acid sites, (mmol/g)			
	Total	Weak (<250°C)	Medium (250-550°C)	Strong (>550°C)
Hβ*	2.85	-	-	-
Sn-Hβ **	1.34	0.62	0.42	0.30
Sn-DAl Hβ**	2.77	0.60	1.86	0.31

* n-butyl-amine titration method, ** NH$_3$-TPD

Table 5.3. Acidity information of catalysts by Py-IR method

Catalyst	Amount of Acidic Sites (mmol/g)	
	Lewis acid sites[a]	Bronsted acid sites[a]
Sn-Hβ	0.31	-

Sn-DAl Hβ	0.93	0.33

5.5.1.5. Study of catalyst activity

Effect of temperature and catalyst loading

The sequential reductive etherification of HMF was conducted under various conditions, including temperatures of 140 °C, 150 °C, 160 °C, and 170 °C; reaction times of 1 h, 2 h, 3 h, and 4 h; and catalyst loadings of 0.15g, 0.2g, and 0.25g. Two different catalysts, Sn-Hβ (with Sn loadings of 0.05M, 0.1M, 0.15M, and 0.3M) and Sn-dAl Hβ (with a Sn loading of 0.15M), were employed. The outcomes are presented in Table 5.4.

The initial experiment employed the Sn-Hβ catalyst (0.3M Sn loading) with a reaction condition of 140°C, and varying times (1 h, 2 h, 3 h, and 4 h) and catalyst loadings (0.15g, 0.2g, and 0.25g). The results indicated a 4% conversion of 5-HMF, with HPMF and BPMF selectivities of 2.27% and 2.04%, respectively, at 140°C, 0.15g catalyst, and 1 h reaction time (entry 1).

Increasing the catalyst loading to 0.2g and 0.25g (entries 2 and 3) while maintaining the other reaction conditions led to increased conversion rates of 5% and 7%, along with enhanced HPMF selectivities of 2.88% and 2.12%, and BPMF selectivities of 2.12% and 2.69%, respectively. Similar trends were observed when experiments were performed with varying reaction times (2 h, 3 h, and 4 h) (entries 4-12). Notably, extended reaction times (4 h) at specific catalyst loadings (entries 10, 11, and 12) achieved the highest 5-HMF conversion of 72% (entry 12). This extended reaction time also brought significant changes in HPMF and BPMF selectivities. HPMF selectivity increased from 50.48% (entry 10) to 60.67% (entry 12), while BPMF selectivity reached around 10.9% with a higher catalyst loading of 0.25g (entry 12). The lower BPMF yield and selectivity could be attributed to inadequate dispersion and agglomeration of Sn on the Hβ catalyst.

Furthermore, to improve product yield and selectivity, Sn-Hβ catalysts with varying metal loadings (0.05 M, 0.1 M, and 0.15 M) were evaluated under reaction conditions of 140°C, 150°C, and 170°C in 4 h (entries 13-21). The outcomes demonstrated that higher temperatures, combined with catalyst loadings of 0.2g and 0.25g, led to increased 5-HMF conversion. Maximum conversion was achieved with a Sn loading of 0.15 M at 170°C and a catalyst loading of 0.2g (entry 21). Interestingly, HPMF selectivity significantly increased to 98.63% with a Sn loading of 0.05 M at 150°C and a catalyst loading of 0.25g (entry 17). However, BPMF selectivities were less promising, with the highest selectivity of 59.10% achieved with a Sn loading of 0.1 M at 150°C and a catalyst loading of 0.2g (entry 19). This discrepancy might stem from inadequate Lewis and Bronsted acid sites on the catalyst responsible for the etherification of 5-HMF to BPMF. The mechanism involved in the reductive etherification of 5-HMF in 2-propanol using a mixed catalyst can be outlined as follows: Initially, the carbonyl group within 5-HMF undergoes hydrogenation through interaction with Lewis acid sites, resulting in the formation of BHMF. Subsequently, BHMF is subject to etherification to yield HPMF, a step that is followed by the further etherification of HPMF into BPMF within the context of 2-propanol. This subsequent etherification process occurs in the presence of an excess of either Lewis acid sites or Bronsted acid sites. Rana et al.(52) documented analogous findings in their investigation of reaction mechanisms concerning the one-pot catalytic transformation of 5-HMF into HPMF and BPMF. Nevertheless, the detection of BPMF within the resultant mixture pointed towards the influence exerted by Sn-Hβ during the etherification stage.

The results show that Sn-Hβ acts as an etherification catalyst in the reductive etherification of 5-HMF to HPMF and BPMF, but the selectivity of BPMF is low as compared to HPMF. Hence, it was decided to change the preparation method (two-step post-synthesis method)

of the Sn-Hβ catalyst to improve the concentration of Lewis and Bronsted acid sites on the catalyst, which is responsible for the conversion of HPMF into BPMF and enhancement of the selectivity of BPMF. Sn-dAl Hβ (Sn loading 0.15 M) was prepared by two step post-synthesis method, which consisted of the de-alumination of parent Hβ and then incorporation of Sn species into the framework of de-aluminated Si-Beta via dry impregnation and calcination to get proper dispersion of Sn into Hβ which will results in sufficient concentration of Lewis acid site and Bronsted acid sites on the surface of the catalyst. Also, from the results of experiments (entry 1 to entry 20) it was decided to carry out reaction with catalyst loading (0.2 g, & 0.25 g), reaction temperature (140°C, 150°C, 160°C, & 170°C) in 4 h with Sn-dAl Hβ catalyst.

Alcohols can also serve as etherifying agents, leading to the creation of BAMFs without necessitating the use of molecular hydrogen (H$_2$)(36–46). In this current study, 2-propanol was employed as both a source of hydrogen and a substrate for the etherification process. To assess the catalyst's impact on 5-HMF conversion and BPMF selectivity, a reaction was conducted using a 0.2 g catalyst weight (entry 23) at 140°C for 4 h. Notably, both 5-HMF conversion and BPMF selectivity increased to 67.76% and 51.54%, respectively, surpassing the outcomes achieved with Sn-Hβ (entries 2 and 14). Moreover, as depicted in Figure 5.6, altering the temperature resulted in higher 5-HMF conversion and BPMF selectivity, reaching 92.55% and 97.28%, respectively, under reaction conditions of T=170°C and catalyst loading=0.2 g (entry 26). This finding confirms the earlier hypothesis that elevated temperatures favor the formation of BPMF.

To gain deeper insights into the function of the Sn-dAl Hβ catalyst and the impact of temperature, the experiment was carried out across different temperature settings, all with a catalyst loading of 0.25 g and a reaction duration of 4 h (entries 27-30). As shown in Figure 5.7, at lower reaction temperatures (entries 27 and 28), notably higher conversions

of 88.24% and 93.57%, respectively, were achieved. Concurrently, selectivity levels of approximately 97.92% and 98.54% were observed. This phenomenon can likely be attributed to the effective integration of Sn within the zeolite framework, resulting in an ample presence of both Lewis and Bronsted acid sites. The rise in reaction temperature also appears to favor the conversion of HPMF into BPMF.

The heightened selectivity further validates that, in contrast to the wet impregnation method, the two-step post-synthesis process facilitated the creation of superior Lewis and Bronsted acid sites. Moreover, proper incorporation of Sn into Hβ was evidenced by the NH$_3$-TPD (Table 5.2), Py-IR (Table 5.3), and TEM (Figure 5.2) outcomes. Upon further temperature elevation (entry 29), the conversion rate slightly decreased to 92.78%, although the selectivity experienced a marginal reduction to 96.59%. Similarly, for the experiment conducted with a 0.25 g catalyst over 4 h (entry 30) at 170°C, the HMF conversion remained around 96.25%, yet BPMF selectivity was further diminished to 95.56%. This trend emphasizes that the catalytic efficiency of etherification thrives due to the synergistic effects of elevated Lewis acid sites and ample Bronsted acid sites.

Figure 5.8 depicts the influence of both temperature and catalyst (Sn-dAl Hβ) loading on the conversion and selectivity of 5-HMF and BPMF. The graph indicates that an elevated temperature corresponds to increased conversion of 5-HMF and higher selectivity towards BPMF, particularly when employing catalyst loadings of 0.2g and 0.25g. However, the utmost selectivity for BPMF (98.54%) was attained at a catalyst loading of 0.25g and a temperature of 150°C in 4h period. This observation underscores that alterations in the catalyst loading of Sn-dAl Hβ induce shifts in the selectivity of BPMF.

Table 5.4. Catalytic activity of different Catalyst (Reaction conditions: 5-HMF – 1g, 2-propanol- 50 ml)

Entry	Catalyst & Sn loading	Catalyst quantity (g)	Temp (°C)	Time (h)	Conv. %	Selectivity%		
						BHMF	HPMF	BPMF
1	Sn-Hβ	0.15	140	1	4	-	2.27	2.04
2	(0.3 M)	0.20	140	1	5	-	2.88	2.12
3		0.25	140	1	7	-	3.39	2.69
4		0.15	140	2	5	-	2.32	2.64
5		0.20	140	2	5	-	1.63	3.33
6		0.25	140	2	8	-	3.42	3.62
7		0.15	140	3	16	-	5.57	9.50
8		0.20	140	3	8	-	2.31	5.33
9		0.25	140	3	9	-	3.69	5.30
10		0.15	140	4	58	-	50.48	7.17
11		0.20	140	4	60	-	52.22	7.47
12		0.25	140	4	72	-	60.67	10.9
13	Sn-Hβ	0.15	140	4	61.96	-	61.34	0.62
14	(0.05 M)	0.20	140	4	85.18	-	84.74	0.19
15		0.25	140	4	85.98	-	85.55	0.14
16		0.20	150	4	15.81	-	67.55	32.45
17		0.25	150	4	45.97	-	98.63	1.37
18		0.2	170	4	80.50	-	95.95	2.80
19	Sn-Hβ	0.2	150	4	27.63	-	40.89	59.10
20	(0.1 M)	0.2	170	4	86.88	-	83.46	-
21	Sn-Hβ	0.2	170	4	90.4	-	80.65	3.98

22	(0.15 M)	0.25	150	4	72.50	-	96.90	1.85
23	Sn-dAlHβ	0.2	140	4	67.76	-	48.4	51.54
24	(0.15 M)	0.2	150	4	79.48	-	4.56	95.44
25		0.2	160	4	87.76	-	44.47	55.21
26		0.2	170	4	92.55	-	2.1	97.28
27		0.25	140	4	88.24	-	2.07	97.92
28		0.25	150	4	93.57	-	1.46	98.54
29		0.25	160	4	92.78	-	3.41	96.59
30		0.25	170	4	96.25	-	4.41	95.56
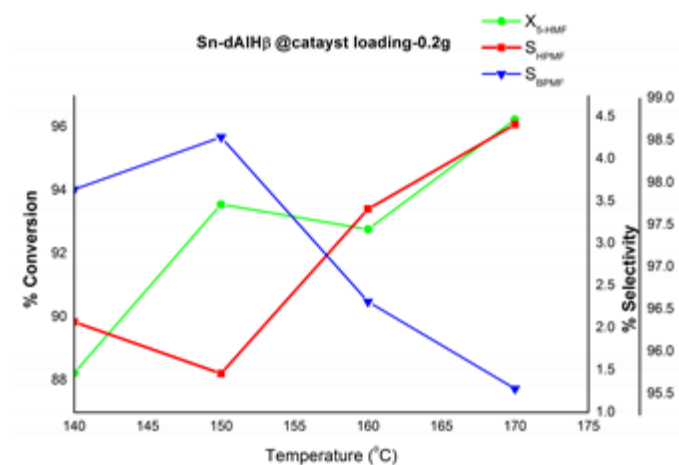
Figure 5.6 Effect of temperature on BHMF, HPMF & BPMF selectivity (Catalyst: Sn dAlHβ loading 0.2g).
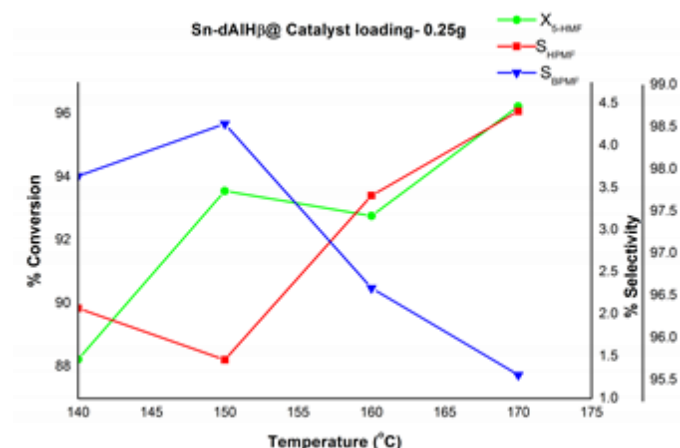
Figure 5.7 Effect of temperature on BHMF, HPMF & BPMF selectivity (Catalyst: Sn dAlHβ loading 0.25g).
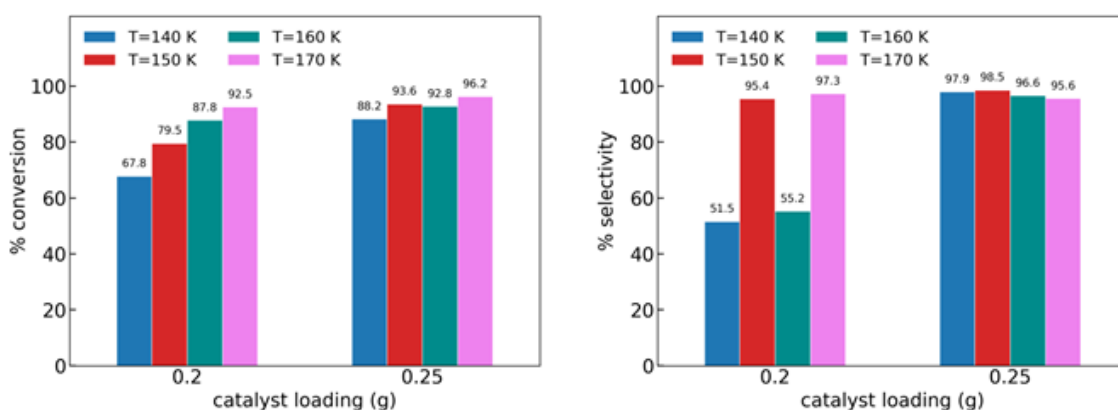
Figure 5.8 Effect of Catalyst (Sn-dAlHβ) loading and Temperature on conversion of 5-

HMF and BPMF selectivity

5.5.1.6. Effect of dealumination on the catalyst properties and catalytic behavior

In this work, Sn-Hβ and Sn-dAlHβ was synthesized by wet impregnation and post synthesis method respectively and used as a catalyst for the conversion of 5-HMF to 2,5-bis(isopropoxymethyl)furan (BPMF) with 2-propanol in order to explore the roles of acidity and preparation methods in the etherification of 5-HMF. Sn-Hβ and Sn-dAlHβ with their pore structure and acidity were studied. It was observed that catalyst (Sn-Hβ) prepared by wet impregnation method shows the fair enough etherification activity to give HPMF but the selectivity of BPMF was surprisingly very low (Table 5.4, entry 13-22). Upon incorporation of Sn into dealuminated zeolite the etherification activity rises

significantly in terms of higher selectivity of BPMF (Table 5.4, entry 23-30), shows successful and proper incorporation of catalytically active Sn metal in to dealuminated zeolite (dAlHβ). As depicted in Figure 5.9, Sn-dAlHβ exhibits a notable increase in the concentration of robust Lewis acid sites, coupled with an ample presence of Bronsted acid sites. This distinctive acid site distribution significantly promotes the reductive etherification process, facilitating the conversion of 5-HMF into BPMF. This contrasts with Sn-Hβ, emphasizing the advantageous impact of the unique acid site composition in Sn-dAlHβ on the desired reaction pathway. Along with that TEM results and textural properties of catalysts shows that Sn-Hβ having big crystal size and small mesopore volume (Table 5.1) which might restrict the mass transfer of reactants towards active sites, leads to the reduction in the selectivity of BPMF. On other hand smaller crystal size and bigger mesopore volume reduces the diffusion issues and providing very high selectivity of BPMF.
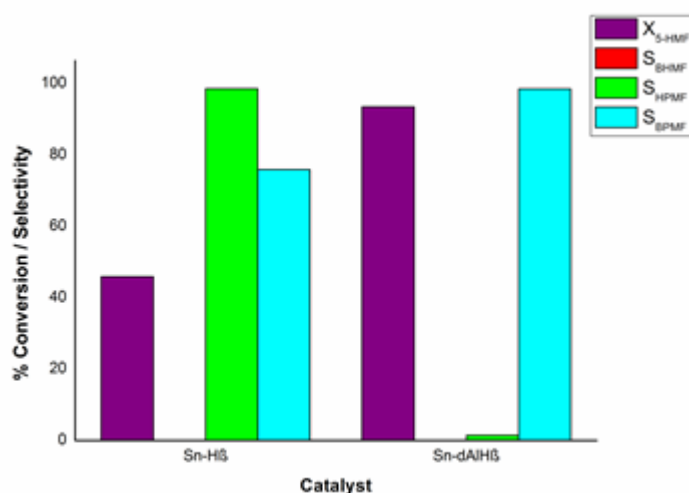
Figure 5.9 Comparison of effect of catalysts (Sn-Hβ and Sn-dAlHβ) on BHMF, HPMF & BPMF
selectivity

5.5.1.7. Effect of acidity of catalyst on product distribution and selectivity

The analysis of adjusting the acidic site characteristics, such as enhancing Lewis acid sites while reducing Bronsted acid sites, was conducted to assess its impact on product

distribution and selectivity. This evaluation was performed through NH_3-TPD and pyridine adsorption studies, which offer deeper insights into the acidic site nature.

As indicated in Table 5.5, Sn-Hβ (0.15M) exhibited only Lewis acidic sites (0.31 mmol/g). Considering that Lewis acidic sites promote the reductive etherification of 5-HMF to yield ethers, the observed product distribution aligned with this trend. Specifically, Sn-Hβ (0.15M) produced both HPMF and BPMF, but HPMF displayed a higher selectivity (96.90%) compared to BPMF (1.85%).

On the other hand, Sn-dAl Hβ (0.15M) demonstrated notably elevated selectivity towards BPMF (98.54%). Figure 5.10 illustrates that Sn-dAl Hβ possessed a higher concentration of Lewis acid sites (0.93 mmol/g) along with an adequate amount of Bronsted acid sites (0.33 mmol/g). The dealumination enabled the effective integration of catalytically active Sn metal into the dealuminated zeolite. This leads to significant increase in Lewis acid sites and reduction in Bronsted acid site. Due to interaction between intrinsic acid sites and Sn species some Bronsted acid sites convert into Lewis acid sites and these Sn-Lewis acid sites have capacity to enhance the etherification process which affects the product distribution. This emphasizes that the successful one-pot reductive etherification of 5-HMF into BPMF necessitates a synergistic interplay between Lewis acid sites and Bronsted acid sites.

Similar findings were also noted in the studies conducted by Luo et al.(49) and Barbera et al.(54) These studies revealed that the carbonyl group within HMF could undergo an initial reduction to generate BHMF through MPV (Meerwein-Ponndorf-Verley) reduction facilitated by the Lewis acid sites present on the catalyst. Subsequently, the produced BHMF could undergo consecutive etherification reactions with isopropanol to yield 2-hydroxymethyl-5-isopropoxymethylfuran (HPMF) and 2,5-bis(isopropoxymethyl)furan (BPMF). This sequence of reactions is promoted when the catalyst possesses an abundance

of Bronsted acid sites or an excessive presence of Lewis acid sites. The collective presence of these acid sites facilitates the efficient transformation of HMF into its etherified derivatives.

Table 5.5. Product distribution and acid site distribution

Catalyst	Amount of Acidic Sites (mmol/g)		% Selectivity		
	Lewis acid sites	Bronsted acid sites	BHMF	HPMF	BPMF
Sn-Hβ (0.15M)	0.31	-	-	96.90	1.85
Sn-dAl Hβ (0.15M)	0.93	0.33	-	1.46	98.54
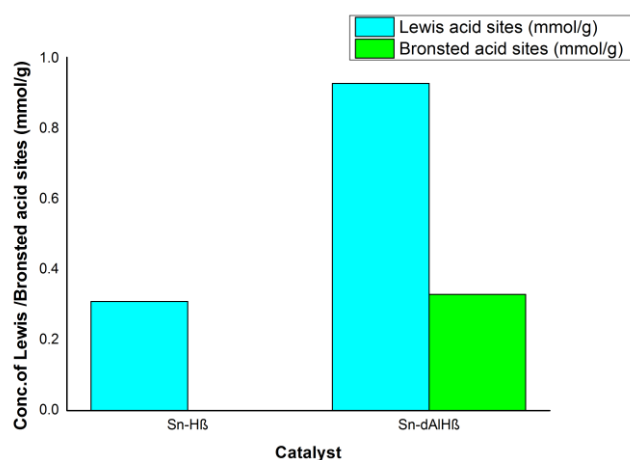
Figure 5.10 Concentration of LAS and BAS on catalyst (mmol/g).

5.5.1.8 Catalyst reusability study

The reusability of Sn-dAlHβ catalyst is investigated in five consecutive reactions run. When the reaction completed, the catalyst was separated by centrifugation and washed with acetone to reuse it in next run. The results of reusability study are as shown in the

Figure 5.11. Reduction in the conversion of 5-HMF was observed after 4th run while selectivity of BPMF was intact after 5 run cycle.
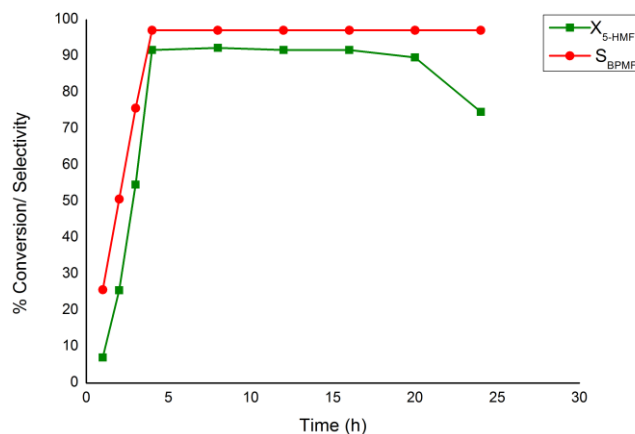
Figure 5.11 Reusability study of Sn-dAlHβ catalyst (Reaction conditions: 5-HMF–1g, 2-propanol- 50 ml, and catalyst loading-0.25 g).

5.5.1.9 Comparison of various supported metal catalyst from literature and present work

The comparison between various supported metal catalysts reported in the literature and the present work reveals distinct trends and performances in different reaction pathways and conditions. Below is a summary of the comparisons:

Researchers have explored a range of supported metal catalysts for various reactions, including the reductive etherification of HMF. Different metals and supports have been investigated, each with their own catalytic properties. These studies have focused on optimizing reaction conditions, catalyst loading, and selectivity.

The present study centers on the reductive etherification of 5-HMF using Sn-dAl Hβ as the catalyst. This work highlights the significance of specific acid site distributions, including Lewis and Bronsted acid sites, in achieving the desired product distribution and selectivity. The synergistic effect of these acid sites is crucial for the conversion of 5-HMF into

BPMF. The study also underscores the impact of temperature and catalyst loading on the conversion and selectivity, with particular emphasis on the role of Sn-dAl Hβ in facilitating the reaction pathway.

In general, the comparison between supported metal catalysts from the literature and the present work underscores the importance of catalyst design, acid site distribution, and reaction conditions in determining product distribution and selectivity in reductive etherification reactions. The use of Sn-dAl Hβ as a catalyst introduces a new avenue for achieving high selectivity towards BPMF through a tailored acid site composition.

In the context of the existing literature, a limited number of studies have explored the use of Sn-dAlHβ catalyst specifically for the conversion of 5-HMF into 2,5-bis(isopropoxymethyl) furan (BPMF). Table 5.6 presents a comparison of the catalytic performance between the catalyst studied in this work and those employed in prior research for the synthesis of BPMF from 5-HMF. Under reaction conditions of 150°C temperature and 4 h duration, Sn-dAlHβ exhibited remarkable performance with 93.57% conversion of 5-HMF and 98.54% selectivity towards BPMF.

Jae et al.(48) synthesized Sn-Hβ and Zr-Hβ catalysts, which were employed in reduction and etherification reactions using 2-propanol. They reported BPMF selectivities of 87% and 77% at 180°C in 6 h, while at 120°C, the selectivities were achieved after 24 h, reaching 66% and 67%, respectively.

Lewis et al.(50) developed a more efficient Lewis acidic Hf-Beta catalyst with 77% selectivity towards BBMF, utilizing 1-butanol as a solvent at 120°C in 24 h. Shinde and Rode(51) achieved high BPMF selectivity (95%) through the combined effect of Zr-Mont catalyst, requiring elevated temperatures of 150°C and 160°C.

Rana et al.(52) reported 91% selectivity of BPMF by combining $Zr(OH)_2$ and Zr-Hβ catalyst at 140°C in 4 h. It was reported by Wei et al.(46) used Zr-SBA-UH as a catalyst

and 2-propanol as a solvent, resulting in BPMF formation. When combined with solvents like 1-propanol, 1-butanol, 2-butanol, and M-PrOH, the reaction yielded BPMF, BBMF, BSBMF, and BMPMF with yields of 38.1%, 17.1%, 4.4%, and 54.1% respectively. Comparing these studies, it becomes evident that a catalyst like Sn-dAlHβ, with tuned Lewis and Bronsted acid sites and their synergistic effect, leads to superior BPMF selectivity. This is achieved through efficient etherification at lower temperatures and shorter reaction times. The careful modulation of acid sites and their interplay emerges as a key factor in achieving enhanced selectivity for BPMF in the reductive etherification of 5-HMF.

Table 5.6. Comparison of various supported metal catalyst from literature and present work

Catalyst	Alcohol	Temperature (°C)	Time ,h	X_{HMF} (%)	S_{BAMF} Yield (%)	$S_{BMMF}/_{BEMF}/_{BPMF}$ (%)	Reference
HZSM-5 (Si/Al=25)	Methanol	100	3	100	70	70	(31)
HZSM-5 (Si/Al=38)	Methanol	100	3	100	68	68	
HZSM-5 (Si/Al=300)	Methanol	100	3	100	69	69	
HZSM-5 (Si/Al=25)	Methanol	120	12	-	68	68	
HZSM-5 (Si/Al=25)	Methanol	140	8	-	59	59	

Cu-HZSM-5	Methanol	120	12	100	68	68	(31)
Hf-Hβ	Ethanol	120	24	87		77	(48)
Zr-Hβ	2-Propanol	180	6	100	77	77	(50)
Sn- Hβ	2-Propanol	180	6	91.5		87	
Zr-Hβ	Ethanol	120	24	81		66	(48)
Sn- Hβ	Ethanol	120	24	69		67	
ZrO(OH)$_2$+ Zr-Mont	2-Propanol	160	1	100	94	94	(51)
ZrO(OH)$_2$+ Zr-Mont	2-Propanol	150	1	100	95	95	
Zr-SBA-UH	2-Propanol	150	4	98.5		93.9	(47)
iUSY@ZrCP	2-Propanol	120	3	78.9		86.9	(62)
ZrO(OH)$_2$+ Zr- Hβ	2-Propanol	140	4	61.62		91	(52)
Hβ		120	4	10		6.86	(52)
Zr-BDC-Sx	2-Propanol	120	3	100		96.9	(63)
Cu/Al$_2$O$_3$ +HP-ZSM-5*	Isopropanol	100	3	100		82.6	(64)
Sn-dAlHβ	2-Propanol	150	4	93.57		98.54	This work

* using H$_2$ gas at 2.5MPa

5.6 Conclusions

The efficient catalytic transformation of 5-HMF to 2,5-bis(isopropoxymethyl)furan (BPMF) within a single reactor was accomplished using Sn-Hβ and Sn-dAlHβ catalysts. These catalysts were prepared through two distinct methods: wet impregnation and post-synthesis approaches. The findings indicated that while both catalysts exhibited commendable etherification activity, the Sn-dAlHβ catalyst outperformed the Sn-Hβ catalyst in terms of converting 5-HMF to BPMF with superior selectivity.

Employing the post-synthesis method to create the Sn-dAlHβ catalyst enabled the effective integration of catalytically active Sn metal into the dealuminated zeolite. As a result, not only were the Lewis acid sites increased, but the catalyst also showcased a larger mesopore volume. This catalyst variant also possessed ample Bronsted acid sites, leading to an enhanced BPMF selectivity. This improvement was attributed to the combined effect of abundant Lewis acid sites, sufficient Bronsted acid sites, and improved reactant diffusion due to the larger mesopore volume.

On the other hand, the Sn-Hβ catalyst exhibited a lower concentration of Lewis acid sites, lacked Bronsted acid sites, and had larger crystal sizes along with reduced mesopore volume. Consequently, these characteristics resulted into a reduced BPMF selectivity.

5.7. References

1. Al-Soof F., Aklil B, Taeb M, Khesali M, Mazraati M, Lubiantara T N, Alawami A, Clemenz C, Guerer N, Brennand J B G, Spitzy J, Linton D, Griffin J, Tallett M, Steiner P, Szalkowska U. World oil outlook. 2010.

2. Hu L, Lin L, Wu Z, Zhou S, Liu S. Recent advances in catalytic transformation of biomass-derived 5-hydroxymethylfurfural into the innovative fuels and chemicals. Renewable and Sustainable Energy Reviews. 2017 Jul;74:230–57.

3. Zhu JY, Pan X, Zalesny RS. Pretreatment of woody biomass for biofuel production: energy efficiency, technologies, and recalcitrance. Appl Microbiol Biotechnol. 2010

Jul;87(3):847–57.

4. Zhou CH, Xia X, Lin CX, Tong DS, Beltramini J. Catalytic conversion of lignocellulosic biomass to fine chemicals and fuels. Chem Soc Rev. 2011;40(11):5588.

5. Zhang Z, Song J, Han B. Catalytic Transformation of Lignocellulose into Chemicals and Fuel Products in Ionic Liquids. Chem Rev. 2017 May 24;117(10):6834–80.

6. Zhang Z, Zhang M, Deng J, Deng K, Zhang B, Lv K, et al. Potocatalytic oxidative degradation of organic pollutant with molecular oxygen activated by a novel biomimetic catalyst ZnPz(dtn-COOH)4. Applied Catalysis B: Environmental. 2013 Mar;132–133:90–7.

7. Sahu R, Dhepe PL. A One-Pot Method for the Selective Conversion of Hemicellulose from Crop Waste into C5 Sugars and Furfural by Using Solid Acid Catalysts. ChemSusChem. 2012 Apr;5(4):751–61.

8. Xia H, Hu H, Xu S, Xiao K, Zuo S. Catalytic conversion of glucose to 5-hydroxymethyfural over Fe/β zeolites with extra-framework isolated Fe species in a biphasic reaction system. Biomass and Bioenergy. 2018 Jan;108:426–32.

9. Tollefson J. Can the world kick its fossil-fuel addiction fast enough? Nature. 2018 Apr;556(7702):422–5.

10. Sun G, An J, Hu H, Li C, Zuo S, Xia H. Green catalytic synthesis of 5-methylfurfural by selective hydrogenolysis of 5-hydroxymethylfurfural over size-controlled Pd nanoparticle catalysts. Catal Sci Technol. 2019;9(5):1238–44.

11. Hu L, Zhao G, Hao W, Tang X, Sun Y, Lin L, et al. Catalytic conversion of biomass-derived carbohydrates into fuels and chemicals via furanic aldehydes. RSC Adv.

2012;2(30):11184.

12. Xu C, Arancon RAD, Labidi J, Luque R. Lignin depolymerisation strategies: towards valuable chemicals and fuels. Chem Soc Rev. 2014;43(22):7485–500.

13. Wang J, Xi J, Wang Y. Recent advances in the catalytic production of glucose from lignocellulosic biomass. Green Chem. 2015;17(2):737–51.

14. Zhang Z, Deng K. Recent Advances in the Catalytic Synthesis of 2,5-Furandicarboxylic Acid and Its Derivatives. ACS Catal. 2015 Nov 6;5(11):6529–44.

15. Liu B, Zhang Z. Catalytic Conversion of Biomass into Chemicals and Fuels over Magnetic Catalysts. ACS Catal. 2016 Jan 4;6(1):326–38.

16. Mascal M, Nikitin EB. Direct, High-Yield Conversion of Cellulose into Biofuel. Angew Chem Int Ed. 2008 Sep 29;47(41):7924–6.

17. Binder JB, Raines RT. Simple Chemical Transformation of Lignocellulosic Biomass into Furans for Fuels and Chemicals. J Am Chem Soc. 2009 Feb 11;131(5):1979–85.

18. Chen B, Li F, Huang Z, Yuan G. Carbon-coated Cu-Co bimetallic nanoparticles as selective and recyclable catalysts for production of biofuel 2,5-dimethylfuran. Applied Catalysis B: Environmental. 2017 Jan;200:192–9.

19. Bai Y, Su S, Wang S, Wang B, Sun R, Song G, et al. Front Cover: Catalytic Conversion of Carbohydrates into 5-Ethoxymethylfurfural by a Magnetic Solid Acid Using γ-Valerolactone as a Co-Solvent (Energy Technol. 10/2018). Energy Tech. 2018 Oct;6(10):1859–1859.

20. Bozell JJ, Petersen GR. Technology development for the production of biobased

products from biorefinery carbohydrates—the US Department of Energy's "Top 10" revisited. Green Chem. 2010;12(4):539.

21. Mika LT, Cséfalvay E, Németh Á. Catalytic Conversion of Carbohydrates to Initial Platform Chemicals: Chemistry and Sustainability. Chem Rev. 2018 Jan 24;118(2):505–613.

22. Mascal M, Dutta S. Chemical-Catalytic Approaches to the Production of Furfurals and Levulinates from Biomass. In: Nicholas KM, editor. Selective Catalysis for Renewable Feedstocks and Chemicals [Internet]. Cham: Springer International Publishing; 2014 [cited 2024 May 27]. p. 41–83. (Topics in Current Chemistry; vol. 353). Available from: https://link.springer.com/10.1007/128_2014_536

23. Fang W, Hu H, Dong P, Ma Z, He Y, Wang L, et al. Improvement of furanic diether selectivity by adjusting Brønsted and Lewis acidity. Applied Catalysis A: General. 2018 Sep;565:146–51.

24. Sacia ER, Balakrishnan M, Bell AT. Biomass conversion to diesel via the etherification of furanyl alcohols catalyzed by Amberlyst-15. Journal of Catalysis. 2014 May;313:70–9.

25. Fang W, Hu H, Ma Z, Wang L, Zhang Y. Two Possible Side Reaction Pathways during Furanic Etherification. Catalysts. 2018 Sep 8;8(9):383.

26. Hu H, Hu D, Jin H, Zhang P, Li G, Zhou H, et al. Efficient Production of Furanic Diether in a Continuous Fixed Bed Reactor. ChemCatChem. 2019 Apr 18;11(8):2179–86.

27. Gupta D, Saha B. Dual acidic titania carbocatalyst for cascade reaction of sugar to

etherified fuel additives. Catalysis Communications. 2018 May;110:46–50.

28. Ras E, Maisuls S, Haesakkers P, Gruter G, Rothenberg G. Selective Hydrogenation of 5-Ethoxymethylfurfural over Alumina-Supported Heterogeneous Catalysts. Adv Synth Catal. 2009 Dec;351(18):3175–85.

29. Gerardus Johannes Maria Gruter. 5-SUBSTITUTED 2-(ALKOXYMETHYL)FURANS. US 8,231,693 B2, 2012.

30. De Jong E, Vijlbrief T, Hijkoop R, Gruter GJM, Van Der Waal JC. Promising results with YXY Diesel components in an ESC test cycle using a PACCAR Diesel engine. Biomass and Bioenergy. 2012 Jan;36:151–9.

31. Cao Q, Liang W, Guan J, Wang L, Qu Q, Zhang X, et al. Catalytic synthesis of 2,5-bis-methoxymethylfuran: A promising cetane number improver for diesel. Applied Catalysis A: General. 2014 Jul;481:49–53.

32. Ikariya T, Blacker AJ. Asymmetric Transfer Hydrogenation of Ketones with Bifunctional Transition Metal-Based Molecular Catalysts. Acc Chem Res. 2007 Dec 1;40(12):1300–8.

33. Wang D, Astruc D. The Golden Age of Transfer Hydrogenation. Chem Rev. 2015 Jul 8;115(13):6621–86.

34. Osatiashtiani A, Lee AF, Wilson K. Recent advances in the production of γ-valerolactone from biomass-derived feedstocks via heterogeneous catalytic transfer hydrogenation. J of Chemical Tech & Biotech. 2017 Jun;92(6):1125–35.

35. Xue Z, Jiang J, Li G, Zhao W, Wang J, Mu T. Zirconium–cyanuric acid coordination polymer: highly efficient catalyst for conversion of levulinic acid to γ-valerolactone.

Catal Sci Technol. 2016;6(14):5374–9.

36. Leng Y, Shi L, Du S, Jiang J, Jiang P. A tannin-derived zirconium-containing porous hybrid for efficient Meerwein–Ponndorf–Verley reduction under mild conditions. Green Chem. 2020;22(1):180–6.

37. Zhou S, Dai F, Xiang Z, Song T, Liu D, Lu F, et al. Zirconium–lignosulfonate polyphenolic polymer for highly efficient hydrogen transfer of biomass-derived oxygenates under mild conditions. Applied Catalysis B: Environmental. 2019 Jul;248:31–43.

38. Rojas-Buzo S, García-García P, Corma A. Hf-based metal–organic frameworks as acid–base catalysts for the transformation of biomass-derived furanic compounds into chemicals. Green Chem. 2018;20(13):3081–91.

39. Li H, He J, Riisager A, Saravanamurugan S, Song B, Yang S. Acid–Base Bifunctional Zirconium *N* -Alkyltriphosphate Nanohybrid for Hydrogen Transfer of Biomass-Derived Carboxides. ACS Catal. 2016 Nov 4;6(11):7722–7.

40. Hu L, Li N, Dai X, Guo Y, Jiang Y, He A, et al. Highly efficient production of 2,5-dihydroxymethylfuran from biomass-derived 5-hydroxymethylfurfural over an amorphous and mesoporous zirconium phosphonate catalyst. Journal of Energy Chemistry. 2019 Oct;37:82–92.

41. Hu L, Dai X, Li N, Tang X, Jiang Y. Highly selective hydrogenation of biomass-derived 5-hydroxymethylfurfural into 2,5-bis(hydroxymethyl)furan over an acid–base bifunctional hafnium-based coordination polymer catalyst. Sustainable Energy Fuels. 2019;3(4):1033–41.

42. Hu L, Li T, Xu J, He A, Tang X, Chu X, et al. Catalytic transfer hydrogenation of biomass-derived 5-hydroxymethylfurfural into 2,5-dihydroxymethylfuran over magnetic zirconium-based coordination polymer. Chemical Engineering Journal. 2018 Nov;352:110–9.

43. Hu D, Hu H, Jin H, Zhang P, Hu Y, Ying S, et al. Building hierarchical zeolite structure by post-synthesis treatment to promote the conversion of furanic molecules into biofuels. Applied Catalysis A: General. 2020 Jan;590:117338.

44. Balakrishnan M, Sacia ER, Bell AT. Etherification and reductive etherification of 5-(hydroxymethyl)furfural: 5-(alkoxymethyl)furfurals and 2,5-bis(alkoxymethyl)furans as potential bio-diesel candidates. Green Chem. 2012;14(6):1626.

45. Han J, Kim YH, Jung B, Hwang S, Jegal J, Kim J, et al. Highly Selective Catalytic Hydrogenation and Etherification of 5-Hydroxymethyl-2-furaldehyde to 2,5-Bis(alkoxymethyl)furans for Potential Biodiesel Production. Synlett. 2017 Oct;28(17):2299–302.

46. Wei J, Wang T, Liu H, Li M, Tang X, Sun Y, et al. Highly Efficient Reductive Etherification of 5-Hydroxymethylfurfural to 2,5-Bis(Alkoxymethyl)Furans as Biodiesel Components over Zr-SBA Catalyst. Energy Tech. 2019 May;7(5):1801071.

47. Wei J, Cao X, Wang T, Liu H, Tang X, Zeng X, et al. Catalytic transfer hydrogenation of biomass-derived 5-hydroxymethylfurfural into 2,5-bis(hydroxymethyl)furan over tunable Zr-based bimetallic catalysts. Catal Sci Technol. 2018;8(17):4474–84.

48. Jae J, Mahmoud E, Lobo RF, Vlachos DG. Cascade of Liquid-Phase Catalytic Transfer Hydrogenation and Etherification of 5-Hydroxymethylfurfural to Potential Biodiesel Components over Lewis Acid Zeolites. ChemCatChem. 2014 Feb;6(2):508–13.

49. Luo J, Yu J, Gorte RJ, Mahmoud E, Vlachos DG, Smith MA. The effect of oxide acidity on HMF etherification. Catal Sci Technol. 2014;4(9):3074–81.

50. Lewis JD, Van de Vyver S, Crisci AJ, Gunther WR, Michaelis VK, Griffin RG, et al. A Continuous Flow Strategy for the Coupled Transfer Hydrogenation and Etherification of 5-(Hydroxymethyl)furfural using Lewis Acid Zeolites. ChemSusChem. 2014 Aug;7(8):2255–65.

51. Shinde S, Rode C. Cascade Reductive Etherification of Bioderived Aldehydes over Zr-Based Catalysts. ChemSusChem. 2017 Oct 23;10(20):4090–101.

52. Rana SP, Rana PH. One-pot reductive etherification of 5-hydroxymethylfurfural into biofuel (2,5-bis(propoxymethyl) furan (BPMF)) using mixed catalyst $ZrO(OH)_2$ and Zr-Hβ. New J Chem. 2023;47(2):891–9.

53. Lanzafame P, Papanikolaou G, Perathoner S, Centi G, Migliori M, Catizzone E, et al. Direct *versus* acetalization routes in the reaction network of catalytic HMF etherification. Catal Sci Technol. 2018;8(5):1304–13.

54. Barbera K, Lanzafame P, Pistone A, Millesi S, Malandrino G, Gulino A, et al. The role of oxide location in HMF etherification with ethanol over sulfated ZrO2 supported on SBA-15. Journal of Catalysis. 2015 Mar;323:19–32.

55. Güleç F, Şimşek EH, Karaduman A. Zr/ZSM5 ZEOLİT KATALİZÖRLERİ VARLIĞINDA 2-METİL NAFTALİNİN DİSPROPORSİYON KİNETİĞİ. Gazi Üniversitesi Mühendislik-Mimarlık Fakültesi Dergisi [Internet]. 2016 Sep 6 [cited 2024 Jun 5];31(3). Available from: http://dergipark.gov.tr/doi/10.17341/gummfd.93160

56. Tang B, Dai W, Wu G, Guan N, Li L, Hunger M. Improved Postsynthesis Strategy to Sn-Beta Zeolites as Lewis Acid Catalysts for the Ring-Opening Hydration of Epoxides. ACS Catal. 2014 Aug 1;4(8):2801–10.

57. Ranjan Sahu H, Ranga Rao G. Characterization of combustion synthesized zirconia powder by UV-vis, IR and other techniques. Bull Mater Sci. 2000 Oct;23(5):349–54.

58. Li N, Wang A, Tang J, Wang X, Liang D, Zhang T. NO reduction by CH4 in the presence of excess O2 over Co/sulfated zirconia catalysts. Applied Catalysis B: Environmental. 2003 Jun;43(2):195–201.

59. He D, Ding Y, Luo H, Li C. Effects of zirconia phase on the synthesis of higher alcohols over zirconia and modified zirconia. Journal of Molecular Catalysis A: Chemical. 2004 Feb;208(1–2):267–71.

60. Ma X, Gong J, Wang S, He F, Yang X, Wang G, et al. Characterization and reactivity of silica-supported bimetallic molybdenum and stannic oxides for the transesterification of dimethyl oxalate with phenol. Journal of Molecular Catalysis A: Chemical. 2004 Aug;218(2):253–9.

61. Kovalenko V, Zhukova A, Rumyantseva M, Gaskov A, Yushchenko V, Ivanova I, et al. Surface chemistry of nanocrystalline SnO2: Effect of thermal treatment and additives. Sensors and Actuators B: Chemical. 2007 Sep 20;126(1):52–5.

62. Wei J, Wang T, Liu H, Liu Y, Tang X, Sun Y, et al. Assembly of Zr-based coordination polymer over USY zeolite as a highly efficient and robust acid catalyst for one-pot transformation of fructose into 2,5-bis(isopropoxymethyl)furan. Journal of Catalysis. 2020 Sep;389:87–98.

63. He A, Gu Q, Shen X, Zheng J, Hu L, Wang X, et al. One-pot reductive etherification of biomass-derived 5-hydroxymethylfurfural to 2,5-bis(isopropoxymethyl)furan over a sulfonic acid-functionalized zirconium-based coordination catalyst. Green Chem. 2023;25(6):2349–60.

64. Yang Y, Hu H, Fang Q, Lu G, He H, Chen H, et al. One-pot synthesis of 2,5-bis(propoxymethyl)furan from 5-hydroxymethylfurfural by using the supported copper catalyst and hierarchical pore ZSM-5 zeolite. Catalysis Today. 2023 Nov;423:114290.

5.8. GC-MS data of synthesized products

2, 5 bis Propoxymethyl furan (BPMF)

GC-MS data: 212(BPMF), 153, 126, 111, 97, 83, 69, 43, 41
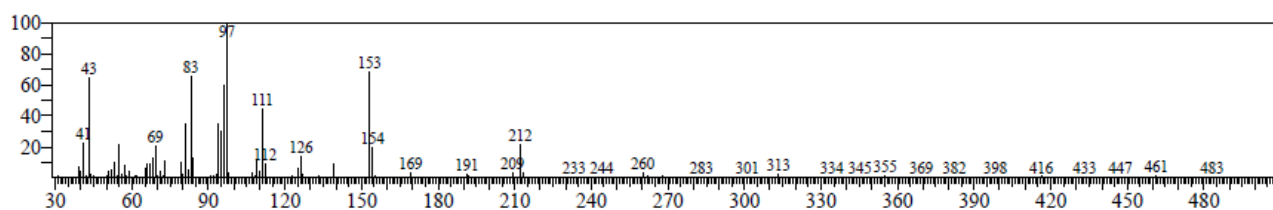
CHAPTER – 6

Highly selective one-pot reductive etherification of bio-derived platform molecule 5-HMF using Zr-HZSM-5 and Sn-HZSM-5 catalysts into potential biofuel/fuel additives 2, 5- Bis Propoxy Methyl furan (BPMF)

As reported in previous chapter 4 and 5 that catalysts Zr-Hβ and Sn- Hβ demonstrated good performance for the reductive etherification of 5-HMF into 2,5-bis(propoxymethyl) furan (BPMF). So, with the aim to achieve furthermore selectivity, decided to explore HZSM-5 as a support. Reductive etherification is very favorable pathway to catalytically convert the bio-platform molecule 5-HMF to 2,5-bis(propoxymethyl) furan (BPMF). BPMF is a potential biofuel/fuel additive candidate, but it is challenging to produce it selectively as MPV (Meerwein−Ponndorf−Verley) and etherification reaction occurs at a time. Sufficient Bronsted acidic sites (BAS) and plenty of Lewis acidic sites (LAS) can favor the etherification reaction, whereas MPV reaction is favored by Lewis acidic sites only. So, LAS and BAS of the catalyst play a key role in the selectivity of BPMF. Hence, developing highly selective catalyst is very important. In this work highly selective

reductive etherification of 5- hydroxymethylfurfural (5-HMF) to 2, 5-bis (propoxymethyl) furan (BPMF) was attained through one-pot pathway using 2-propanol as a hydrogen donor, which was conducted by Zr-HZSM-5 and Sn-HZSM-5 catalysts. Because of excellent synergistic action of BAS and LAS, Sn-HZSM-5 shows high selectivity of BPMF. The catalysts were characterize using techniques such as transmission electron microscopy, BET surface area measurement, powder X-ray diffraction, temperature-programmed desorption of ammonia (NH_3-TPD), Pyridine-IR spectroscopy and Fourier transform infrared spectroscopy. Under the optimized reaction conditions, which included a temperature of 160°C, a catalyst loading of 0.20 grams, a reaction time of 4 h, and a concentration of 1 gram of 5-HMF, impressive results were obtained: a 95.97% conversion of 5-HMF and a 98.63% selectivity towards BPMF.

6.1. Introduction

Conventional energy sources like coal, oil, and natural gas are crucial to modern human life. However, their excessive and uncontrolled usage led to rise critical issues i.e. environmental degradation, global warming, and the availability of fossil fuels for future generations(1−6). Renewable resources like lignocellulosic biomass can be used to produce valuable chemicals and biofuels to address these issues (7−12). Abundant availability, renewability and cost-effectiveness of biomass making it a prominent contributor for sustainable chemical production (13−15). Therefore, converting bio-derived platform molecules into valuable chemicals is both a lucrative and imperative approach in the present scenario(16−19). Various bio-platform molecules such as 5-hydroxymethylfurfural (5-HMF), levulinic acid, furfurals, sugar alcohols, lactic acid, succinic acid, and phenols, are considered as building block chemicals. Among them in recent years, 5-HMF has gained significant attention as HMF derived ethers and its derivatives can be used as fuel additive, paint remover, pharmaceuticals, food additives, polymers, surfactants and

pesticides (20). Consequently, methods to manufacture biofuels from 5-HMF are being increasingly developed. For example, the reductive derivative of 5-HMF, 2,5-bis(hydroxymethyl)furan (BHMF), can be transformed into diethers, which are potential biofuels(21) and previous studies have reported the etherification of BHMF(22–25). 5-Alkoxymethylfurfural (AMF's) is considered a promising biodiesel or additive due to its energy density (30.3 MJ/L) being similar to that of commercially available gasoline (31.1 MJ/L) or diesel (33.6 MJ/L)(26). However, recent findings indicate(27) that the aldehyde group in EMF affects its stability, causing phase separation issues when blended with conventional diesel fuel. In contrast, diethers and 2,5-bis(alkoxymethyl)furans (BAMFs) exhibit superior energy densities and better compatibility with diesel fuel(28). Research has shown that blending 2,5-bisethoxymethylfuran (BEMF) with diesel results in no significant change in engine performance and reduces emissions. Additionally, 2,5-bismethoxymethylfuran (BMMF) has demonstrated full compatibility with diesel fuel(30,31). Catalytic conversion of 5-HMF to BAMF is two steps process which includes hydrogenation of 5-HMF to BHMF followed by the etherification of BHMF to BAMF in presence of alcohol using solid acid catalyst. Literature shows that different type of catalysts such as Bronsted acids, Lewis acids and transition metal ions were used for the etherification reaction. Cao et al. reported synthesis of (BAMFs) using methanol as solvent and HZSM-5 catalyst with a Si/Al ratio of 25 from BHMF with 70% yield in the presence of external hydrogen gas(29). Balakrishnan et al. demonstrated a one-pot reductive etherification process converting 5-HMF to BAMFs by using various catalysts, such as Amberlyst-15 and Dowex DR-2030, along with solvent such as ethanol and butanol, yielding up to 80% product in the presence of external H_2 gas. (30) Similarly, Han et al. reported an Amberlyst-15 catalyst for the etherification of BHMF into BAMFs using different solvents (methanol, ethanol, propanol, and butanol), leading to yields of 50%,

70%, 74%, and 71% for BMMF, BEMF, BPMF, and BBMF, respectively using H_2 gas as hydrogen donor(31). Li et al. utilized Co-400 catalyst for the reduction etherification of HMF to (BMMF) at 140°C under 2 MPa pressure of external hydrogen and achieved 98.5% yield (32).There are two approaches generally reported in literature for the synthesis of BAMF (i) direct use of H_2 gas and (ii) catalytic transfer hydrogenation in which alcohol is act as hydrogen donor. Second approach is more attractive looking at the cost and safety considerations associated with producing and handling H_2 gas(33–36). Many researchers have documented the sequential process of hydrogenation followed by etherification to generate BAMFs from HMF. This strategy lowers production costs and streamlines the process by reducing the number of required unit operations. Various catalysts and reaction conditions(37–44) have been investigated to achieve the reductive etherification of 5-HMF. However, selectivity of di ethers from the bio-platform molecule 5-HMF is a bigger challenge in its manufacturing. Wi et al. performed reductive etherification of 5-HMF to BEMF and BIPMF using Zr-SBA-UH catalyst with solvent such as ethanol and 2-propanol at 150°C for 4 h and achieved 88% and 94% yields respectively(45). Wei et al.(46) prepared Zr-SBA to synthesized BPMF via reductive etherification of 5-HMF and obtained 81.% selectivity of BPMF after 4 h at 180°C. Jae et al.(47) employed Sn-beta catalyst to carry out reduction and etherification reactions with 2-propanol and reported 79.5% yield of BIPMF after 6 h at 180°C. In a similar vein, Luo et al.(48) achieved a 61% BPMF yield using the same reaction conditions and catalyst (Sn-beta) for a 3 h duration. Lewis et al.(49) manipulated the Lewis acidity of an Hf-Beta catalyst which led to elevated yield of BBMF (81%). This was accomplished by utilizing 1-butanol as a solvent and conducting the reaction at 120°C for 1 h. Shinde and Rode(50) synthesized Zr-Mont catalyst through wet-impregnation method, demonstrating its efficacy in both reduction and etherification reactions. Robust interaction between Zr and Mont imbued the Zr-Mont catalyst with

enhanced Lewis acidity, culminating in superior yields of 95% BIPMF and 96% BBMF at 150°C, surpassing the performance of Sn-Beta and Hf-Beta catalysts. Rana et al.(51) prepared BPMF by one-pot reductive etherification using mixed catalyst Zr-Hβ + ZrO(OH)$_2$ and obtained 91 % selectivity of BPMF. It was noted that competitive reactions reduce selectivity of BAMFs. So, highly selective and efficient catalysts are required to achieve high selectivity of BAMFs. As indicated in recent literature, the presence of Lewis and Bronsted acidic sites has been highlighted for their significant influence on achieving heightened product selectivity and minimizing undesirable secondary reactions. Certain studies have suggested that the process of etherifying 5-HMF with alcohol is primarily governed by the presence of Lewis acid, while concurrent competitive reactions are primarily regulated by the presence of Bronsted acid(21). Lanzafam et al.(52)) showed that strong Bronsted acidity was responsible for the furan ring opening reaction, whereas Lewis acidity led to formation of EMF. On other hand, Barbera at el.(53) used sulphated zirconia and reported that formation of EMF was suppressed due to increased Bronsted acidity and decreased Lewis acidity. However, Luo et at.(48) concluded that both Lewis and Bronsted acid were essential for the etherification of 5-HMF.

In this study, Zr-HZSM-5 and Sn-HZSM-5catalysts were synthesized through wet impregnation and post-synthesis methods, respectively. These catalysts were then employed to facilitate selectively convert 5-HMF to 2,5-bis(isopropoxymethyl)furan (BPMF) using 2-propanol. The aim was to synthesize highly selective BPMF; study the effect of Zr and Sn supported HZSM-5 catalyst on 5-HMF conversion and to understand role of acidic sites on the selectivity of the BPMF. A detailed study of textural properties and acidity of Zr-HZSM-5 and Sn-HZSM-5 was conducted. It was observed that Sn-HZSM-5 showed higher activity and selectivity as compared to Zr-HZSM-5. Results of NH$_3$-TPD and Py-IR revealed that Sn-HZSM-5 possesses large amount of Lewis acid sites

(LAS) along with sufficient number of Bronsted acid sites (BAS), whereas Zr-HZSM-5 has high no of LAS with a few BAS. This study showed that 5-HMF converted into both HPMF and BPMF via one pot reductive etherification using different Lewis acid catalyst such as Zr and Sn supported on HZSM-5. It also exhibits the role of different Lewis acidic metal ions to achieve higher selectivity of BPMF by tuning LAS and BAS. Remarkably, the current study showcases the completion of one-pot reductive etherification of 5-HMF into BPMF at optimize reaction conditions of 160°C in 4h, achieving an impressive selectivity of 99% using the Sn-HZSM-5 catalyst whereas Zr-HZSM-5 afford 83% selectivity at similar reaction conditions.

6.2. Materials and methods

6.2.1. Materials

The chemicals acquired were utilized without further modification. In India, 5-(hydroxymethyl) furfural (98% purity) was provided by SSRL (Sisco Research Laboratories Pvt. Ltd.). All the alcohols and solvents, aq. ammonia (30%), ZrO_2 and metal precursors such as Zirconyl Nitrate Hydrate (99.5%) were purchased from LobaChemie, Mumbai, India and metal precursors including Tin Chloride pentahydrate ($SnCl_4.5H_2O$) were procured from Sigma-Aldrich, India. HZSM-5 was bought from Sud-cheme India Private Limited, located in Vadodara, Gujarat.

6.2.2. Catalyst Preparation

6.2.2.1. Preparation of Zr-HZSM-5

The ammonium form of ZSM-5 catalyst was calcined at 550 °C in 4 h to get proton form ZSM-5 catalysts. Next, zirconium (IV) nitrate hydrate metal ions were impregnated into the structure of ZSM-5 using a typical wet impregnation method (54). To prepare Zr-impregnated ZSM-5 catalyst, 4.05 gm zirconium (IV) oxynitrate hydrate was dissolved into 20 ml deionized water. After all zirconium (IV) nitrate salt dissolved, 16 gm of ZSM-5

was added to the aqueous solution. The mixture was then kept at room temperature overnight for impregnation. After impregnation, sample was dried at 120 °C in 4 h and then, calcined at 550 °C in 6 h.

6.2.2.2. Preparation of Sn-HZSM-5

Sn-HZSH-5 catalysts were prepared using a two-step post-synthesis procedure(55), which consisted of the de-alumination of parent HZSM-5 and then incorporation of Sn species into the framework of de-aluminated Si-ZSM-5 via dry impregnation and calcination. Briefly, commercial HZSM-5 with nominal nSi/nAl ratio of 3.5 was stirred in a 13 mol L^{-1} nitric acid aqueous solution (20 mL gzeolite^{-1}) at 100°C overnight to obtain a de-aluminated HZSM-5 (Si-HZSM-5). The powder was filtered, washed thoroughly with deionized water, and dried at 180°C overnight. Before the incorporation of Sn, the sample was pre-treated at 200°C overnight under vacuum to remove physisorbed water. The solid mixture was put into a reactor, then sealed and heated to 600 ^{o}C in 6 h (heating rate at 5 ^{o}C /min) under vacuum. After that, it was calcined under flowing air at 600 ^{o}C in 6 h.

6.3. Catalyst Characterization

6.3.1. Powder X-ray diffraction measurements

Powder X-ray diffraction (PXRD) profiles were acquired utilizing a Bruker D8 Advance X-ray diffractometer. The LynxEye Superspeed detector and Cu Kα radiation sourced from a PW Bragg–Brentano (BB) goniometer (θ/2θ) were employed for this purpose, with operational settings at 40 kV and 35 mA. The recorded diffractograms spanned the 2θ range of 5° to 90°, employing a 2θ step increment of 0.02°.

6.3.2. BET measurements

The surface areas according to the Brunauer–Emmett–Teller (BET) method, along with pore volume and pore size distribution using Barrett–Joyner–Halenda (BJH) analysis, were evaluated for the catalysts under investigation. This assessment involved N_2 adsorption-

desorption analysis performed at a temperature of -196°C. Prior to the analysis, the catalysts were subjected to vacuum degassing at a temperature of 200 ± 2°C.

6.3.3. TEM

Images of the catalyst were captured using a JEOL JEM2100 transmission electron microscope (TEM).

6.3.4. Temperature Programmed Desorption of NH_3 (NH_3-TPD)

The acidity strength and quantity of acid sites located on the catalyst's surface were ascertained *via* Temperature Programmed Desorption (TPD), utilizing the Belcat-II instrument from BEL Japan. In a standard protocol, a 75 mg catalyst sample underwent pretreatment at 300°C with a continuous flow of helium for 2 h within a quartz U-tube, preceding the chemisorption step. Subsequently, the temperature was lowered to 50°C, and a mixture of 10% NH_3 in helium was directed through the catalyst for duration of 30 min. Following this, any physically adsorbed NH_3 gas was purged out by flowing helium for 15 min at 50°C. Subsequent to this, the TPD analysis of NH_3 adsorbed onto the acidic sites was conducted. Temperature was raised at a rate of 10°C per min, elevating the samples up to 800°C within a helium environment, while utilizing a Thermal Conductivity Detector (TCD) to quantify the quantity of desorbed gas.

6.3.5. Pyridine FTIR

Infrared spectra for pyridine adsorption (Py-IR) were recorded using a Cary630 FT-IR Spectrometer. The initial step involved subjecting a self-supporting sample pellet, weighing approximately 20 mg and measuring 10 mm in diameter, to a temperature of 500°C for a duration of 2 h under a vacuum. This step was taken to eliminate any moisture and other adsorbed gases from the sample. The subsequent phase consisted of saturating all the acid sites on the sample by exposing it to pyridine at a temperature of 150°C for a

period of 1 h. The identification of Lewis and Bronsted acid sites was achieved by analyzing the bands located at 1445 cm^{-1} and 1543 cm^{-1}.

6.4. Catalytic Activity

Experiment was carried out in a 100 mL stainless steel autoclave reactor. Autoclave was loaded with 1 g of hydroxymethylfurfural (HMF), catalyst (0.2g and 0.25 g), and 50 mL of 2-propanol. After sealing the autoclave, it was heated to the desired reaction temperature of 140°C, 150°C, 160°C, and 170°C under continuous stirring at 550 rpm for reaction duration of 4 h. Following each reaction, the autoclave was cooled. At the conclusion of each run, the mixture of products was separated from the catalyst through centrifugation and subsequently subjected to analysis using Gas Chromatography-Mass Spectrometry (GC-MS). The GC-MS was equipped with a DB-1701 column (60M x 0.32mm x 1μm film thickness), consisting of a 14% cyanopropylphenyl phase and an 86% dimethylpolysiloxane phase.

To assess the performance of the catalytic systems, two metrics were defined: conversion of 5-HMF (X_{5-HMF}, %) and selectivity to products (Si). The calculation of 5-HMF conversion (X_{5-HMF}) involved determining the ratio of the amount of 5-HMF converted to the initial amount of 5-HMF. Selectivity values for reaction products such as BHMF, HPMF, and BPMF (Si) were calculated by dividing the quantity of formed products by the amount of 5-HMF that underwent conversion. The reaction for the reductive etherification of 5-HMF to BPMF is as shown in Figure 6.1.

$$\text{conversion } (\%) = \frac{(I.N.)_i - (I.N.)_f}{(I.N.)_i} * 100 \quad ,$$

Where, $(I.N.)i$ = Initial moles of 5-HMF   & $(I.N.)f$ = Final moles of 5-HMF

$$\text{selectivity } (\%) = \frac{\text{moles of product formed}}{\text{moles of 5-HMF converted}} * 100$$
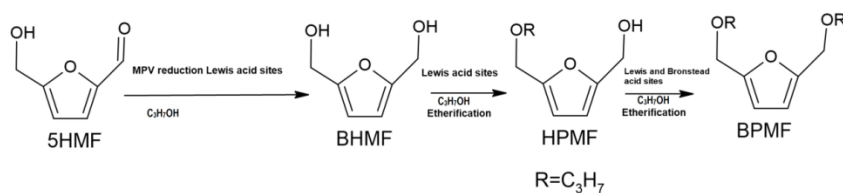
Figure 6.1 Reductive etherification of 5-HMF to BPMF

6.5. Results and discussions

6.5.1. Physical and chemical properties of catalysts

6.5.1.1. Transmission Electron Microscopy

Transmission Electron Microscopy (TEM) analysis was performed to acquire information about the particle size and morphology of the catalysts. The TEM images, displayed in Figure 6.2 ((a) and (b)), revealed that average Zr particle size are in the range of 8-10 nm and that of Sn particle size are in the range of 10-12 nm. However, the identification of metal particles proved challenging due to their tendency to aggregate during the synthesis method for the Zr-HZSM-5.

Figure 6.2 TEM Images and particle size (a) Zr-HZSM-5 (b) Sn-HZSM-5

6.5.1.2. Powder X-ray diffraction (PXRD) analysis

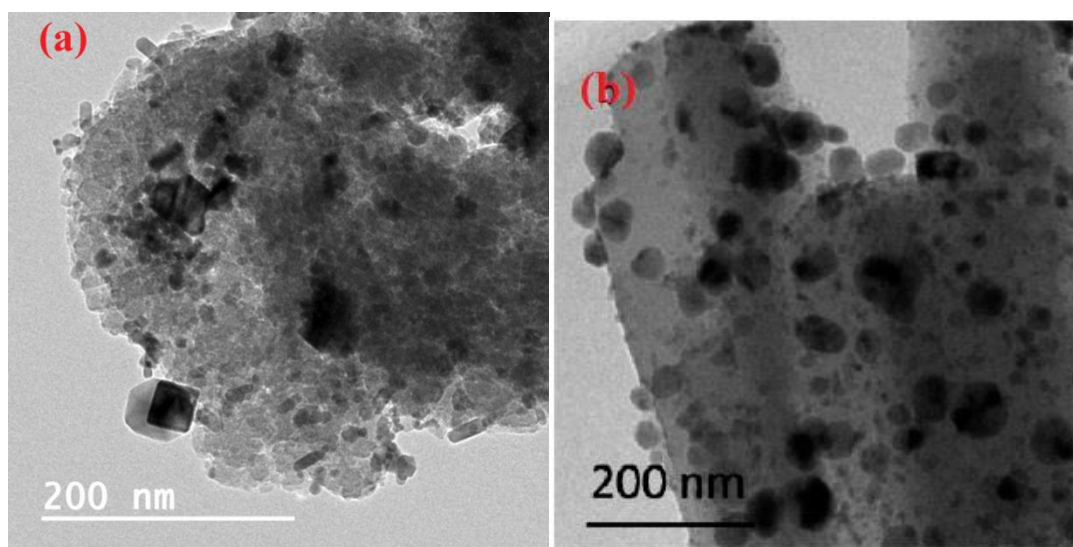In Figure 6.3(a), the PXRD patterns of the Zr-HZSM-5 catalysts exhibit distinctive peaks at diffraction angles of $2\theta = 14°, 20°, 24°, 26.75°, 30°, 32°, 34.55°$ and $54.34°$. Moving on to Figure 6.3(b ,c and d), the PXRD patterns of the HZSM-5, dAl-HZSM-5 and Sn-HZSM-5catalysts displayed a pattern that closely resembles to HZSM-5, with evident peaks at $2\theta = 14°, 20°, 24°, 24.57°, 26.02°, 27.05°, 29.22°, 29.9°, 30.10°, 34.3°$ and $45.44°$. The PXRD pattern of the Zr and Sn impregnated HZSM-5 completely matched with that of the parent HZSM-5, which indicates that the impregnation has no obvious effect on the parent zeolite structure and its structure remains intact after loading metal over the HZSM-5 catalyst. Presence of distinct diffraction peaks at $34.3°$, attributed to Sn (JCPDS file No.-00-004-0673)(56,57) was distinctly observed in the Sn-HZSM-5catalyst samples. The diffractions at $34.55°$ and $54.34°$, due to tetragonal zirconia phase (57,58) were clearly observed on the Zr-HZSM-5 catalyst sample.
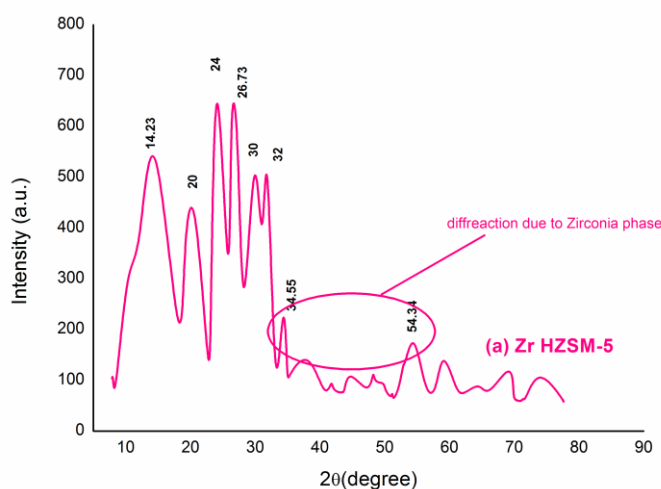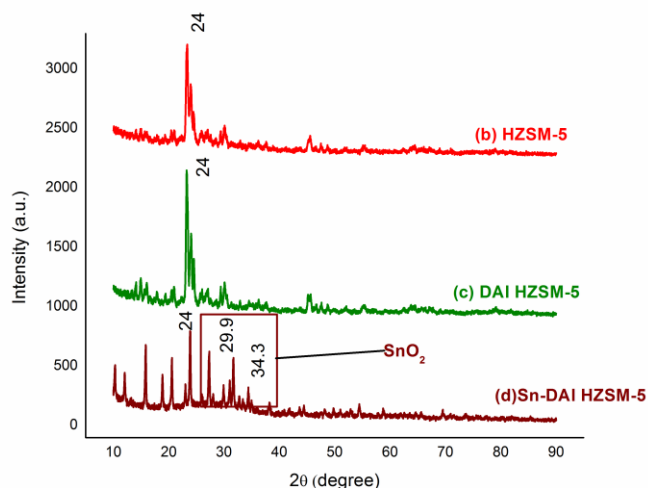
Figure 6.3 PXRD patterns of (a) Zr-HZSM-5 (b) HZSM-5 (c) DAl-HZSM-5 and (d) Sn-HZSM-5 catalysts.

6.5.1.3. Surface areas, external surface area and pore volumes

The N_2 adsorption results for the catalysts are summarized in Table 6.1. It is evident from Table 6.1 that the surface area has decreased for both Zr-HZSM-5 and Sn-HZSM-5. Introduction of Zr and Sn metal to HZSM-5 does not significantly impact the specific surface area and micro pore volume and a slight reduction in surface area and micropore was observed. However, an increase in mesopore volume has been noted which is attributed to the extraction of Al atoms from the zeolites(59). Sn-HZSM-5 catalyst exhibits a notably larger external surface area and mesopore volume as compared to the Zr-HZSM-5. Higher mesopore volume in the catalyst sample aids in enhancing mass transfer during heterogeneous catalytic reactions, consequently leading to heightened intrinsic site activity(60).

156

Table 6.7 Textures of HZSM-5, Sn- HZSM-5 and Zr-HZSM-5 catalyst

Sample	Surface area, m^2/g	Pore volume, cm^3/g			External surface area, m^2/g
	S.A^a	$V_{pore,}^b$	V_{micro}^c	V_{meso}	S_{meso}^c
HZSM-5	553.19	0.30	0.22	0.08	34.35
Sn-HZSM-5	436.50	0.55	0.12	0.42	141.75
Zr-HZSM-5	393.157	0.28	0.13	0.15	79.69

a-S.A- BET surface area, b-Total pore volume measured at P/P0= 0.9999,c-t-plot method, $V_{meso}= V_{pore}- V_{micro}$, External surface area.

6.5.1.4. Acidity of catalysts

The NH_3-TPD analysis was conducted to assess the quantity and strength of acidic sites in HZSM-5, Zr-HZSM-5, and Sn-HZSM-5 catalysts. The distribution of products, their selectivity, and the rates of desired and undesired reactions are significantly influenced by both BAS and LAS. The MPV reduction reaction is favored by LAS which also enhance the etherification step. Whereas, the rate of undesired product formation decreases with a reduction in BAS. Therefore, the rate of etherification is enhanced by the synergistic effect of LAS and BAS(47).

Distinct peaks of Sn-HZSM-5 and Zr-HZSM-5 catalysts shown in lower temperature region (<300°C), middle temperature range (301°C to 550°C), and higher temperature range (>550°C) in Figure 6.4 (a) and (b). Three characteristic desorption peaks of Sn-HZSM-5 are observed at 136 °C, 434 °C, and 550 °C and that for Zr-HZSM-5 peaks at 164°C, 300 °C, and 550 °C. These peaks are identified as NH_3 desorption from weak, moderate, and strong acid sites. The middle and higher temperature peaks correspond to

desorption from strong acidic sites, while lower temperature peaks are attributed to release of NH_3 from weak acidic sites(61).

NH_3-TPD results indicate that catalysts possess both strong and weak acidic sites. Middle and high-temperature peaks around 434 °C and 550 °C for Sn-HZSM-5, and at 550 °C for Zr-HZSM-5 are due to desorption from LAS. Table 6.2 shows that impregnation of Sn and Zr onto HZSM-5 led to change in its total acidity. This alteration in acidity is linked to introduction of metal (Zr and Sn) species. Sn and Zr impregnation induce a significant improvement in LAS and a reduction in BAS as evidenced by the values of weak, moderate, and strong acid sites in Table 6.2. Notably, total acidity of Sn-HZSM-5 and Zr-HZSM-5 reduced to 1.58 mmol/g and 1.62 mmol/g, respectively. Sn-HZSM-5 exhibited a higher value of moderate acidic sites (0.72 mmol/g) compared to Zr-HZSM-5 (0.52 mmol/g). This change in Bronsted and Lewis acid sites is attributed to the strong interaction between intrinsic acid sites and Sn species. This strong interaction ultimately resulted in conversion of some Bronsted acid sites into Sn-Lewis acid sites(48). These Sn-Lewis acid sites are capable of fastening the etherification process. Lewis et al. have also observed a similar trend of higher etherification rate with Sn-Lewis acid sites for conversion of 5-HMF to 2,5 BBMF (2,5 bis butoxymethyl furan)(48,49).

Furthermore, Py-IR analysis was conducted to quantify concentration of Lewis and Bronsted acid sites for confirmation. The LAS, Lewis + Bronsted acidic sites, and BAS are observed around 1445, 1490, and 1542 cm^{-1}, respectively depicted in Figure 6.5 for all three catalysts. Pyridine, acting as a Lewis base which interacts with BAS to form pyridinium ions. The formed pyridinium ions can be seen between 1525 and 1542 cm^{-1}(Figure 6.5)(62). It can also adsorb on the surface of LAS, indicated by FTIR bands at 1445 cm^{-1}.

Table 6.3 provides a quantitative analysis of Bronsted and Lewis acid sites for both Sn-HZSM-5 and Zr-HZSM-5. As seen in table 6.3, Sn-HZSM-5 exhibits a higher quantity of both Lewis and Bronsted acid sites compared to Zr-HZSM-5. This may be due to higher Lewis acidity of Sn than to Zr. Higher value of LAS with Sn compared to Zr was also reported by Corma et al(63,64).
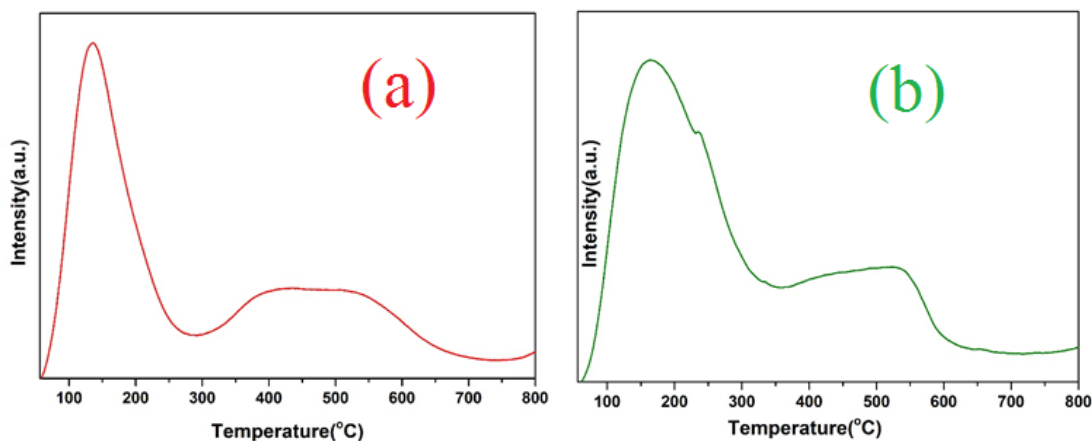

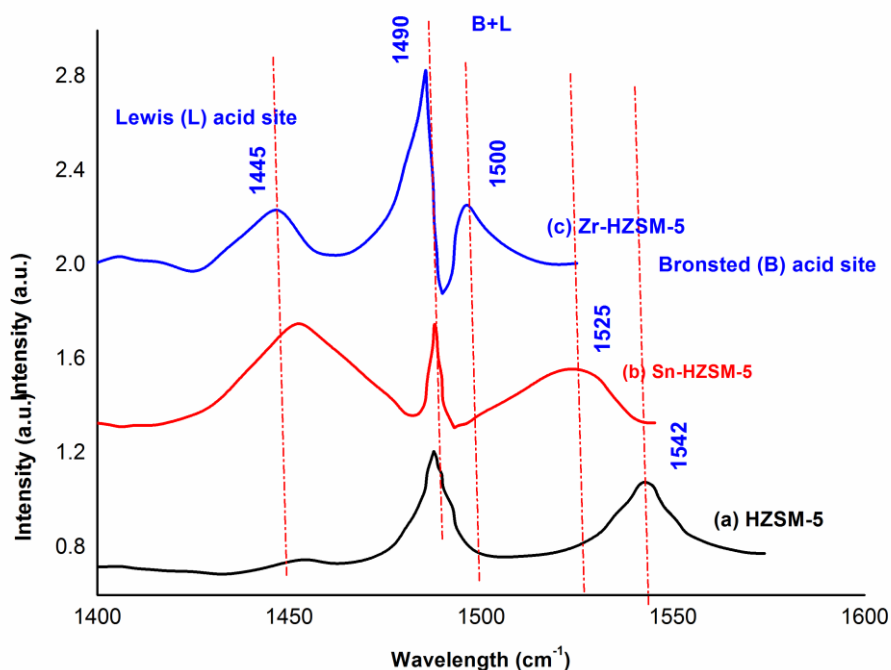**Figure 6.4** NH$_3$-TPD profiles of (a) Sn- HZSM-5 (b) Zr-HZSM-5

Figure 6.5 Py-FTIR of (a) HZSM-5 (b) Sn-HZSM-5 (c) Zr-HZSM-5.

Table 6.8 Acidity information of catalysts by NH$_3$-TPD & Titration method

Sample	Amount of acid sites, (mmol/g)			
	Total	Weak (<300°C)	Moderate (301-550°C)	Strong (>550°C)
HZSM-5	2.060	0.814	0.762	0.431
Sn-HZSM-5	1.58	0.56	0.72	0.30
Zr-HZSM-5	1.62	0.85	0.52	0.25

Table 6.3 Acidity information of catalysts by Py-IR method

Catalyst	Amount of Acidic Sites (mmol/g)	
	Lewis acid sites[a]	Bronsted acid sites[a]
HZSM-5	2.18	27.78
Sn-HZSM-5	27.30	16.28
Zr-HZSM-5	24.58	5.45

[a]Determined by Py-IR

6.5.1.5. Study of catalyst activity

Effect of temperature and catalyst loading

The sequential reductive etherification of HMF was conducted in temperature range of 140 - 170 °C, catalyst loading of 0.1 - 0.25 g with three different catalyst namely HZSM-5, Zr-HZSM-5, and Sn-HZSM-5 (with metal loadings of 0.15 M) in 4 h reaction time. Obtained results are demonstrated in Table 6.4.

Initial experiment employed HZSM-5 with a reaction condition of 140°C in 4 h and 0.1g catalyst loadings. About 12% conversion of 5-HMF with 5% and 8% selectivity of HPMF and BPMF, respectively were obtained (entry 1).

Upon increasing catalyst loading to 0.2g, a marginal increase in conversion and selectivity of HPMF and BPMF was observed (entry 2). Lower selectivity of BPMF was due to few LAS and more BAS of HZSM-5. Yang et al also concluded that LAS and BAS played a vital role in selectivity of BPMF(65). Therefore, to enhance BPMF selectivity, Zr-HZSM-5 was tested for a reaction condition of 140°C in 4 h (entries 3-6). Incorporation of Zr to HZSM-5 led to increased 5-HMF conversion and HPMF and BPMF selectivities. Maximum 99 % conversion with 35 % and 65 % selectivity of HPMF and BPMF, respectively, were attained with catalyst loading of 0.2 g (entry 5). However, further increase in catalyst loading to 0.25 g did not impact positively on 5-HMF conversion and it reduced to 61 %.Whereas, selectivity of both HPMF and BPMF remains intact. This can be due to an increase in Lewis acid sites and a reduction in the Brønsted acid sites on the catalyst, which favours the etherification. To check the effect of temperature on conversion and selectivity, experiments were carried out at 150°C and 160°C with 0.2 g and 0.25 g catalyst (entry 7- 10). Selectivity of BPMF increases with increase in temperature and reaches 83 % maximum at 160°C and catalyst loading 0.25g (entry10).

Process of reductive etherification of 5-HMF in 2-propanol using a catalyst can be described as follows: Initially, the carbonyl group in 5-HMF undergoes hydrogenation through interaction with LAS to produce BHMF. Produced BHMF then undergoes etherification to form HPMF which is subsequently converted to BPMF *via* etherification in the presence of 2-propanol. This second etherification step occurs with an excess of either LAS or BAS. Similar findings reported by S. Rana and P. Rana(51,66) in study of one-pot catalytic transformation of 5-HMF into HPMF and BPMF.

Obtained results reveal that Zr-HZSM-5 acts as an etherification catalyst in reductive etherification of 5-HMF to HPMF and BPMF. However, analysis of the product mixture indicates that HPMF was not efficiently converted into BPMF which reflects in selectivity

of BPMF. Reaction mechanism for above reaction involves following steps, in which first carbonyl group of 5-HMF endures hydrogenation reaction *via* in contact with LAS, which led to formation of BHMF and then, BHMF is etherified to produce HPMF in the presence of 2-Propanol. This etherification requires ample of LAS and sufficient BAS to convert BHMF to HPMF followed by production of BPMF.

Therefore, it was further decided to replace Zirconia (Zr) with Tin (Sn) since Sn exhibits higher Lewis acidity compared to Zr(47,49). Consequently, Sn-HZSM-5 was synthesized to improve concentration of Lewis and Bronsted acid sites on the catalyst and employed at reaction conditions to examine its effect on conversion of HPMF into BPMF and BPMF selectivity. Higher conversion and selectivity was achieved with 0.2 g and 0.25 g of catalyst (entries 5 to 10). Hence, subsequent reactions with Sn-HZSM-5 were performed with 0.2 g and 0.25 g of catalyst in a temperature range of 140 - 170 °C in 4 h (entries 11 to 18).

Alcohols can also act as etherifying agents which enable formation of BAMFs without the need for molecular hydrogen (H_2)(30,31,37–45). At 140°C in 4 h (entry 11), 95 % conversion of 5-HMF was attained. However, the selectivity of HPMF and BPMF was around 49% and 51 %, respectively. With increased catalyst loading to 0.25 g (entry 12), a slight increase in BPMF selectivity was noticed and it was around 54%. As illustrated in Figure 6.6, higher temperatures augmented both 5-HMF conversion and BPMF selectivity and reached 92% and 97% respectively. Whereas, selectivity of HPMF significantly reduced to 1% under reaction conditions of 150°C and a catalyst loading of 0.2 g (entry 13). This observation confirms the effective integration of Sn within the zeolite framework which provides abundant Lewis and Bronsted acid sites. Elevated temperatures also seem to favor conversion of HPMF into BPMF. To further investigate temperature effects, experiments were performed at higher temperatures (160°C, 170°C) in 4 h with 0.2 g

catalyst (entries 14 and 15). These resulted in higher 5-HMF conversions (93%) and a slight decrease in BPMF selectivity to 96%.

Similarly, experiments were conducted with a 0.25 g catalyst loading in 4 h (entries 16-18) at temperature ranges of 150°C-170°C. Figure 6.7 indicates that at 160°C, 5-HMF conversion reached approximately 96%, with HPMF and BPMF selectivity at 1% and 99%, respectively. Increased selectivity further confirms that Sn demonstrates superior catalytic activity due to its proper incorporation into HZSM-5 and the presence of abundant LAS alongside sufficient BAS, as evidenced by the NH_3-TPD (Table 6.2) and Py-IR (Table 6.3) results. This trend highlights that the catalytic efficiency of etherification benefits from the synergistic effects of elevated LAS and ample BAS.

Table 6.4. Catalytic activity of different Catalyst (Reaction conditions: 5-HMF – 1g, 2-propanol- 50 ml)

Entry	Catalyst & Sn loading	Catalyst loading (g)	Temp (°C)	Time (h)	Conv. %	Selectivity%		
						BHMF	HPMF	BPMF
1	HZSM-5	0.1	140	4	12.50	-	4.50	8.00
2		0.2	140	4	14.36	-	5.45	8.91
3	Zr-HZSM-5 (0.15 M)	0.1	140	4	60.88	-	45.90	54.09
4		0.15	140	4	96.16	0.21	52.25	45.17
5		0.2	140	4	99.00	0.24	34.43	65.01
6		0.25	140	4	61.37	0.21	34.54	65.16
7		0.20	150	4	80.50	-	24.05	75.95
8		0.25	150	4	85.97	-	21.37	78.63
9		0.20	160	4	90.4	-	19.35	80.65
10		0.25	160	4	84.86	-	17.00	83.00

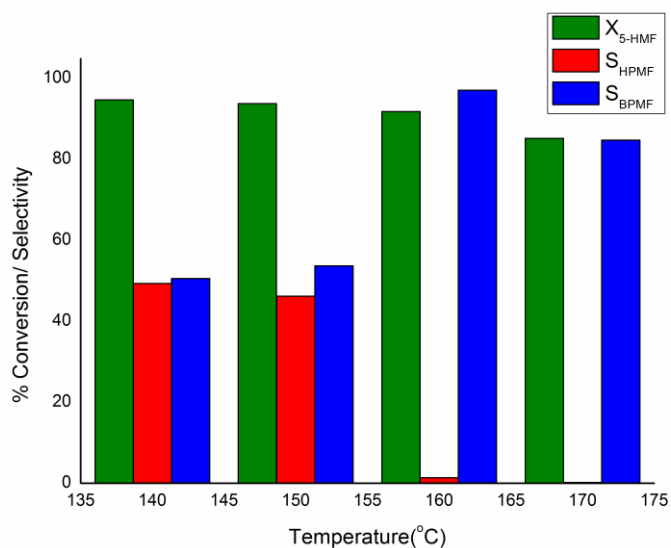| 11	Sn-HZSM-5	0.2	140	4	95.00	-	49.00	51.00
12	(0.15 M)	0.25	140	4	93.79	-	46.00	54.00
13		0.20	150	4	92.00	-	1.34	97.00
14		0.20	160	4	85.98	-	0.15	85.54
15		0.20	170	4	93.00	-	4.00	96.00
16		0.25	150	4	85.18	-	0.19	84.74
17		0.25	160	4	96.00	-	1.00	99.00
18		0.25	170	4	86.88	-	-	83.46

Figure 6.6 Effect of temperature on BHMF, HPMF & BPMF selectivity (Catalyst: Sn HZSM-5 loading 0.2g)
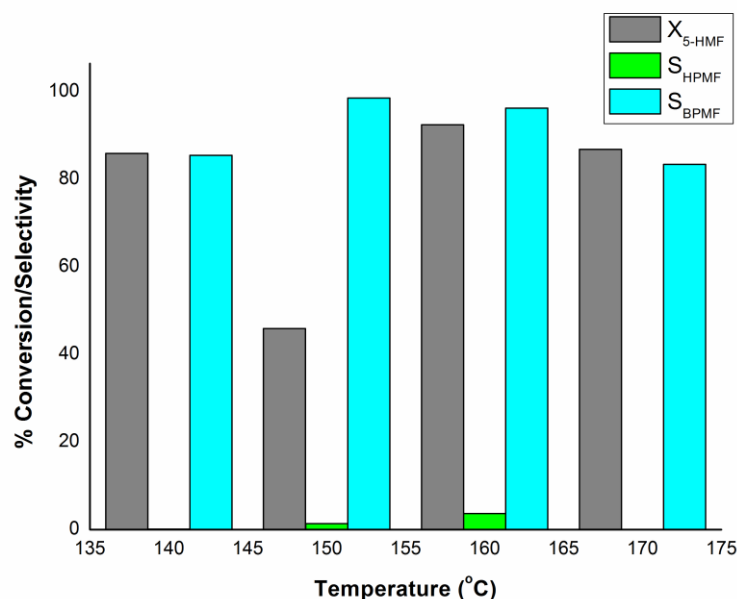
Figure 6.7 Effect of temperature on BHMF, HPMF & BPMF selectivity (Catalyst: Sn HZSM-5 loading 0.25g)

6.5.1.6. Effect of impregnation of Zr and Sn on the catalyst properties and catalytic behavior

In this study, Zr-HZSM-5 and Sn-HZSM-5 were synthesized and employed as catalysts for the conversion of 5-hydroxymethylfurfural (5-HMF) to 2, 5-bis (isopropoxymethyl)furan (BPMF) using 2-propanol. The aim was to investigate the roles of acidity and the interaction of Zr and Sn with the HZSM-5 support in the etherification of 5-HMF. The textural properties and acidity of Zr-HZSM-5 and Sn-HZSM-5 were examined.

It was observed that the Zr-HZSM-5 catalyst demonstrated adequate etherification activity, yielding both HPMF and BPMF; however, the selectivity towards BPMF was not upto the mark (Table 6.4, entries 3-10). In contrast to this, Sn-HZSM-5 catalyst exhibited significantly enhanced etherification activity, with higher selectivity for BPMF (Table 6.4, entries 13-18). This indicates the successful and proper incorporation of the catalytically active Sn metal into the zeolite (HZSM-5), leading to the effective conversion of BAS into LAS.

165

Figure 6.8 compares the catalytic performance of Sn-HZSM-5 and Zr-HZSM-5. The Sn-HZSM-5 catalyst exhibits outstanding performance of 5-HMF and the selectivity of BPMF. This can be due to the presence of robust LAS along with sufficient BAS. Distribution of this distinct acid site significantly enhances the reductive etherification process and facilitates conversion of 5-HMF into BPMF.

 In addition to these results of NH$_3$-TPD, Py-IR results, and the textural properties of catalysts represent that Zr-HZSM-5 possesses reasonably good LAS but very poor BAS and a small mesopore volume (Table 6.1). These factors may limit the conversion of HPMF to BPMF and hinder the mass transfer of reactants to active sites and thereby reduce BPMF selectivity in case of Zr-HZSM-5. On the other hand, Sn-HZSM-5, with its ample LAS, sufficient BAS, and larger mesopore volume, mitigates diffusion issues and achieves exorbitant selectivity for BPMF through the proper synergistic effect of the acid sites.
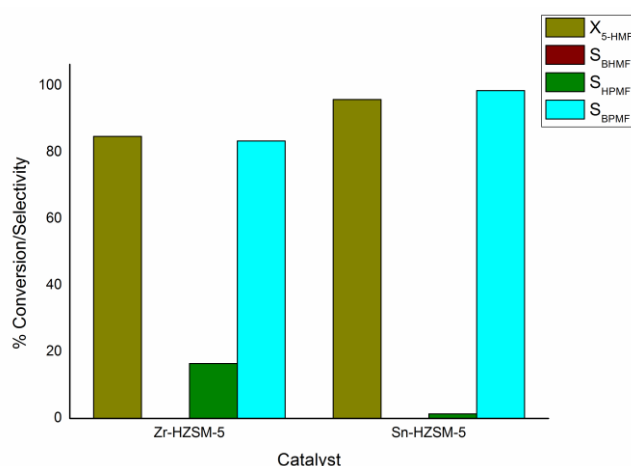

Figure 6.8 Comparison of effect of catalysts (Zr-HZSM-5 and Sn-HZSM-5) on BHMF, HPMF & BPMF selectivity

6.5.1.7. Effect of acidity on catalyst performance

Our goal was to modify the acidic sites of HZSM-5 by increasing LAS and reducing the BAS through the incorporation of Sn and Zr. More emphasis was given to detailed analysis of pyridine adsorption data that provides more detailed information on the nature of acidic sites compared to NH3-TPD.

As shown in Table 6.3, HZSM-5 had a smaller quantity of LAS (2.18 mmol/g) and a larger quantity of BAS (27.78 mmol/g). Since LAS promote the Meerwein-Ponndorf-Verley (MPV) reaction and the synergistic effect of LAS and BAS facilitates the reductive etherification of 5-HMF to yield ethers, the observed product distribution aligned with this trend (Table 6.4). Impregnation of Sn and Zr metal ions altered the quantities/concentrations of Lewis and Bronsted acidic sites which led to changes in product distribution.

Figure 6.9 express that Sn-HZSM-5 had a substantial amount of LAS (27.30 mmol/g) and a reasonable amount of BAS (16.28 mmol/g), while Zr-HZSM-5 had a large amount of LAS (24.58 mmol/g) and very few BAS (5.45 mmol/g). Using the Zr-HZSM-5 catalyst, 5-HMF could convert into HPMF and BPMF, but the selectivity for BPMF was not high (83%). In contrast, Sn-HZSM-5 demonstrated remarkably high selectivity towards BPMF (99 %).

High Lewis acidity Sn metal ion and the effective integration of catalytically active Sn metal into the zeolite significantly increased the LAS and reduced the BAS. Due to the interaction between intrinsic acid sites and Sn species, some BAS converted into LAS. These Sn-Lewis acid sites have the capacity to enhance the etherification process which ultimately affects the product distribution. This emphasizes that the successful one-pot reductive etherification of 5-HMF into BPMF requires a synergistic interplay between LAS and BAS.

Similar findings were also noted in the studies conducted by Luo et al.(48) and Barbera et al.(53) These studies revealed that the carbonyl group within HMF could undergo an initial reduction to generate BHMF through MPV (Meerwein-Ponndorf-Verley) reduction which facilitated by the LAS present on the catalyst. Subsequently, the produced BHMF could undergo consecutive etherification reactions with isopropanol to yield 2-hydroxymethyl-5-isopropoxymethylfuran (HPMF) and 2,5-bis(isopropoxymethyl)furan (BPMF). This sequence of reactions is promoted when the catalyst possesses an abundance of BAS or an excessive presence of LAS. The collective presence of these acid sites facilitates the efficient transformation of HMF into its etherified derivatives.

Table 6.5 Product distribution and acid site distribution

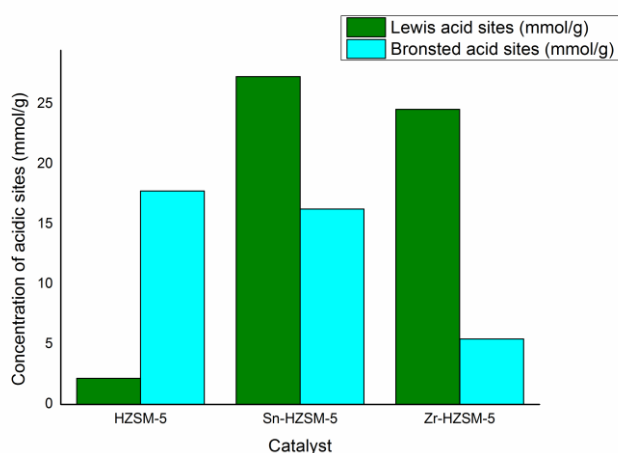| Catalyst	Amount of Acidic Sites (mmol/g)		% Selectivity		
	Lewis acid sites	Bronsted acid sites	BHMF	HPMF	BPMF
Zr-HZSM-5	24.58	5.45	-	17.00	83.00
Sn-HZSM-5	27.30	16.28	-	1.00	99.00

Figure 6.9 Concentration of LAS and BAS on catalyst (mmol/g)

6.5.1.8. Catalyst reusability study

The reusability of Sn-HZSM-5 catalyst is investigated in five consecutive reactions run. When the reaction completed, the catalyst was separated by centrifugation and washed with acetone to reuse it in next run. The results of reusability study are as shown in the Figure 6.10. Reduction in the conversion of 5-HMF was observed after 4th run while selectivity of BPMF was intact after 5 run cycle.
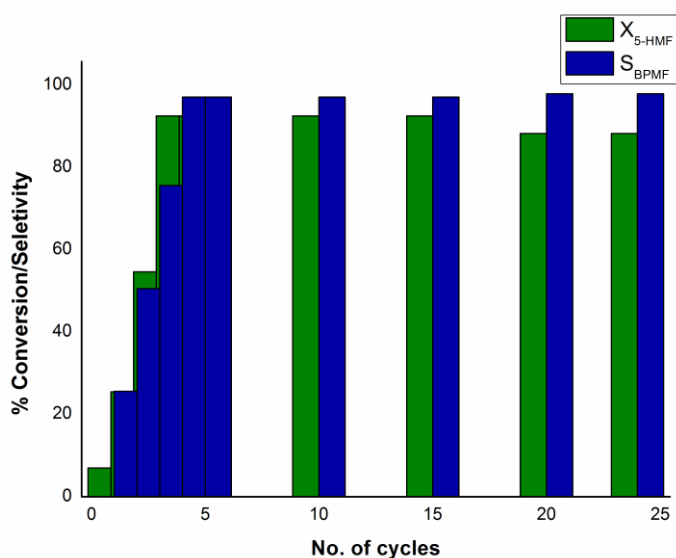

Figure 6.10 Reusability study of Sn-HZSM-5 catalyst (Reaction conditions: 5-HMF–1g, 2-propanol- 50 ml, and catalyst loading-0.25 g).

6.6 Conclusions

This study demonstrated that Sn-HZSM-5 is a more effective catalyst than Zr-HZSM-5 for the etherification of 5-HMF to BPMF using 2-propanol. Lewis acid sites are generated through the incorporation of metal ions, resulting in observable Lewis acidity is Sn-HZSM-5 > Zr-HZSM-5. Superior performance of Sn-HZSM-5 is attributed to its higher selectivity for BPMF, which results from the successful incorporation of Sn. This enhances the conversion of Bronsted acid sites to Lewis acid sites that led to a robust concentration of Lewis acid sites and sufficient Bronsted acid sites which subsequently promote

reductive etherification process. In contrast, Zr-HZSM-5, with its limited Bronsted acid sites and smaller mesopore volume, exhibited lower BPMF selectivity. The study highlights the importance of acid site distribution and textural properties in catalyst performance for etherification reactions.

6.7. References

1. Al-Soof F., Aklil B, Taeb M, Khesali M, Mazraati M, Lubiantara T N, Alawami A, Clemenz C, Guerer N, Brennand J B G, Spitzy J, Linton D, Griffin J, Tallett M, Steiner P, Szalkowska U. World oil outlook. 2010.

2. Hu L, Lin L, Wu Z, Zhou S, Liu S. Recent advances in catalytic transformation of biomass-derived 5-hydroxymethylfurfural into the innovative fuels and chemicals. Renewable and Sustainable Energy Reviews. 2017 Jul;74:230–57.

3. Zhu JY, Pan X, Zalesny RS. Pretreatment of woody biomass for biofuel production: energy efficiency, technologies, and recalcitrance. Appl Microbiol Biotechnol. 2010 Jul;87(3):847–57.

4. Zhou CH, Xia X, Lin CX, Tong DS, Beltramini J. Catalytic conversion of lignocellulosic biomass to fine chemicals and fuels. Chem Soc Rev. 2011;40(11):5588.

5. Zhang Z, Song J, Han B. Catalytic Transformation of Lignocellulose into Chemicals and Fuel Products in Ionic Liquids. Chem Rev. 2017 May 24;117(10):6834–80.

6. Zhang Z, Zhang M, Deng J, Deng K, Zhang B, Lv K, et al. Potocatalytic oxidative degradation of organic pollutant with molecular oxygen activated by a novel biomimetic catalyst ZnPz(dtn-COOH)4. Applied Catalysis B: Environmental. 2013 Mar;132–133:90–7.

7. Sahu R, Dhepe PL. A One-Pot Method for the Selective Conversion of Hemicellulose

from Crop Waste into C5 Sugars and Furfural by Using Solid Acid Catalysts. ChemSusChem. 2012 Apr;5(4):751–61.

8. Xia H, Hu H, Xu S, Xiao K, Zuo S. Catalytic conversion of glucose to 5-hydroxymethyfural over Fe/β zeolites with extra-framework isolated Fe species in a biphasic reaction system. Biomass and Bioenergy. 2018 Jan;108:426–32.

9. Tollefson J. Can the world kick its fossil-fuel addiction fast enough? Nature. 2018 Apr;556(7702):422–5.

10. Sun G, An J, Hu H, Li C, Zuo S, Xia H. Green catalytic synthesis of 5-methylfurfural by selective hydrogenolysis of 5-hydroxymethylfurfural over size-controlled Pd nanoparticle catalysts. Catal Sci Technol. 2019;9(5):1238–44.

11. Hu L, Zhao G, Hao W, Tang X, Sun Y, Lin L, et al. Catalytic conversion of biomass-derived carbohydrates into fuels and chemicals via furanic aldehydes. RSC Adv. 2012;2(30):11184.

12. Xu C, Arancon RAD, Labidi J, Luque R. Lignin depolymerisation strategies: towards valuable chemicals and fuels. Chem Soc Rev. 2014;43(22):7485–500.

13. Wang J, Xi J, Wang Y. Recent advances in the catalytic production of glucose from lignocellulosic biomass. Green Chem. 2015;17(2):737–51.

14. Zhang Z, Deng K. Recent Advances in the Catalytic Synthesis of 2,5-Furandicarboxylic Acid and Its Derivatives. ACS Catal. 2015 Nov 6;5(11):6529–44.

15. Liu B, Zhang Z. Catalytic Conversion of Biomass into Chemicals and Fuels over Magnetic Catalysts. ACS Catal. 2016 Jan 4;6(1):326–38.

16. Mascal M, Nikitin EB. Direct, High‑Yield Conversion of Cellulose into Biofuel. Angew Chem Int Ed. 2008 Sep 29;47(41):7924–6.

17. Binder JB, Raines RT. Simple Chemical Transformation of Lignocellulosic Biomass into Furans for Fuels and Chemicals. J Am Chem Soc. 2009 Feb 11;131(5):1979–85.

18. Chen B, Li F, Huang Z, Yuan G. Carbon-coated Cu-Co bimetallic nanoparticles as selective and recyclable catalysts for production of biofuel 2,5-dimethylfuran. Applied Catalysis B: Environmental. 2017 Jan;200:192–9.

19. Bai Y, Su S, Wang S, Wang B, Sun R, Song G, et al. Front Cover: Catalytic Conversion of Carbohydrates into 5-Ethoxymethylfurfural by a Magnetic Solid Acid Using γ-Valerolactone as a Co-Solvent (Energy Technol. 10/2018). Energy Tech. 2018 Oct;6(10):1859–1859.

20. Kong X, Zhu Y, Fang Z, Kozinski JA, Butler IS, Xu L, et al. Catalytic conversion of 5-hydroxymethylfurfural to some value-added derivatives. Green Chem. 2018;20(16):3657–82.

21. Fang W, Hu H, Dong P, Ma Z, He Y, Wang L, et al. Improvement of furanic diether selectivity by adjusting Brønsted and Lewis acidity. Applied Catalysis A: General. 2018 Sep;565:146–51.

22. Sacia ER, Balakrishnan M, Bell AT. Biomass conversion to diesel via the etherification of furanyl alcohols catalyzed by Amberlyst-15. Journal of Catalysis. 2014 May;313:70–9.

23. Fang W, Hu H, Ma Z, Wang L, Zhang Y. Two Possible Side Reaction Pathways during Furanic Etherification. Catalysts. 2018 Sep 8;8(9):383.

24. Hu H, Hu D, Jin H, Zhang P, Li G, Zhou H, et al. Efficient Production of Furanic Diether in a Continuous Fixed Bed Reactor. ChemCatChem. 2019 Apr 18;11(8):2179–86.

25. Gupta D, Saha B. Dual acidic titania carbocatalyst for cascade reaction of sugar to etherified fuel additives. Catalysis Communications. 2018 May;110:46–50.

26. Ras E, Maisuls S, Haesakkers P, Gruter G, Rothenberg G. Selective Hydrogenation of 5-Ethoxymethylfurfural over Alumina-Supported Heterogeneous Catalysts. Adv Synth Catal. 2009 Dec;351(18):3175–85.

27. Gerardus Johannes Maria Gruter. 5-SUBSTITUTED 2-(ALKOXYMETHYL)FURANS. US 8,231,693 B2, 2012.

28. De Jong E, Vijlbrief T, Hijkoop R, Gruter GJM, Van Der Waal JC. Promising results with YXY Diesel components in an ESC test cycle using a PACCAR Diesel engine. Biomass and Bioenergy. 2012 Jan;36:151–9.

29. Cao Q, Liang W, Guan J, Wang L, Qu Q, Zhang X, et al. Catalytic synthesis of 2,5-bis-methoxymethylfuran: A promising cetane number improver for diesel. Applied Catalysis A: General. 2014 Jul;481:49–53.

30. Balakrishnan M, Sacia ER, Bell AT. Etherification and reductive etherification of 5-(hydroxymethyl)furfural: 5-(alkoxymethyl)furfurals and 2,5-bis(alkoxymethyl)furans as potential bio-diesel candidates. Green Chem. 2012;14(6):1626.

31. Han J, Kim YH, Jung B, Hwang S, Jegal J, Kim J, et al. Highly Selective Catalytic Hydrogenation and Etherification of 5-Hydroxymethyl-2-furaldehyde to 2,5-Bis(alkoxymethyl)furans for Potential Biodiesel Production. Synlett. 2017

Oct;28(17):2299–302.

32. Li H, Govind KS, Kotni R, Shunmugavel S, Riisager A, Yang S. Direct catalytic transformation of carbohydrates into 5-ethoxymethylfurfural with acid–base bifunctional hybrid nanospheres. Energy Conversion and Management. 2014 Dec;88:1245–51.

33. Ikariya T, Blacker AJ. Asymmetric Transfer Hydrogenation of Ketones with Bifunctional Transition Metal-Based Molecular Catalysts. Acc Chem Res. 2007 Dec 1;40(12):1300–8.

34. Wang D, Astruc D. The Golden Age of Transfer Hydrogenation. Chem Rev. 2015 Jul 8;115(13):6621–86.

35. Osatiashtiani A, Lee AF, Wilson K. Recent advances in the production of γ-valerolactone from biomass-derived feedstocks via heterogeneous catalytic transfer hydrogenation. J of Chemical Tech & Biotech. 2017 Jun;92(6):1125–35.

36. Xue Z, Jiang J, Li G, Zhao W, Wang J, Mu T. Zirconium–cyanuric acid coordination polymer: highly efficient catalyst for conversion of levulinic acid to γ-valerolactone. Catal Sci Technol. 2016;6(14):5374–9.

37. Leng Y, Shi L, Du S, Jiang J, Jiang P. A tannin-derived zirconium-containing porous hybrid for efficient Meerwein–Ponndorf–Verley reduction under mild conditions. Green Chem. 2020;22(1):180–6.

38. Zhou S, Dai F, Xiang Z, Song T, Liu D, Lu F, et al. Zirconium–lignosulfonate polyphenolic polymer for highly efficient hydrogen transfer of biomass-derived oxygenates under mild conditions. Applied Catalysis B: Environmental. 2019

Jul;248:31–43.

39. Rojas-Buzo S, García-García P, Corma A. Hf-based metal–organic frameworks as acid–base catalysts for the transformation of biomass-derived furanic compounds into chemicals. Green Chem. 2018;20(13):3081–91.

40. Li H, He J, Riisager A, Saravanamurugan S, Song B, Yang S. Acid–Base Bifunctional Zirconium *N* -Alkyltriphosphate Nanohybrid for Hydrogen Transfer of Biomass-Derived Carboxides. ACS Catal. 2016 Nov 4;6(11):7722–7.

41. Hu L, Li N, Dai X, Guo Y, Jiang Y, He A, et al. Highly efficient production of 2,5-dihydroxymethylfuran from biomass-derived 5-hydroxymethylfurfural over an amorphous and mesoporous zirconium phosphonate catalyst. Journal of Energy Chemistry. 2019 Oct;37:82–92.

42. Hu L, Dai X, Li N, Tang X, Jiang Y. Highly selective hydrogenation of biomass-derived 5-hydroxymethylfurfural into 2,5-bis(hydroxymethyl)furan over an acid–base bifunctional hafnium-based coordination polymer catalyst. Sustainable Energy Fuels. 2019;3(4):1033–41.

43. Hu L, Li T, Xu J, He A, Tang X, Chu X, et al. Catalytic transfer hydrogenation of biomass-derived 5-hydroxymethylfurfural into 2,5-dihydroxymethylfuran over magnetic zirconium-based coordination polymer. Chemical Engineering Journal. 2018 Nov;352:110–9.

44. Hu D, Hu H, Jin H, Zhang P, Hu Y, Ying S, et al. Building hierarchical zeolite structure by post-synthesis treatment to promote the conversion of furanic molecules into biofuels. Applied Catalysis A: General. 2020 Jan;590:117338.

45. Wei J, Wang T, Liu H, Li M, Tang X, Sun Y, et al. Highly Efficient Reductive Etherification of 5-Hydroxymethylfurfural to 2,5-Bis(Alkoxymethyl)Furans as Biodiesel Components over Zr-SBA Catalyst. Energy Tech. 2019 May;7(5):1801071.

46. Wei J, Cao X, Wang T, Liu H, Tang X, Zeng X, et al. Catalytic transfer hydrogenation of biomass-derived 5-hydroxymethylfurfural into 2,5-bis(hydroxymethyl)furan over tunable Zr-based bimetallic catalysts. Catal Sci Technol. 2018;8(17):4474–84.

47. Jae J, Mahmoud E, Lobo RF, Vlachos DG. Cascade of Liquid-Phase Catalytic Transfer Hydrogenation and Etherification of 5-Hydroxymethylfurfural to Potential Biodiesel Components over Lewis Acid Zeolites. ChemCatChem. 2014 Feb;6(2):508–13.

48. Luo J, Yu J, Gorte RJ, Mahmoud E, Vlachos DG, Smith MA. The effect of oxide acidity on HMF etherification. Catal Sci Technol. 2014;4(9):3074–81.

49. Lewis JD, Van de Vyver S, Crisci AJ, Gunther WR, Michaelis VK, Griffin RG, et al. A Continuous Flow Strategy for the Coupled Transfer Hydrogenation and Etherification of 5-(Hydroxymethyl)furfural using Lewis Acid Zeolites. ChemSusChem. 2014 Aug;7(8):2255–65.

50. Shinde S, Rode C. Cascade Reductive Etherification of Bioderived Aldehydes over Zr-Based Catalysts. ChemSusChem. 2017 Oct 23;10(20):4090–101.

51. Rana SP, Rana PH. One-pot reductive etherification of 5-hydroxymethylfurfural into biofuel (2,5-bis(propoxymethyl) furan (BPMF)) using mixed catalyst ZrO(OH)$_2$ and Zr-Hβ. New J Chem. 2023;47(2):891–9.

52. Lanzafame P, Papanikolaou G, Perathoner S, Centi G, Migliori M, Catizzone E, et al. Direct *versus* acetalization routes in the reaction network of catalytic HMF

etherification. Catal Sci Technol. 2018;8(5):1304–13.

53. Barbera K, Lanzafame P, Pistone A, Millesi S, Malandrino G, Gulino A, et al. The role of oxide location in HMF etherification with ethanol over sulfated ZrO2 supported on SBA-15. Journal of Catalysis. 2015 Mar;323:19–32.

54. Güleç F, Sher F, Karaduman A. Catalytic performance of Cu- and Zr-modified beta zeolite catalysts in the methylation of 2-methylnaphthalene. Pet Sci. 2019 Feb;16(1):161–72.

55. Tang B, Dai W, Wu G, Guan N, Li L, Hunger M. Improved Postsynthesis Strategy to Sn-Beta Zeolites as Lewis Acid Catalysts for the Ring-Opening Hydration of Epoxides. ACS Catal. 2014 Aug 1;4(8):2801–10.

56. Li N, Wang A, Tang J, Wang X, Liang D, Zhang T. NO reduction by CH4 in the presence of excess O2 over Co/sulfated zirconia catalysts. Applied Catalysis B: Environmental. 2003 Jun;43(2):195–201.

57. He D, Ding Y, Luo H, Li C. Effects of zirconia phase on the synthesis of higher alcohols over zirconia and modified zirconia. Journal of Molecular Catalysis A: Chemical. 2004 Feb;208(1–2):267–71.

58. Córdoba LF, Sachtler WMH, Montes De Correa C. NO reduction by CH4 over Pd/Co-sulfated zirconia catalysts. Applied Catalysis B: Environmental. 2005 Apr;56(4):269–77.

59. Silaghi MC, Chizallet C, Raybaud P. Challenges on molecular aspects of dealumination and desilication of zeolites. Microporous and Mesoporous Materials. 2014 Jun;191:82–96.

60. Kärger J, Freude D. Mass Transfer in Micro- and Mesoporous Materials. Chem Eng Technol. 2002 Aug 6;25(8):769.

61. Ma X, Gong J, Wang S, He F, Yang X, Wang G, et al. Characterization and reactivity of silica-supported bimetallic molybdenum and stannic oxides for the transesterification of dimethyl oxalate with phenol. Journal of Molecular Catalysis A: Chemical. 2004 Aug;218(2):253–9.

62. Zhang GQ, Bai T, Chen TF, Fan WT, Zhang X. Conversion of Methanol to Light Aromatics on Zn-Modified Nano-HZSM-5 Zeolite Catalysts. Ind Eng Chem Res. 2014 Oct 1;53(39):14932–40.

63. Corma A. Water-resistant solid Lewis acid catalysts: Meerwein–Ponndorf–Verley and Oppenauer reactions catalyzed by tin-beta zeolite. Journal of Catalysis. 2003 Apr 25;215(2):294–304.

64. Corma A, Domine ME, Nemeth L, Valencia S. Al-Free Sn-Beta Zeolite as a Catalyst for the Selective Reduction of Carbonyl Compounds (Meerwein−Ponndorf−Verley Reaction). J Am Chem Soc. 2002 Apr 1;124(13):3194–5.

65. Yang Y, Hu H, Fang Q, Lu G, He H, Chen H, et al. One-pot synthesis of 2,5-bis(propoxymethyl)furan from 5-hydroxymethylfurfural by using the supported copper catalyst and hierarchical pore ZSM-5 zeolite. Catalysis Today. 2023 Nov;423:114290.

66. Rana SP, Rana PH. Effect of tunable acidic properties on the selectivity of biofuel candidate 2, 5-BIS (PROPOXYMETHYL)furan (BPMF) using Sn-H β and SN-DALH B catalysts. Biofuels Bioprod Bioref. 2024 Mar;18(2):495–509.

6.8. GC-MS data of the synthesized product
2, 5 bis Propoxymethyl furan (BPMF)

GC-MS data: 212(BPMF), 169, 153, 139, 111, 97, 83, 69, 43, 41, 30
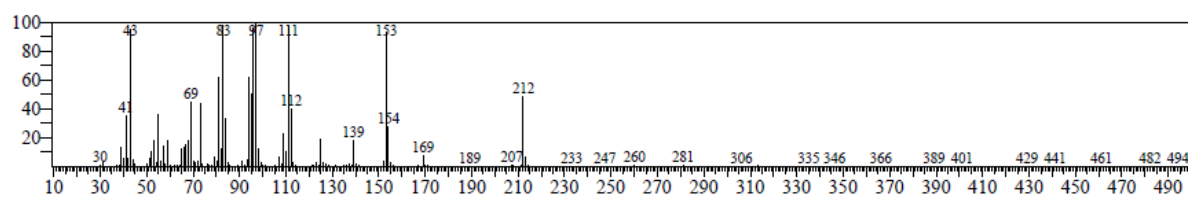
CHAPTER – 7

Conclusions and Future scope

7.1 Conclusion

In conclusion, transitioning from fossil fuels to renewable resources is crucial for addressing the issues of resource depletion, price instability, and environmental impact. Biomass, a carbon-based renewable resource, offers numerous benefits, including low cost, environmental friendliness, and wide availability. Converting biomass-derived platform molecules into valuable chemicals and biofuels is a promising approach for sustainable development. The synthesis of platform chemicals like 5-hydroxymethylfurfural (HMF) and its derivatives, such as 2,5-bis(alkoxymethyl)furans (BAMFs), shows significant potential for industrial applications. Processes combining hydrogenation and etherification, especially catalytic transfer hydrogenation (CTH), are economically viable and efficient methods for producing these chemicals. Optimizing yield and selectivity depends on the choice of catalysts and solvents. Overall, advancing biomass conversion into valuable chemicals and biofuels through innovative processes and mixed catalyst systems is essential for achieving sustainable energy solutions and reducing reliance on fossil fuels.

This thesis describes the catalytic conversion of 5-HMF into 2,5-bis(Propoxymethyl)furan using different catalysts. Zirconium (Zr) and tin (Sn) were impregnated on various supports (Hβ and HZSM-5) using wet impregnation and post-synthesis methods. The catalysts were characterized using various techniques. The thesis includes a study of the roles of Lewis acidic sites, Bronsted acidic sites, and supports, as well as the effect of metal ions on the reductive etherification of 5-HMF. This chapter concludes and summarizes the work presented in the previous chapters and discusses the future scope

based on this thesis.

Chapter 1 discussed the significance of biomass derive platform chemicals, its conversion into valuable chemicals and motivation of study.

Chapter 2 gives detail about the literature review of catalytic conversion of bio-derived 5-HMF into valuable chemicals using different catalyst, effect of temperature, reaction time, types of solvent, pressure etc. it summarizes that conversion of 5-HMF depends on the various affected parameters, metal ions and supports. It also provides details about the various characterization methods used to characterize catalyst.

Chapter 3 describes Various catalysts, including Zr over different zeolites (HZSM-5, HY, Hβ) and $ZrO(OH)_2$, were synthesized using the wet impregnation method and characterized using PXRD and FTIR. The characterization showed that the structures of HZSM-5, HY, and Hβ remained intact after metal impregnation, with the presence of Zr confirmed by characteristic peaks. The $ZrO(OH)_2$ catalyst had a lower yield and selectivity for BPMF, likely due to its role as a charge transfer hydrogenation catalyst. The Zr-Hβ catalyst achieved the highest conversion of 5-HMF at 79.41%, followed by Zr-HY at 64.76% and Zr-HZSM-5 at 60.88%. In terms of product distribution, 2,5-bis(isopropoxymethyl)furan (BPMF) was the main reaction product. The selectivity towards BPMF was 38.50% for Zr-Hβ, 35.4% for Zr-HY, and 54.09% for Zr-HZSM-5.

Chapter 4 explored the catalytic conversion of 5-HMF into 2,5-bis(isopropoxymethyl)furan (BPMF) using a mixed catalyst system of $ZrO(OH)_2$ and Zr-Hβ in a single reactor. The catalyst demonstrated good selectivity in converting 5-HMF to BPMF, primarily producing BHMF and HPMF, with HPMF selectivity being significantly higher. This higher selectivity is attributed to hydrogen transfer facilitated by the combined

Bronsted and Lewis acidic sites on ZrO(OH)$_2$. The mixed catalytic system increased Lewis acid sites and reduced Brønsted acid sites, enhancing BPMF selectivity. Zr-Lewis acid sites were found to strongly promote etherification over hydrogen transfer. The single-pot reaction, combining catalytic transfer hydrogenation and etherification, simplifies the process and reduces production costs by minimizing unit operations.

Chapter 5 shows the efficient catalytic transformation of 5-HMF to 2,5-bis(isopropoxymethyl)furan (BPMF) was achieved using Sn-Hβ and Sn-dAlHβ catalysts, prepared through wet impregnation and post-synthesis methods. Both catalysts showed good etherification activity, but the Sn-dAlHβ catalyst had superior selectivity for BPMF. The post-synthesis method for Sn-dAlHβ effectively integrated catalytically active Sn into the dealuminated zeolite, resulting in increased Lewis acid sites, a larger mesopore volume, and sufficient Bronsted acid sites. This combination enhanced BPMF selectivity due to better reactant diffusion. In contrast, the Sn-Hβ catalyst had fewer Lewis acid sites, no Bronsted acid sites, larger crystal sizes, and reduced mesopore volume, leading to lower BPMF selectivity.

Chapter 6 reported that Sn-HZSM-5 is a more effective catalyst than Zr-HZSM-5 for the etherification of 5-HMF to BPMF using 2-propanol. This is due to the higher Lewis acidity of Sn-HZSM-5, which results from the incorporation of tin ions. Sn-HZSM-5 demonstrates superior performance because it has a higher selectivity for BPMF, driven by a successful conversion of Bronsted acid sites to Lewis acid sites. This balance of acid sites promotes the reductive etherification process more efficiently. In comparison, Zr-HZSM-5, with fewer Bronsted acid sites and smaller mesopore volume, showed lower selectivity for BPMF. The study underscores the significance of acid site distribution and textural properties in the performance of catalysts for etherification reactions.

7.2 Future scope

- Further exploration of different metal ion incorporations in Hβ and HZSM-5 to enhance etherification efficiency.

- Detailed investigation of the mechanistic pathways involved in the etherification process.

- Kinetic study of reductive etherification of 5-HMF to 2,5 Bis Propoxymethyl furan.

- Modeling the catalytic processes to better understand and design improved catalysts.

- Instead of batch process continuous system can be explored.

LIST OF PUBLICATION

1. Rana SP, Rana PH. One pot reductive etherification of 5-HydroxyMethylFurfural into biofuel (2, 5-Bis (Propoxymethyl) Furan (BPMF)) using mixed catalyst $ZrO(OH)_2$ and Zr-Hβ. **New J. Chem** 2023; 47: 891-899. (**Impact Factor-3.925**).

2. Rana SP, Rana PH. Effect of tunable acidic properties on the selectivity of biofuel candidate 2, 5-bis (propoxymethyl) furan (BPMF) using Sn-H β and Sn-dAlH β catalysts. **Biofuels, Bioproducts and Biorefining**. 2024 Mar;18(2):495-509. (**Impact Factor-3.2**)

Papers to be submitted:

3. Synthesis of alkoxy methyl furfural and Bis alkoxymethyl furan a biofuel candidate: A review

4. Highly selective one-pot reductive etherification of bio-derived platform molecule 5-HMF using Zr-HZSM-5 and Sn-HZSM-5 catalysts into potential biofuel/fuel additives 2, 5- Bis Propoxy Methyl furan (BPMF).

ROYAL SOCIETY
OF CHEMISTRY

PAPER

One-pot reductive etherification of 5-hydroxymethylfurfural into biofuel (2,5-bis(propoxymethyl) furan (BPMF)) using mixed catalyst ZrO(OH)$_2$ and Zr-Hβ

Srujal P. Rana[ac] and Paresh H. Rana [iD] *[bc]

One pot synthesis of 2,5-bis(propoxymethyl)furan (BPMF) from 5-hydroxymethylfurfural (5-HMF) is essential and simultaneously difficult. In the present work, a mixed heterogenous catalyst (ZrO(OH)$_2$ and Zr-Hβ) was used to study the conversion of 5-HMF to BPMF using 2-propanol as the hydrogen donor in a one-pot process. The prepared catalysts were characterized *via* temperature-programmed desorption of ammonia (NH$_3$-TPD), powder X-ray diffraction, transmission electron microscopy, BET surface area, and Fourier transform infrared spectroscopy. The Brønsted acid sites and Lewis acid sites of the catalyst played a vital role in the selectivity for BPMF. Under the optimized reaction conditions (temperature of 140 °C, catalyst loading of 0.25 g, reaction time of 4 h and 5-HMF concentration of 1 g), 61.6% 5-HMF conversion and 91.23% BPMF selectivity were achieved.

Introduction

Human life is significantly affected by energy derived from fossil fuels. The massive use of fossil fuel resources has resulted in numerous issues including depletion of reserves, price volatility, and environmental concerns.[1–3] In this regard, the exploration of renewable resources as an alternative of fossil fuel has become urgent.[4–6] Biomass is a carbon-based renewable resource with many advantages including low cost, environmental friendly nature and availability, making it an important source for the sustainable development of valuable chemicals.[7–9] Hence, the conversion of biomass-derived platform molecules into valuable chemical and derivatives is a very attractive approach to alleviate the above-mentioned issues.[10,11] Bio refineries have emerged as a viable route to maximize the use of biomass. Biomass-derived chemicals, such as 5-hydroxymethylfurfural (5-HMF), levulinic acid, furfurals, sugar alcohols, lactic acid, succinic acid, and phenols, are considered platform chemicals. These platform chemicals can be further used for the production of a variety of important chemicals on an industrial scale.[12–14] Accordingly, various methods for the transformation of lignocellulosic biomass to platform chemicals such as 5-hydroxymethylfurfural (HMF), which can be

further converted to polymer building blocks and potential biofuel candidates, have been reported recently. Thus, the manufacturing of biofuels from HMF is gaining momentum. For instance, 5-ethoxymethylfurfural (EMF) produced by the etherification of HMF with ethanol is considered a promising bio-diesel or additive because of its high energy density of 30.3 MJ L^{-1}, which is very close to that of commercially available gasoline (31.1 MJ L^{-1}) and diesel (33.6 MJ L^{-1}).[15] Gruter *et al.*[16] reported that the aldehyde group of EMF affects the stability of the molecules when it is blended with regular diesel as phase separation occurs. Alternatively, products such as di-ethers and 2,5-bis(alkoxymethyl)furans (BAMFs) exhibit higher energy densities and good blending properties with diesel.[17] Cao *et al.*[18] reported the complete miscibility of 2,5-bismethoxymethylfuran (BMMF) with diesel. For the synthesis of BAMFs from HMF, two types of catalytic systems have been reported in literature: (i) using H$_2$ gas directly as a hydrogen source (conventional hydrogenation) and (ii) catalytic transfer hydrogenation (CTH). Compared to conventional hydrogenation with molecular H$_2$, CTH is a favourable alternative because carbonyl compounds, including aldehydes and ketones, can be completely reduced to corresponding alcohols through the Meerwein–Ponndorf–Verley (MPV) reaction using formic acid and alcohols as hydrogen donors.[19–22] Many researchers have reported the combination of hydrogenation and subsequently etherification to produce BAMFs from HMF. This approach can be considered economically viable due to the reduced production cost of BAMFs, and the process becomes simple as the number of operations is reduced.

^{a} Department of Chemical Engineering, Sarvajanik College of Engineering & Technology, Gujarat, India. E-mail: srujal.rana@scet.ac.in

^{b} Department of Chemical Engineering L.D College of Engineering, Gujarat, India. E-mail: ranaph78@gmail.com

^{c} Gujarat Technological University Gujarat, India

Effect of tunable acidic properties on the selectivity of biofuel candidate 2,5-bis (propoxymethyl)furan (BPMF) using Sn-Hβ and Sn-dAlHβ catalysts

Srujal P. Rana, Department of Chemical Engineering, Sarvajanik College of Engineering and Technology, Surat, India; Research Scholar, Gujarat Technological University, Ahmedabad, India
Paresh H. Rana, ⓘD Department of Chemical Engineering, L. D. College of Engineering, Ahmedabad, India

Abstract: 2,5-Bis(propoxymethyl)furan (BPMF) is a potential biofuel candidate but it is difficult to synthesize it selectively. The Lewis acid sites and Brønsted acid sites of the catalyst play a key role BPMF's selectivity. In the present work, the effect of tunable acidic properties such as the Lewis and Brønsted acidity of Sn-Hβ and Sn-dAlβ (Sn in dealuminated Hβ) catalysts on the selectivity of BPMF was studied by carrying out one-pot reductive etherification of 5-hydroxymethylfurfural (5-HMF) using 2-propanol as a hydrogen donor. The catalysts that were prepared underwent analysis using techniques such as temperature-programmed desorption of ammonia (NH$_3$-TPD), powder X-ray diffraction, transmission electron microscopy, pyridine-IR spectroscopy, Brunauer–Emmett–Teller (BET) surface area measurement, and Fourier transform infrared spectroscopy. Under the optimized reaction conditions, which included a temperature of 150 °C, a catalyst loading of 0.25 g, a reaction time of 4 h, and a concentration of 1 g of 5-HMF, impressive results were obtained: 93.57% conversion of 5-HMF and 98.54% selectivity towards BPMF. It was observed that the catalysts remained active for up to five cycles and slight/moderate change was observed in the conversion of 5-HMF, while the selectivity of BPMF remained intact. © 2024 Society of Industrial Chemistry and John Wiley & Sons Ltd.

Key words: 5-HMF; 2,5-bis(isopropoxymethyl)furan (BPMF); catalytic transfer hydrogenation; reductive etherification; Sn-Hβ; Sn-dAlHβ; Lewis acid site; Brønsted acid site

---

Correspondence to: Paresh H. Rana, Department of Chemical Engineering, L. D. College of Engineering, Ahmedabad, Gujarat, India. E-mail: ranaph78@gmail.com

SCI
where science
meets business